u Ottawa

L'Université canadienne
Canada's university

FACULTÉ DES ÉTUDES SUPÉRIEURES ET POSTOCTORALES

uOttawa

L'Université canadienne
Canada's university

FACULTY OF GRADUATE AND POSDOCTORAL STUDIES

Ajoy Biswas

AUTEUR DE LA THÈSE / AUTHOR OF THESIS

M.A.Sc. (Mechanical Engineering)

GRADE / DEGREE

Department of Mechanical Engineering

FACULTÉ, ÉCOLE, DÉPARTEMENT / FACULTY, SCHOOL, DEPARTMENT

Dynamic Gait Stability Index Using a Fuzzy Logic Model

TITRE DE LA THÈSE / TITLE OF THESIS

Dr. Kofman

DIRECTEUR (DIRECTRICE) DE LA THÈSE / THESIS SUPERVISOR

E. Lemaire

CO-DIRECTEUR (CO-DIRECTRICE) DE LA THÈSE / THESIS CO-SUPERVISOR

EXAMINATEURS (EXAMINATRICES) DE LA THÈSE / THESIS EXAMINERS

Dr. M. Munro

Dr. D. Russell

Gary W. Slater

Le Doyen de la Faculté des études supérieures et postdoctorales / Dean of the Faculty of Graduate and Postdoctoral Studies

DYNAMIC GAIT STABILITY INDEX USING A FUZZY LOGIC MODEL

By Ajoy Biswas

Thesis submitted to the
Faculty of Graduate and Postdoctoral Studies
in partial fulfillment of the requirements
for the M.A.Sc. degree in Mechanical Engineering

Faculty of Mechanical Engineering
University of Ottawa

Your file Votre référence
ISBN: 978-0-494-25747-0
Our file Notre référence
ISBN: 978-0-494-25747-0

Abstract

The field of physical rehabilitation needs a quantitative technique for measuring dynamic gait stability (walking stability) to make decisions regarding treatment, assistive devices, potential for falls, and to track progress during rehabilitation. This measure should be easily applied in a clinical setting, valid across physical disabilities, and must provide a quantitative index that can be used for comparisons over a range of tasks and environments. This research project developed and evaluated a gait stability index using a portable pressure measurement system.

This study examined current stability analysis methods and evaluated dynamic gait stability assessment parameters. Six gait parameters were identified and extracted from a commercial foot pressure measurement system (F-Scan). A fuzzy logic controller combined the six parameters and generated an index value. Fifteen healthy subjects were evaluated at four stability levels. All parameter combinations (57 indices in total) were assessed to isolate the most effective index.

Table of Contents

List of Tables

List of Figures

List of Abbreviations

A/P	Anterior / Posterior
ADL	Activities of Daily Living
ApEn	Approximate Entropy
BVH	Bilateral Vestibular Hypofunction
CA	Centroid Average
COF	Centre of Force
COG	Centre of Gravity
COG_{HAT}	Centre of Gravity of the Head/Arms/Trunk
COP	Centre of Pressure
COVS	Clinical Outcome Variables Scale
DGI	Dynamic Gait Index
FGA	Functional Gait Assessment
FM-B	Fugl-Meyer Test Balance Subscale
FR	Functional Reach
FSST	Four Square Step Test
GABS	Gait and Balance Scale
LyE	Lyapunov Exponent
M/L	Medial / Lateral
MF	Maximum Force
PASS	Postural Assessment Scale for Stroke patients
POMA	Performance-Oriented Mobility Assessment
RMS	Root Mean Square
SD	Standard Deviation
TUG	Timed Up and Go
VB6	Microsoft Visual Basic 6.0
VT	Vertical

Stability Parameters:

AP	Anterior/Posterior
ML	Medial/Lateral
DST	Double Support Time
ST	Stride Time
CellTrig	Cell Triggering Frequency
MaxLat	Maximum Lateral Position

Acknowledgements

First and foremost, I'd like to thank Dr. Lemaire and Dr. Kofman for your support and guidance throughout this project. I am indebted to you for helping me complete this research.

As well, this would not have been possible without the support of my family and friends. Ma and Baba, you guys are my constant inspiration. I cannot tell you enough how much I owe everything to you. And of course, Dada, Janet, Femke, Hart, Noel, Grant, and of course Shawn, you've helped me so much (and kept me sane!) in completing this thesis.

Chapter 1. Introduction

According to the National Center for Injury Prevention and Disease Control, by 2020 the cost of all fall-related injuries will reach $32.4 billion in the USA [1]. In fact, among older adults, falling is the leading cause of death and the most common cause of nonfatal injuries and hospital admissions for trauma [2]. Of those who survive a fall, 20-30 percent will suffer debilitating injuries that affect them the rest of their lives [3].

Stability is defined as "the property of a body that causes it, when disturbed from a condition of equilibrium or steady motion, to develop forces or moments that restore the original condition" [4]. Specifically, "mechanical stability is that property of a body that causes it to develop forces opposing any position or motion disturbing influence. Static stability is concerned with the production of restoring forces, while dynamic stability is concerned with the oscillations that are set up in the system as a result of the restoring forces" [5]. For the purposes of this thesis, walking stability is considered to be the smooth transition of weight from the heel to the toes while maintaining forward progression (Section 2.1).

Poor walking stability is a major cause of falls and leads to a general decrease in quality of life [6]. Assessment and rehabilitation of walking stability is therefore a very important socioeconomic concern. Observational evaluations are presently the only accepted method for quickly obtaining balance and stability measures. These tests typically rate common activities of daily living (ADL) on a scale and combine the overall performance as a mobility indicator. Mobility indicators cannot provide precise gait stability measurement since they use broad scales that incorporate a wide range of activities. Other methods used to analyze gait stability involve equipment that produces precise gait data; however, this equipment is typically confined to a laboratory.

A fast, portable, precise, accurate, and concentrated analysis method does not exist for gait stability. The solution would be to establish a validated dynamic gait stability index that is easy to obtain and can be derived from a single data source, such as foot pressure data obtained from a single measurement device. Pressure-sensitive insoles and a portable data-

logging system can be used to acquire foot-pressure distribution patterns during various activities and in many environments. Appropriate data processing could extract a valid dynamic stability index.

1.1 Scope of Thesis

In this thesis, a dynamic gait stability index, determined by a fuzzy-logic model, was developed from portable foot-pressure measurement data. The fuzzy logic control system optimally combined various gait stability parameters into a single index value. The fuzzy-logic model determination of the new dynamic stability index was validated in gait laboratory tests for four conditions of increasing levels of instability.

The dynamic gait stability index developed in this thesis was designed for people who are sufficiently mobile in the forward direction and for people who can activate an adequate portion of a pressure sensor. Therefore, the system is not intended for people who cannot walk due to severe balance or cognitive problems, as well as people who have had partial foot amputations.

The stability index validation process was limited to a healthy subject population (with normal gait patterns). These healthy subjects were evaluated at levels of decreasing stability that ensured a progression through the range of the index. The constructed system is limited to only normal forward-progressing gait patterns. Running, slipping and walking backwards or sideways is not within the scope of this research.

1.2 Overview of Thesis

Following the introduction, Chapter 2 provides background information about the human gait cycle, parameters used in quantifying gait, instrumentation employed to acquire gait data, as well as various techniques to measure gait stability. Chapter 2 also describes other attempts at creating indices of gait stability and reviews fuzzy logic controllers. Next, Chapter 3 establishes the rationale and objectives, respectively, for research on the new gait stability fuzzy-logic model and index. Chapter 4 then reviews some preliminary tests and

details the gait and foot-pressure parameters that were considered in establishing a quantitative stability index. Chapter 4 also describes the fuzzy logic model that was used for fusion of the different parameters into a dynamic stability index. Chapter 5 focuses on the methods of the clinical testing and Chapter 6 provides the results of the clinical gait and foot-pressure data acquisition trials, the fuzzy logic model processing and computation of the stability index. This is followed by a discussion of results, the study limitations, and recommendations for future work in Chapter 7. The thesis finishes with conclusions in Chapter 8.

Chapter 2. Literature Review

This chapter reviews the literature on human gait and examines gait stability assessment methods that have been established in both the clinical and research communities. This chapter also reviews gait parameters and instrumentation for gait parameter measurement, and explains gait parameters that are associated with both static and dynamic stability. As well, previous attempts at developing a gait-stability index and potential foot-pressure measurement systems for a gait-stability measurement system are discussed. Finally, fuzzy logic theory is also briefly reviewed.

2.1 Components of Human Gait

Before addressing the components that make up the human gait cycle, an understanding of the anatomical terminology used when describing position and direction of the human body is required. The term *medial* refers to the direction towards the middle of the body. The *lateral* direction points to the side of the body away from the centre. The *anterior* side of the body is the front while the *posterior* is the back (Figure 2.1).

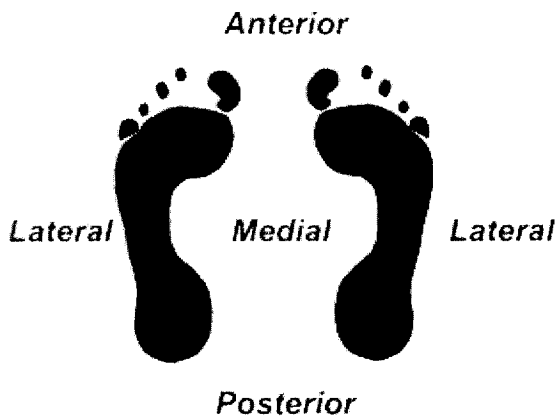

Figure 2.1: Anatomical terms of direction [7].

The human gait cycle, shown in Figure 2.2, is a complex series of coordinated movements that result in walking. The two main phases are *stance* and *swing*.

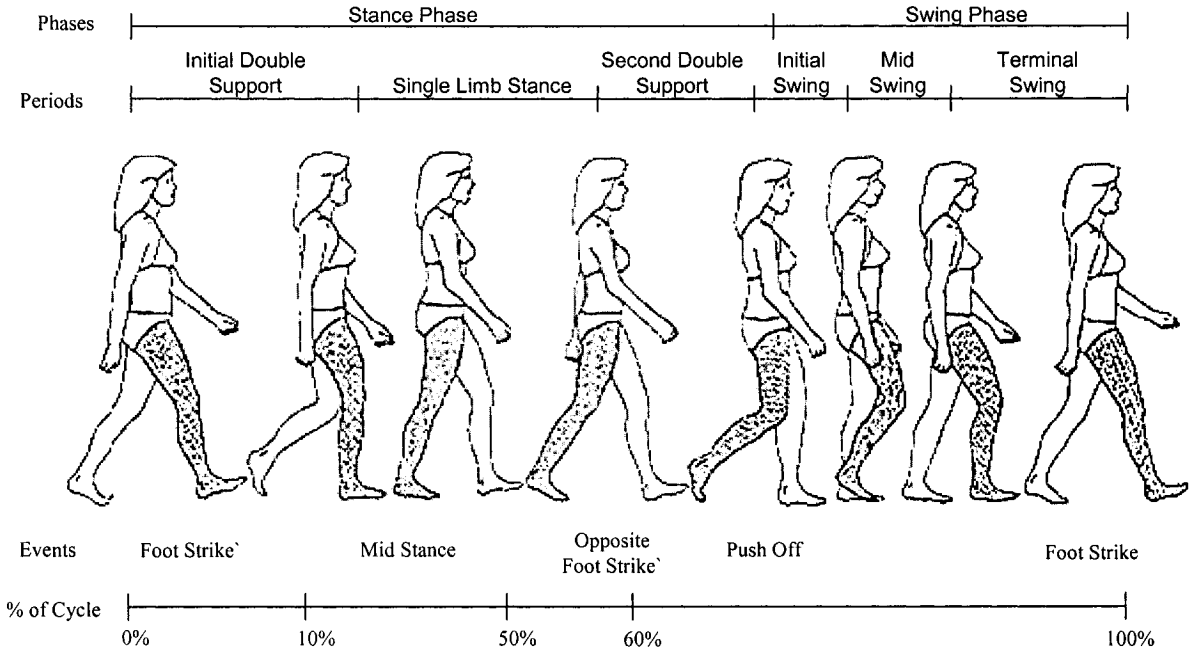

Figure 2.2: Illustration of the gait cycle showing the different phases and events for the right limb [modified from 8].

Stance-phase occurs when the foot is in contact with the ground and the leg is weight bearing. Stance-phase can be divided into *foot-strike*, *mid-stance*, and *push-off* [9]. Foot-strike occurs when the foot makes initial contact with the ground and the lower body absorbs the major impact forces. Mid-stance is the period between foot-strike and push-off when body weight is transferred onto one foot. During this phase, the body pivots over the foot in the forward direction. The center of pressure shifts laterally over one limb to free the other limb from support so that the unsupported leg may advance forward [10]. Therefore, slight lateral center of pressure (COP) motion is expected (Figure 2.3).

The foot is normally supinated (Figure 2.4) during mid-stance [11, 12]. Supination is the natural flattening of the arch when the foot strikes the ground. The foot supinates to absorb shock after the heel hits the ground. This outward rolling of the ankle also assists in maintaining balance during the transfer of weight [12, 13].

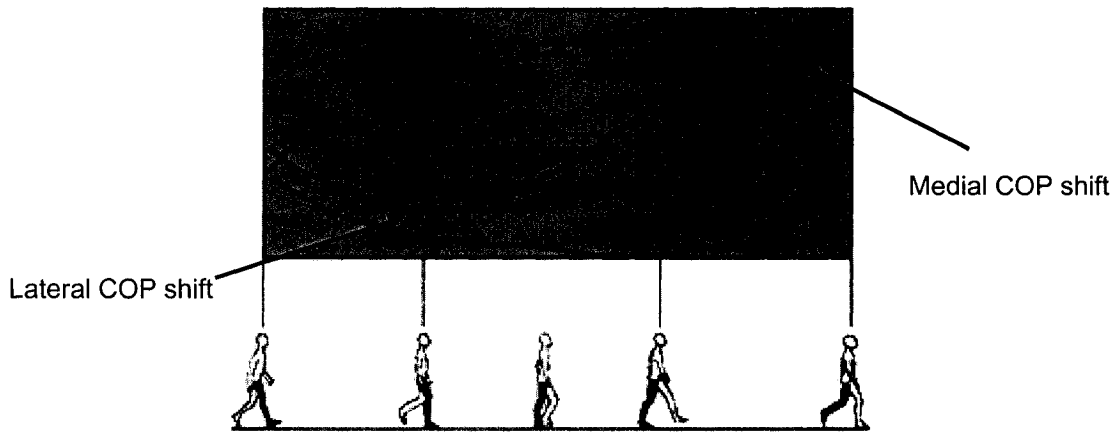

Figure 2.3: Centre of pressure pattern of normal gait [modified from 11].

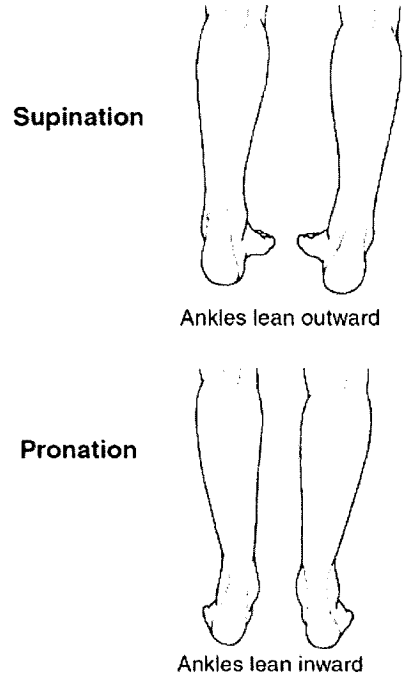

Figure 2.4: Pronation and supination of the ankle [modified from 14].

As mid-stance ends, ankle plantar-flexion propels the body upwards and forwards until only the ball of the foot is in contact with the ground [15]. While moving into push-off, the foot tends to pronate (Figure 2.4) however it should be fully re-supinated to terminate stance-phase [11]. Supination transforms the foot into a more stable, rigid structure for a powerful push-off [13]. Stance-phase is terminated when the toes lift from the ground. COP patterns during stable walking follow a smooth transition from the hindfoot to the forefoot

throughout stance phase (Figure 2.3) [16-19]. During regular paced walking, push-off partly coincides with the opposite foot's foot-strike, known as *double-support phase*, when both feet are simultaneously in contact with the ground. The highest peak power in the gait cycle is generated during push-off [20].

Swing-phase begins with push-off and ends with foot-strike. Ankle dorsiflexion, the flexing of the foot upward, combined with knee and hip flexion, raise the foot to clear the ground (Figure 2.5). Concentric power generated at the hip acts to swing the leg forward. During terminal swing-phase, the hamstring muscles activate to decelerate the leg and control foot placement. Throughout the full gait cycle, a person spends approximately 40% of the time in swing-phase and 60% in stance-phase [9].

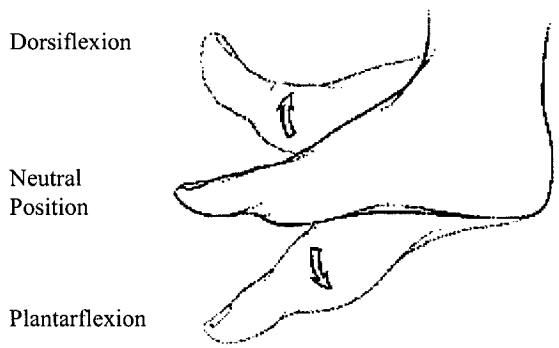

Figure 2.5: Diagram showing ankle dorsiflexion and plantarflexion [21].

2.2 Plantar Pressure

Plantar pressure data refers to the interface pressures between the plantar surface of the foot and a contact surface [18, 22]. Plantar pressure data is important for podiatrists, physicians, biomechanists, and researchers [23] since the derived information can assist in determining and managing impairments associated with various musculoskeletal, skin, and neurological disorders. The most common applications of plantar pressure data involve evaluating orthotic stabilizers and braces, predicting diabetic ulcers, and detecting lower limb instability. Plantar pressure data is also evaluated to find unnatural pressure points on the foot that lead to hindered mobility [23-27]. Bennett et al. [28] state that "a clear understanding of abnormal

foot function is central to its effective treatment, and a quantitative plantar pressure analysis of function would appear an important adjunct in clinical management."

Plantar pressure can be measured by various types of sensors and sampled at frequencies from 50 to 200 Hz (discussed later in Section 2.4.4) The sensors are either spread out evenly across the plantar surface of the foot or strategically placed to obtain the most pertinent plantar pressure information. The most commonly observed foot regions are the heel, mid-foot, metatarsal heads, and the great toe [12, 18, 25, 27-35]. The foot is typically divided into a number of sub-sections during analysis to pinpoint abnormalities in particular areas of the foot (Figure 2.6).

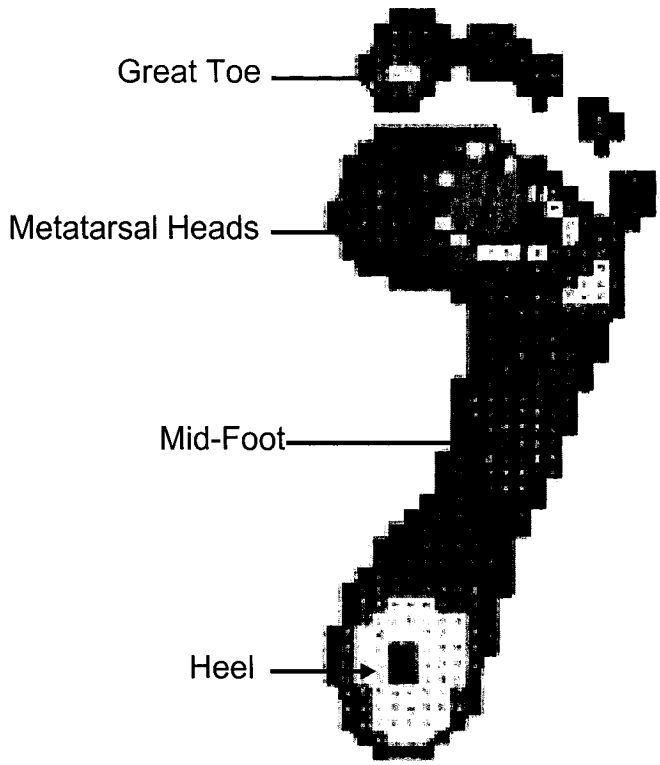

Figure 2.6: Plantar pressure distribution measurement shown by image colour (collected with the EMED system) [26]. Red indicates high pressure, while dark blue indicates low pressure.

The most common foot pressure assessment technique is an analysis of peak pressure locations. Other aspects of plantar pressure data that are often evaluated are mean and peak pressure values, frequency, centre of force (COF), contact area, contact time, and pressure-

time integral [12, 19, 27, 30-35]. Typically, the highest peak pressure distribution is found under the heel, the second and third metatarsal heads, and the great toe [12, 18, 19, 23, 25, 28, 29, 33-35]. Pressure readings at these regions were also shown to increase linearly with faster gait speeds [27]. The lowest pressure tends to be located at the medial side of the mid-foot under the arch [19].

2.3 Clinical Observational Measures of Balance and Stability

This section reviews relevant clinical observational measures of stability assessment, usually conducted by physiotherapists. These tests are based on the ability to perform simple ADL and tend to be either a subjective method of evaluating a subject's mobility level or are heavily dependent on the reaction time of the investigator.

2.3.1 Sharpened Romberg Test

The Sharpened Romberg Test is a standing balance test. To perform the test, the patient stands with their feet heel to toe. This test was slightly adapted from the original Romberg test that requires the patient's feet to be side-by-side (Figure 2.7). The physician supports the patient to attain the Sharpened Romberg position but timing does not begin until the patient stands unsupported. The score is the number of seconds that the patient can maintain balance without grasping for support or moving their feet [36]. The Sharpened Romberg stance is a commonly used basic mobility assessment technique [37-52]. One test variation that quantifies the stabilizing effect of visual perception is called the Romberg quotient, the stability ratio between performance with eyes open and eyes closed [53].

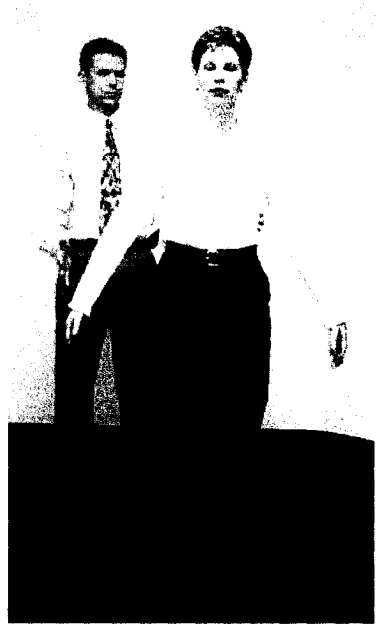

Figure 2.7: Original Romberg test [54].

2.3.2 One Legged Stance Test

The One Legged Stance Test of balance is more difficult for the patient than the Sharpened Romberg because they must balance on a much narrower base of support. To perform the One Legged Stance Test, the patient stands on one leg without upper-extremity support and without bracing the suspended leg against the stance leg. The score is the number of seconds this position is maintained without grasping for support and without allowing the suspended foot to touch the ground [36, 40, 41, 43-45, 47-50, 55-58]. The difficulty can be increased by having the subject close their eyes.

2.3.3 Functional Reach

The Functional Reach (FR) test, commonly used for gait and mobility evaluation [37, 43, 44, 50, 56, 57, 59-65], was developed by Duncan et al. [66]. The test is defined as the maximum distance one can reach forward beyond arm's length while maintaining a fixed base of support in standing. The FR score is the difference in reach between the start and end positions. Measurements are taken at the shoulder level and each subject must place their feet a set distance apart and keep the heels in contact with the floor. The FR test can be easily administered in both hospital and home environments.

Wernick-Robinson et al. [67] found that the FR test did not compare well with gait speed variations or with abnormal centre of gravity (COG) motion. This contradictory outcome could be attributed to different reaching strategies (slightly squatting or bending at the hip) or because the patient's vestibular dysfunction severity was not taken into account.

2.3.4 Tinetti Assessment Tool

The Tinetti Assessment Tool is used to predict a patient's risk of falling. This test is divided into two sections: a balance section with ten components and a gait section with eight components. The patient begins the balance section seated in a straight chair and performs numerous activities: maintaining sitting balance, rising from the chair, standing, standing with feet close together and receiving a slight push to the sternum (breastbone), standing with feet close together and eyes closed, turning 360 degrees, and sitting down.

During the gait section, the patient walks at a normal pace on level surfaces and the evaluator grades various gait parameters: gait initiation time, step length, foot clearance, step symmetry, excursions from the path, trunk posture, and base of support. The maximum score for the entire test is 28 [36, 68-71].

2.3.5 Performance-Oriented Mobility Assessment

The Performance-Oriented Mobility Assessment (POMA) test, also developed by Tinetti, consists of daily tasks and balance-based tests such as rising from a chair, standing, sitting down, standing with eyes closed, withstanding a nudge on the chest, turning, extending the back, turning 360 degrees, standing on one leg, bending down, and reaching up. Gait-based tests are also involved and include height and length of stride and step-symmetry. The POMA test is appropriate for assessing older adults and predicting their propensity to fall. There have been slight alterations in the POMA format since its creation in 1986, adding slightly easier and more difficult tasks for evaluation. The most recent version, POMA II, has a score of 0, 1 or 2 for each task for a total of 54 points [56, 62, 72, 73].

2.3.6 The Duke Mobility Scale

The Duke Mobility Scale consists of 13 items that combine easier tasks, such as sitting, with mobility tasks, such as walking, stopping suddenly, stepping over a shoe box, and going up and down stairs. The scale classifies patients into low and high-risk categories for falls. Each item is graded on a three-point scale, giving a total score ranging from 0 to 26 [65, 72].

2.3.7 Gait and Balance Scale

The Gait and Balance Scale (GABS) is an easy-to-use comprehensive clinical scale that contains two parts: history of balance problems and measurement of 14 gait parameters; including, full and half-turn, Romberg test, tandem stance, one-limb stance, modified POMA, foam posturography, timed tasks to assess gait speed, and the 'Timed Up and Go' (TUG) Test [74], explained later in Section 2.3.13.

GABS was created by Thomas et al. [74] who validated the system through comparison with GAITRite (Section 2.4.4.5) and a force plate-based system called Pro

Balance Master System. According to their study, GABS was a well-constructed, comprehensive clinical scale that reliably measured gait, balance, and posture.

2.3.8 Dynamic Gait Index

The Dynamic Gait Index (DGI) evaluates the patient's ability to modify their gait in response to changing task demands. Subjects are rated from 0 to 3 on eight different gait tasks: walking on even surfaces, changing speeds, with head turns in a vertical and horizontal direction, while stepping over or around obstacles, and with pivot turns and steps. Scores on the DGI range from 0 to 24. Scores that are greater than 19 indicate a low risk for falling during gait [49, 60, 75-81].

2.3.9 Functional Gait Assessment

The Functional Gait Assessment (FGA) is a 10-item gait assessment created and validated by Wrisley et al. [82] that is based on the DGI. The test retains seven of the eight original items from the DGI and implements three new items: gait with narrow base of support, ambulating backwards, and gait with eyes closed. The new items were added because these activities are difficult for people with vestibular disorders. The FGA demonstrated what the authors considered moderate reliability when used by physical therapists with patients with vestibular disorders.

2.3.10 Four-Square Step Test

The Four-Square Step Test (FSST) (Figure 2.8) is a clinical test designed by Dite et al. [64] that measures rapid stepping and obstacle avoidance. This test requires the subject to rapidly step forwards, backwards, and sideways while stepping over a cane lying flat on the ground. The time to complete the process is measured. The main objective is to identify subjects who fall.

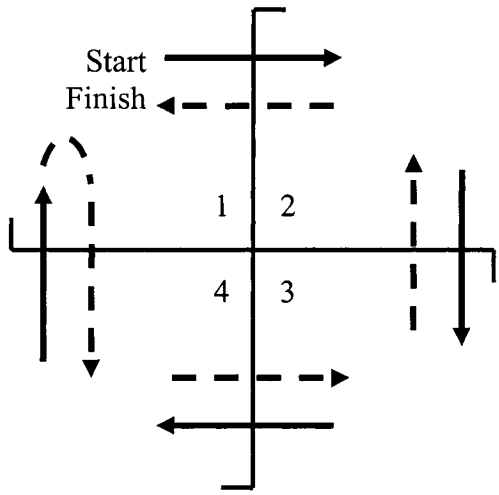

Figure 2.8: FSST test [64].

2.3.11 Fugl-Meyer Test Balance Subscale

The Fugl-Meyer Test Balance Subscale (FM-B) is 1 of 6 subscales from the original Fugl-Meyer test (FM) that was designed for impairment evaluation after a stroke. The FM-B contains seven, three-point tasks: three for sitting and four for standing. The total score ranges from 0 to 14. Previous studies have shown the FM-B reliability to be controversial. As a result, the scoring criteria were altered while maintaining the original testing procedure. The modified FM-B validity was acceptable and is now used regularly [83].

2.3.12 Postural Assessment Scale for Stroke Patients

The Postural Assessment Scale for Stroke patients (PASS) was developed for all stroke patients, including those with poor postural stability. The assessment scale contains 12 four-point measures that evaluate the ability to cope with progressively difficult situations in maintaining or changing a lying, sitting, or standing position. The PASS has a score that ranges from 0 to 36 and has been proven to have high reliability [83].

2.3.13 Timed Up and Go Test

The Timed Up and Go (TUG) test was deemed by Cole et al. [84] to be a quick and practical method to test basic mobility manoeuvres, both clinically and for research purposes. The test [6, 72, 85] is adapted from the original "Get Up and Go" test and has shown a strong association to the Barthel Index of Daily Living that was developed to monitor functional independence before and after rehabilitative treatment [84, 86]. The protocol involves rising from a seated position, walking 10 paces, turning, and returning to the seat. The time necessary to complete the task reflects directly on locomotion abilities.

TUG is considered a basic functional mobility test rather than a measure of balance [72]. Times can range from six seconds to four minutes [85]. Berg et al. [72] report that most adults can complete the task in 10 seconds. Eleven to 20 seconds is the typical range for frail elderly or disabled patients. If the task takes more than 20 seconds, a more comprehensive assessment is needed. TUG is one of the most common techniques of assessing general mobility [43, 50, 51, 56, 59, 64, 69, 78, 79, 81, 82, 87-92].

2.3.14 Berg Balance Scale

The Berg Balance Scale rates the patient on a score of zero to four for 14 tasks that are common in everyday life. The tasks include a sitting test; three transferring tests (from sitting to standing, etc.); five standing tests; and five tests to gauge mobility, such as turning 360 degrees and reaching forward while standing. The test elements measure the ability to perform tasks and maintain certain positions while diminishing the base of support from sitting, standing, to single leg stance. The Berg Balance scale has been described as an objective measure of balance abilities [84] and has also been accepted as a comparison tool for validation of experimental balance assessment techniques [36, 37, 56, 59, 60, 63, 80, 81, 88, 91-104].

2.3.15 Clinical Outcome Variables Scale (COVS)

The Clinical Outcome Variables Scale (COVS) Mobility Test is another test based on ability to perform activities of daily living. The tasks are rated on a 7-point scale and the mobility subscale includes: rolling (2), lying to sitting balance, weight transfers (2), ambulation (4), and wheelchair mobility. There are also two measures for arm function. COVS is used to measure mobility in an active rehabilitation population including individuals with spinal cord injury, stroke, other neurological conditions, amputation, multiple trauma, and post-surgical hip or knee replacement [100, 101].

2.3.16 Summary of Clinical Observational Measures of Balance and Stability

The observational measures mentioned in the preceding sections describe some of the most commonly used techniques of assessing balance and stability in a clinical setting. The tests involve various combinations of sitting, standing, reaching, and mobility tasks that are common in ADL. These tests are used by clinicians due to the low time requirements for obtaining a general assessment of balance and mobility and the ability to take measurements at the point of patient contact.

The main limitation with the previously mentioned clinical observational measures is that they either require the subjective scoring of an evaluator or involve the reaction time of the assessor when timing the subject on an activity. As well, many of these tests evaluate the

subject's ability to perform certain movements that would make the tests biased for people who are adept to these tasks or for people with task-specific deficiencies not related to balance. By observing and evaluating people on only a small number of activities, the full scope of their stability cannot be determined. The goal of this study is to have an accurate, objective and quantitative measure of gait stability, to replace these observational-based tests.

2.4 Instrumentation for Measuring Stability of Human Walking

Balance, in its broadest sense, involves the capability to control upright posture under a variety of conditions and the ability of an individual to sense their stability limitations [72]. In many studies, kinematic parameters have been acquired with various instruments and analyzed to assess human locomotor stability. A force plate combined with a motion analysis system is the most widely reported method of quantitative balance measurement in the literature [6]. Other commonly used systems depend on foot pressure analysis. These techniques are explained in the following sections.

2.4.1 Force Plate Systems

Force plates (Figure 2.9), also known as force platforms, measure three-dimensional (3D) ground reaction forces and moments as a subject contacts the device. The typical design is approximately 10 cm high with a flat surface measuring 40 cm x 60 cm. Transducers are used to record force components along three axes (anterior-posterior shear, medio-lateral shear, vertical force normal to the plate surface). The force plate must be secured to eliminate vibrations and is often bolted to a steel frame or a concrete foundation. The most commonly used commercial platforms are manufactured by Kistler (Kistler Instrumente AG, Winterthur, Switzerland), AMTI (Advanced Mechanical Technology, Inc., Watertown, ME), and Bertec (MIE Medical Research Ltd., United Kingdom).

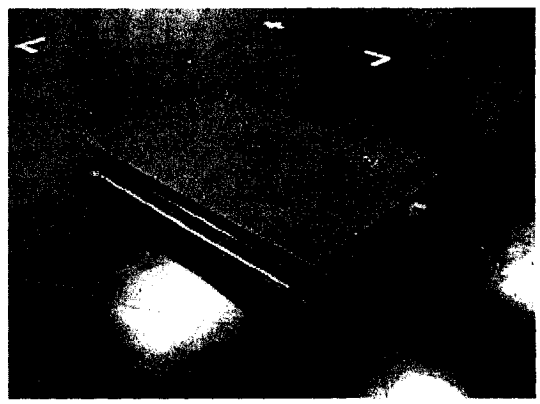

Figure 2.9: Bertec force platform [105].

A drawback with force plates is the inability to obtain discrete plantar force data when both feet are in contact with the plate. Therefore, to correctly analyze gait pattern data, only single foot contact per platform is permitted. No single arrangement of positioning two platforms can accommodate all subjects. As well, force plates should be concealed within the floor so that subjects do not know their location, otherwise gait patterns would be unavoidably altered as the subject aims for the platform. This often results in repeated void trials while the researcher must wait for the subject to correctly load the force plate. As well, a force plate only gives a single 3D force vector and moment with the placement of the foot. Foot pressure distribution over the entire foot cannot be extracted with a force plate alone. However, the major disadvantage of the force plate is that it is typically restricted to a laboratory.

2.4.2 Camera and Marker-Based Systems

The most common gait analysis technique is to combine force plates with a camera/marker-based system (Figure 2.10), thereby effectively collecting kinetic and kinematic data simultaneously. A grid or cube of reflective markers with known coordinates is used to calibrate the cameras so that accurate marker positions can be calculated from the video images. 3D motion analysis systems require at least two cameras, but more are often used to minimize the occurrences of hidden markers. If two or more cameras cannot see a marker, the 3D marker position cannot be tracked. The marker's position could be interpolated, but this may introduce an error. Other marker-based systems involve scanning the field of view with moving light beams, detecting reflections from prisms mounted on a subject, and detecting small wire coils placed on subjects by means of a magnetic field [15]. The most commonly used systems rely on either passive reflective markers or active light emitting diodes.

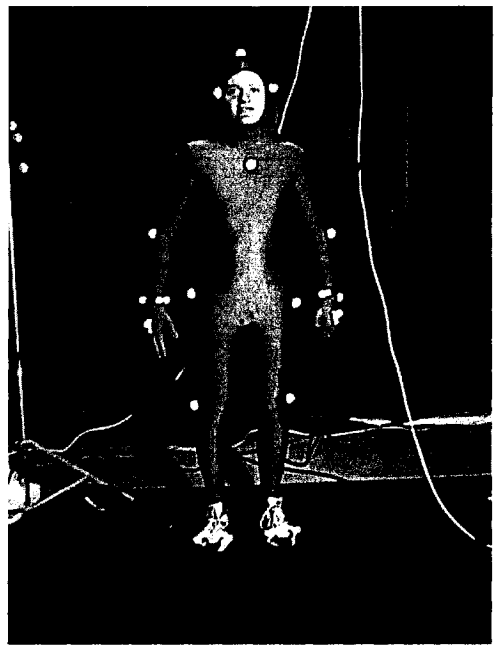

Figure 2.10: Marker-based motion analysis system showing reflective markers placed on a body [106].

Although cameras can be made portable, the cameras should not be moved after the system has been calibrated. Video systems are also difficult to use as a routine patient assessment technique. The major drawback of a marker-based system is the time for set up, camera calibration, and marker placement. As well, there must be an adequate number of markers used in order to minimize the occurrence of an insufficient number of visible markers.

2.4.3 Accelerometers

Accelerometers detect acceleration and deceleration in any direction [107]. These transducers are often strategically placed at joint locations for accurate biomechanical gait cycle analysis. When placed at the lower trunk, accelerometers can be used to determine body sway, walking speed, step length, cadence [108], and accelerations in anterior/posterior (A/P) and medial/lateral (M/L) directions [109]. The devices can also be made portable with a data logger and power source.

2.4.4 Pressure Measurement Systems

The following pressure measurement systems are commonly used to analyze foot pressure during gait. The systems vary in applications ranging from observing high-pressure zones of the foot with low spatial resolution to analyzing precise pressure values over the full plantar surface of the foot. Similar to the force plates, camera/marker-based systems, and accelerometers described earlier, these pressure measurement systems can also be used to assess gait stability. One benefit is that these systems can be made portable. Portability is of primary importance, and pressure measurement systems are therefore especially of interest for this research.

2.4.4.1 Parotec Pressure Measurement System

The Parotec system (Paromed Medizintechik, Neubeuern, Germany) contains thin insoles (Figure 2.11) connected to a small controller box. Parotec implements a hydrocell technology that was developed for pressure measurement and independently rated to perform with less than 2% measurement error across the expected pressure, temperature, and humidity ranges of normal use [110, 111]. The hydrocell consists of a discrete piezoelectric sensor contained in a fluid-filled cell that is embedded in an insole. When a load is applied to

the hydrocell, the applied force causes increased pressure within the water environment of the hydrocell. The piezoelectric sensor within the cell generates an electrical charge as a result of this increased pressure and measures the vertical component of the applied force [112].

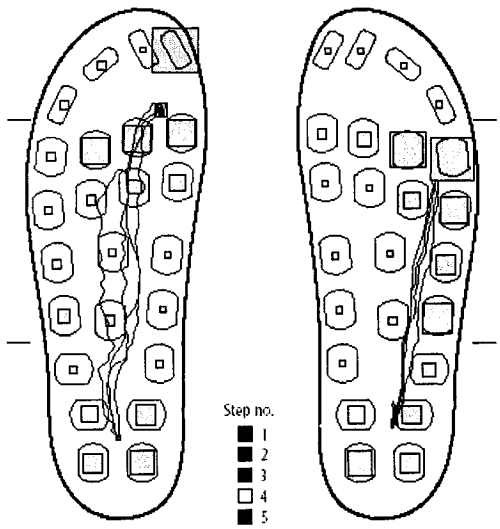

Figure 2.11: Parotec system load sensors. [110].

The Parotec system's drawback is that it embeds only 24 individual hydrocells in each insole. This allows for large-scale pressure data to be evaluated, but it cannot obtain fine spatial resolution. Schaff [112] reviewed some foot-pressure measurement systems and mentioned that the Parotec system can describe foot pressure patterns sufficiently, while pinpoint and atypically located pressure peaks may not be observed. Davis et al. [113] also claimed that larger transducers will yield data of substantially lower resolution.

2.4.4.2 Pedar-X In-Shoe Pressure Measurement System

The Pedar-X system (Novel, Munich, Germany - Figure 2.12) consists of insole sensors that measure plantar pressure distributions. The system can be made portable with built-in flash memory storage [114]. Each insole is equipped with 84-99 capacitive sensors that span the area of the foot. The system can also enhance the resolution by a method of interpolation to approximately one sensor per cm^2. However, the sampling abilities of capacitive sensors are limited to a frequency of approximately 50 Hz [112, 115].

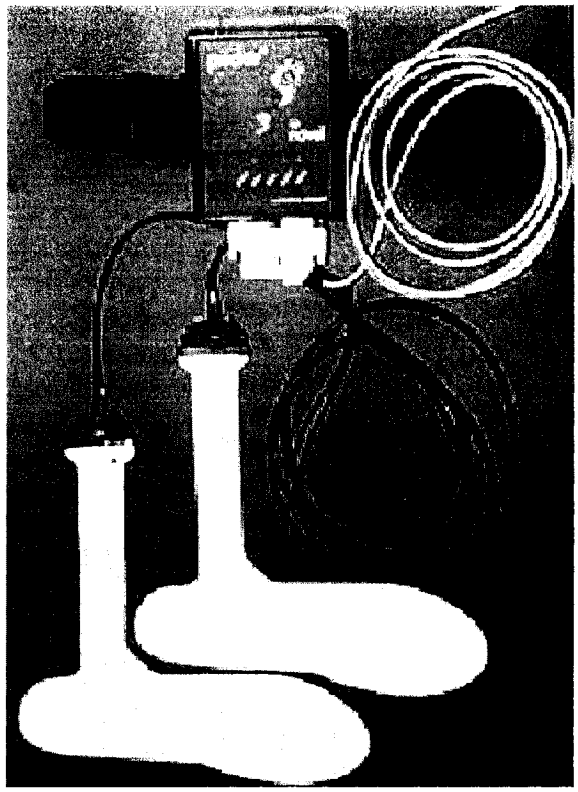

Figure 2.12: Pedar-X in-shoe pressure measurement system [115].

2.4.4.3 Piezoelectric Film Transducers

Piezoelectric film transducers are another approach for obtaining gait data by placing sensors under a subject's feet while they walk. The typical piezoelectric film transducer is approximately 10 x 10 mm^2 and 2.8 mm thick. These transducers use a 500 μm copolymer piezoelectric film sandwiched between a brass electrode and a double-sided circuit board. The electrodes provide electrical connections to the film surface and prevent critical bending under loading. During the testing process, sensors are placed in the subject's shoes and an ankle box is strapped to each leg [116].

Nevill et al. [116] created in-shoe pressure measurement sensors using piezoelectric film transducers; however, each sensor contained only eight transducers. The rationale behind this design is that pertinent information resides only at the great toe, five metatarsal heads, the arch, and the heel. Data outside these regions were considered redundant. As a result, the sensor could miss important stability information when dealing with uncommonly

used areas of the foot. Even if Nevill and colleagues had used as many transducers as possible, given the dimensions of a piezoelectric film transducer, each sensor would contain less than 200 transducers.

Also, the sensor is quite rigid due to the circuit board required in the design. The inflexible sensor may result in erroneous data, or omit valid data, and could also interfere with the gait pattern by hindering or masking natural flexion of the foot. Another disadvantage is that the system is not fully portable because the subject must remain tethered to an electronic console during testing. The 10 m cable used in experimentation allowed for recording multiple footsteps, but lacked the ability to venture outside a laboratory.

2.4.4.4 Optical Techniques

Plantar pressure distribution measurement was also investigated by Urry [22]. Optical pedobarographs [117, 118] detect the amount of internally reflected light through a glass plate (Figure 2.13). The index of refraction of glass changes very slightly by applying pressure. Transmitted light is measured to indicate pressure distribution. The disadvantages of this method are that any interference from external light sources would be a source of error and this pressure measurement technique is not portable.

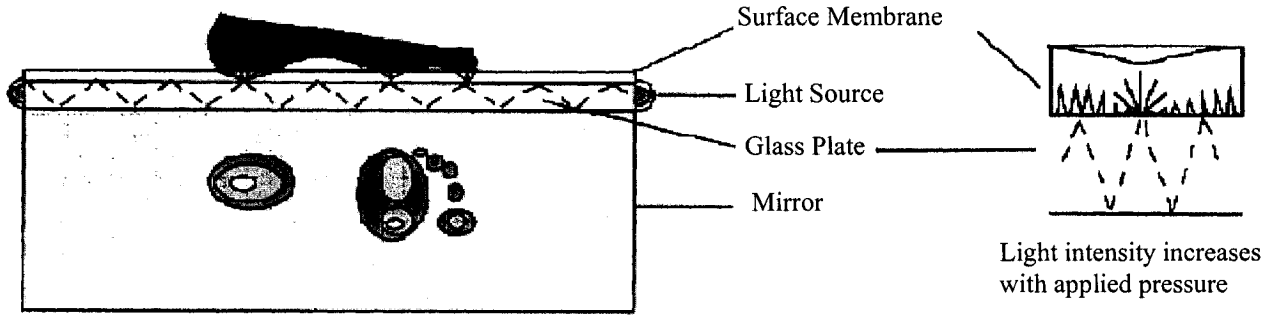

Figure 2.13: Optical pedobarograph [22].

Another optical method uses photoelasticity [119], where an applied load is transmitted to an optically sensitive (photoelastic) sheet by an array of semi-spherical solids. The pressure distribution beneath the foot would be represented by discrete circular interference patterns [22]. Although most optical methods tend to have high spatial resolution and work well for dynamic gait evaluation, they are not portable.

2.4.4.5 GAITRite Pressure Measurement Mat

GAITRite (CIR Systems Inc., Havertown, PA) is a compact computer-based instrumented electronic roll-up walkway connected to a computer with application software for calculating temporal and spatial gait parameters. The walkway is 3 m long with a pressure sensitive mat (61 cm x 366 cm) containing a series of sensors organized in a 48 x 288 grid pattern, sandwiched between two vinyl layers [74]. On average, 20 x 10 sensors are contacted during foot contact. The main limitations with GAITRite are low resolution, non-portability, and the inability to handle irregular terrain.

2.4.4.6 Force Sensing Resistors

Force sensing resistors (FSR) are devices that exhibit a decrease in resistance with any increase in force applied to the active surface [120]. A typical FSR (Figure 2.14) consists of [121]:

- A layer of insulating plastic
- An active area consisting of conductors that are supplied with an electrical voltage
- A plastic spacer
- A flexible substrate coated with a polymer conductive film that is aligned with the active area

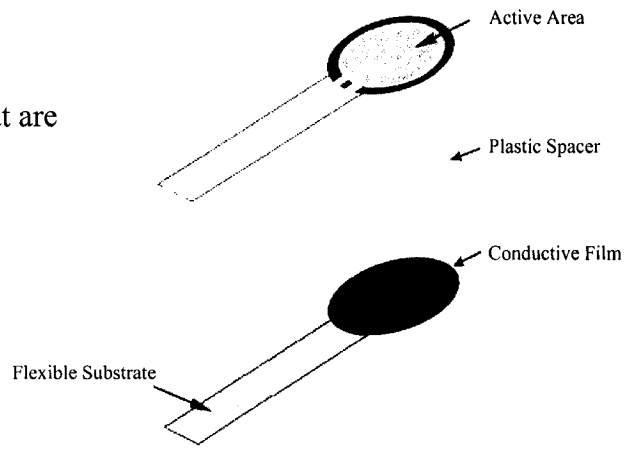

Figure 2.14: FSR components [modified from 121].

When an external force is applied to the sensor, the active area comes into contact with the conductive film and completes an electrical connection through the sensor. As the applied force increases, more of the active area comes into contact with the film and reduces the resistance in the circuit. The resistance can be measured and used to determine the applied force. The advantages of FSR sensors include flexibility, durability, reliability, overload tolerance, electronic simplicity, and low cost.

2.4.4.7 F-Scan In-Shoe Pressure Measurement System

The F-Scan measurement system, (TekScan Inc., South Boston, MA) uses a sensor that is shaped like a shoe sole and placed under the patient's foot inside their shoe. The sensor contains FSR cells (Section 2.4.4.6) in a conductive grid of rows and columns containing pressure-sensitive, semi-conducting ink sandwiched between two polyester film sheets (Figure 2.15). This system has a 165 Hz sampling rate, spatial resolution of 960 pressure readings per sensor (4 sensors/cm^2) [34, 112], and insole sensors that range from 0.2 mm to 0.4 mm in thickness.

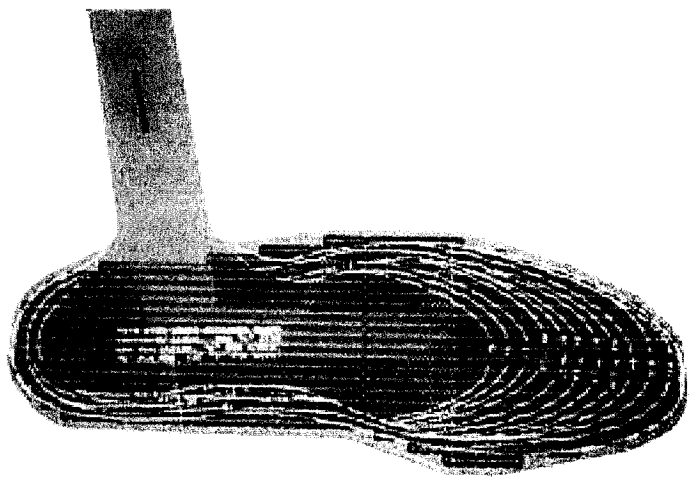

Figure 2.15: F-Scan pressure sensitive insole. The sensor can be trimmed along the white lines to fit inside different shoe sizes.

When force is applied, the ink layer resistance decreases in proportion to the force magnitude [122]. The portable F-Scan-Mobile measurement system (Figure 2.16) incorporates data logging within a belt-pack. The small and fully self-contained accessory pack can be worn around the waist or strapped to the lateral calf to power the system and record pressure data [123, 124].

F-Scan in-soles do not interfere with gait and can be customized for any shoe size. The sensors can be used to analyze the effects of walking in various types of footwear and orthoses [124]. Chen et al. [125] compared measurements made by the F-Scan system with those by an AMTI force plate. The F-Scan system demonstrated some inaccuracies in

registered pressure readings in the double support phase, confirming similar results found by Sumiya et al. [122]. This inaccuracy was associated with increased shear forces at heel-on and toe-off. F-Scan cannot measure shear force; therefore large force components that are not normal to the sensor would not be detected. However, both groups of authors agree that the F-Scan and force plate data correlate quite well, making F-Scan a reliable and clinically valid tool for relative comparisons of plantar pressure distributions.

Figure 2.16: F-Scan Mobile system [123].

Schaff et al. [112] did a comparison study with commonly used pressure measurement systems and found that the F-Scan system had the highest in-shoe resolution by a large margin. Han et al. [126] studied COP path quantification measured by F-Scan transducers and found that the results were reliable by test-retest analysis.

Table 2.1: Specifications for the available mobile pressure measurement systems [112].

System	Resolution (sensors/insole)	Method	Frequency (Hz)	Type
F-Scan	960	Resistive	100	Matrix sole
Parotec	24	Piezoelectric	100-200	Single point
Pedar-X	84-99	Capacitive	50	Matrix sole

The F-Scan system has a high spatial resolution. FSR sensors are also excellent switches and can be used for accurate stride timing parameters. The system can be portable and has shown to provide accurate results when compared to the force plate gold standard within the limitations described above. The system can also output raw pressure values for each cell and provide a calculated COF location.

2.4.4.8 Summary of Pressure Measurement Systems

A number of different methods can be used to analyze foot pressure data. Some systems are very useful for observing the common pressure zones (Figure 2.6) with larger sensors such as

the Parotec System (Section 2.4.4.1) and the Pedar-X System (Section 2.4.4.2). In contrast, the optical techniques described in Section 2.4.4.4 have high spatial resolution and work well for dynamic gait evaluation; however, these systems cannot be made portable to observe gait in environments outside a laboratory. F-Scan is a pressure measurement system that uses FSR sensors to span an insole. The insoles contain approximately 1000 sensors and can be trimmed to fit inside different shoe sizes. The F-Scan system can be made portable, has a high spatial resolution, and has proven to be a reliable method for dynamic gait analysis.

2.4.5 Summary of Gait Stability Measurement Instrumentation

The most commonly used technique of quantitatively measuring gait stability is by combining force plates with a camera/marker-based system to obtain both kinetic and kinematic gait information. However, force plates must be concealed from the subject and data cannot be separated from two feet on the same platform. This results in repeated void trials while the researcher must wait for the subject to correctly load the force plate. As well, camera/marker-based systems take some time to calibrate and have to deal with occurrences of hidden markers. Yet, the most important drawback of both these systems is that they are typically not portable. A force plate has to be well-secured to eliminate any vibrations and the cameras used in a camera/marker-based setup cannot be moved after the system has been calibrated.

Another method of obtaining stability information is to use accelerometers. Accelerometers can obtain quantitative joint motion information and can be made portable. A number of accelerometers would be needed to obtain adequate information to assess stability, whereas plantar foot pressures can be obtained with a single insole.

The F-Scan pressure measurement system is ideal for this research. The sensors fit inside a shoe of any size and can obtain accurate pressure measurements with a high spatial resolution. This system can also be made portable with an accessory belt pack to obtain gait stability information without being restricted to a laboratory. Accelerometers would be a feasible addition to the system; however, to limit the amount of equipment necessary to obtain a stability index, accelerometers were omitted from the project. In future research, accelerometers may be introduced to broaden the scope of the index.

2.5 Methods of Objective Stability Measurement

The methods discussed in this section involve isolation of quantitative stability parameters that are analyzed to yield an objective stability assessment. These evaluation techniques involve the instrumentation described in Section 2.4 and are not based on human decision or reaction time. This section also reviews previous studies on static and dynamic stability.

2.5.1 Methods of Measuring Static Stability

Static stability refers to a person's ability to maintain balance in a standing position. Typically, static stability investigation is considerably simpler than examining dynamic stability [127]. Static stability tests are often observation-based but sometimes involve data and signal processing.

COP can be a key component when determining static stability. "Limits of stability are the boundaries within which the COP can move back and forwards, as well as sideways, before requiring a step to regain balance and avoid a fall. Subjects who can control their COP in a larger range within their base of support are considered to have better postural control [87]." Observing COP motion during quiet standing is used regularly for assessing static stability [10, 37, 39, 53, 58, 71, 88, 100, 128-130].

A subject's ability to stand still without swaying can also indicate their level of static stability [47, 50, 52, 53, 55, 57, 58, 61, 65, 68, 71, 73, 78, 86, 129-133]. Postural stability measures how stable people are in a standing position. Measurement approaches include accelerometers, force plates, and motion analysis systems.

The main methods for static stability evaluation are observation of COP, COG, and body sway. Abnormal changes in these parameters during quiet standing are thought to be a sign of instability. According to the studies mentioned above, the COP and COG are reliable for determining a subject's level of static stability while body sway does not always correlate with other stability tests.

2.5.1.1 Previous Studies Involving Static Stability

Ringsberg et al. [134] assessed postural sway using a computerized balance system to calculate how far the center of balance deviated from the mean center of balance during four different 20-second balance tests. The tests were (1) standing on a stationary platform with eyes open, (2) standing on the same stationary platform with eyes closed, (3) standing on a platform with eyes closed and with the platform gliding horizontally backwards and forwards, and (4) standing on the platform with eyes open and with the platform moving up and down. The results were correlated with a separate one-leg standing test that the authors asserted as an assured method of static stability evaluation. Unfortunately, the authors found no relationship between the one-leg standing test and any of the computerized centre of balance tests. As well, the four computerized tests were poorly correlated with each other. The authors concluded that the tests may have measured different aspects of postural control and are not comparable.

Observing the COG is another technique used by Patton et al. [135] to acquire static stability information. Their study involved a balance recovery test where subjects would squat to develop posterior momentum, generate a brief and abrupt pull on a fixed bar in front of them that reversed the COG motion, and then recover their balance. To assess stability, the investigators defined conditions based on COG dynamics that cause the base of support to move (called torque boundaries) and conditions beyond which movement cannot be terminated (called state boundaries). These values were dependent on a body dynamics model that required extensive kinematic data to predict when a fall was about to occur. The research team used an AMTI force plate to measure ground reaction forces and an Elite video analysis system to acquire body kinematics. The empirical data coincided with the model predictions in all but 0.2% of the trials, in which the authors suspected the subjects to have performed the balance test incorrectly.

2.5.2 Methods of Measuring Dynamic Stability

Dynamic stability refers to a person's ability to maintain control and balance of their body while walking at a self-selected pace. Many aspects of gait can be used to measure dynamic stability. Body sway, body COG and/or COP motion, and various stride parameters have all

been known to reveal a level of dynamic stability. The following sections describe these techniques of measuring dynamic gait stability.

2.5.2.1 Dynamic Upper-Body Sway

For a stable gait pattern, the body's momentum should be controlled at all times to minimize sudden shifts in balance. Upper-body motion in the medial/lateral (M/L) direction, also known as body sway, occurs in normal gait. However, studies have shown that increased amplitude and frequency of body sway during walking can indicate instability and that fall frequency increases as sway increases. Poor momentum control leads to increased lateral sway during walking, hence a lack of stability [38, 52, 55, 74, 89, 103, 130, 131, 136-139].

2.5.2.2 Centre of Gravity Dynamics

To maintain stable gait, the COG must remain within the base of support. Currently, the body COG position can only be obtained with a whole body, marker-based, data collection system. Typically, the body is separated into rigid segments with six degrees of freedom [140]. The 3D COG position over time can then be calculated from segment positions. COG vertical projection, COG velocity, and vertical COG oscillations are commonly used variables for analyzing stability. Other good measures involve inverted pendulum comparisons and observing the relationship between mechanical work, energy consumption, and COG motion [68, 102, 141-153].

According to past studies, unsteady COG motion results in abnormal foot pressure patterns that can also be observed in the COP motion. In a study of the biomechanics of posture and balance, Riley et al. [140] stated that COG motion shows a damped form of the COF motion. Adkin et al. [58] and Oates et al. [154] both agree that COP observation can provide insight into the COG movement. Regarding application to this thesis, the issue of portability is quite important. Since the total body COG can only be accurately obtained with markers and cameras, data collection is largely restricted to a laboratory setting. Therefore total body COG-based stability parameters will not be useful for this study.

2.5.2.3 Stride Timing Parameters

Stride length, cadence, stride velocity and double-support time have demonstrated a strong correlation with gait stability and are commonly used in gait analysis. In gait, *cycle time* refers to the time for one foot to go from heel-strike to heel-strike. The distance from heel-strike to heel-strike is known as the *stride length*. Stride length is divided by cycle time to obtain *stride velocity*. These measures are commonly used as a comparison for testing a dynamic stability assessment technique and are normally obtained with a stopwatch, footswitches, or through video data analysis [10, 38, 39, 41, 43, 45, 49, 51, 52, 55, 57, 59, 65, 74, 78, 79, 89, 91, 95-101, 103, 108, 131, 137, 141, 142, 146, 150, 152, 157-176].

Double support time is the period when both feet are in contact with the ground. In able-bodied gait, this phase is approximately 20% of the full gait cycle [15]. Double support time is either obtained from foot switches, video data analysis, or by analyzing foot pressure data. People who are unstable spend more time in double support to maintain their balance. Double support time is another commonly used parameter in stability analysis [43, 74, 96, 98, 108, 128, 131, 141-144, 150, 157, 158, 160, 161, 169].

2.5.2.4 Dynamics of Centre of Pressure Under the Foot

Anterior/Posterior (A/P) motion of the COP under the foot is an important parameter for determining dynamic stability. A stable gait plantar pressure pattern follows a smooth transition from the hindfoot to the forefoot (Figure 2.3) [16]. Therefore, A/P deviations hindering a smooth transfer could indicate unstable gait [17, 102, 130, 135, 141, 144, 148, 178-183]. Motion of the COP in the A/P direction can be obtained with a force plate or other plantar-pressure measurement techniques.

M/L motion of the COP is a common indicator for stability analysis. Throughout stance-phase, motion from the foot's medial side to the foot's lateral side is expected. When transferring from double support to single support, pressure shifts toward the outside of the foot. Likewise, while transferring from single support to double support, pressure shifts towards the inside of the foot. Any deviations from this simple pattern (Figure 2.3) would be perceived as a sign of instability [17, 88, 102, 130, 135, 136, 141, 144, 148, 150, 151, 173,

176, 178-183]. As well, instability can be seen in an excessive lateral shift in COP [110, 184, 185]. Studies have shown that older people with poor lateral stability are three times more prone to falling [88]. Similar to A/P direction, M/L COP motion can be obtained with force plates or with a foot pressure measurement system.

2.5.2.5 Previous Studies involving Dynamic Stability

Karcnik et al. [155, 156] used patient COG, COG velocity, and the foot's supporting area dimensions to create a "relative kinematic stability index" (RKSI) for kinematic stability and an "absolute velocity index" (AVI) for dynamic stability (Equations 2.1 and 2.2):

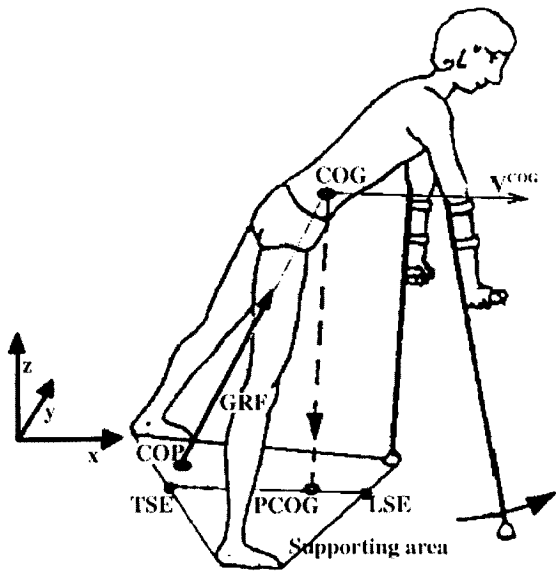

Figure 2.17: Biomechanical parameters used in the equations created by Karcnik et al. for the assessment of gait stability [155].

$$RKSI = \frac{d(PCOG, CS)}{\frac{|d(TSE, LSE)|}{2}} \qquad \textbf{(2.1)}$$

$$AVI = \sqrt{\frac{g}{z^{COG}(t)}} d(PCOG, LSE) - v_x^{COG}(t) \qquad \textbf{(2.2)}$$

In the RKSI formula (Equation 2.1), *d* denotes the distance between two points, *PCOG* is the vertical projection of the COG on the ground plane, *CS* is the centre of the supporting area, *LSE* is the leading supporting edge of the supporting area, and *TSE* is the

trailing supporting edge (Figure 2.17). In the AVI formula (Equation 2.2), g is the acceleration due to gravity, $z^{COG}(t)$ is the height of the COG above ground level and it moves forward in the x-direction, and $v_x^{COG}(t)$ is the velocity of the COG in the x-direction (Figure 2.17).

The two indices, RKSI and AVI, were used to determine if a gait pattern was stable or unstable yet they did not always agree with each other. The RKSI falls outside the stable range when the COG goes outside the base of support. If the COG velocity exceeds a 'critical' velocity, then the system is in a dynamically unstable state. The authors postulated that kinematic stability and dynamic stability are mutually independent and that a system can be dynamically stable while kinematically unstable and vice versa. Therefore, a subject should be able to maintain stability while moving quickly with their COG within their base of support, or while moving slowly with their COG outside their base of support. This is a feasible argument; however, the stability assessment would largely depend on the value assigned to 'critical velocity'. This parameter would vary for every person making it very difficult to calculate precisely. It would also be a source of error. The researchers also encountered problems with measuring the angle between the foot and the ground during push-off and with small inaccuracies and fluctuations in the COG trajectory. The imprecision of these parameters led to inexact assessments of the stability indices.

Kaya et al. [177] tried to correlate gait cycle time and double support time with linear and angular momentum of the human body. The researchers looked at the influence of momentum shifts on balance maintenance in a balance-impaired population (elderly and bilateral vestibular hypofunction (BVH) patients). Linear and angular momentum, cycle time, whole-body A/P COG velocity, and A/P velocity of the head/arms/trunk COG were observed using four motion analysis cameras and two force-plates. According to their study, BVH subjects walked noticeably slower than healthy subjects and, in turn, generated less linear whole-body momentum in the sagittal and vertical planes during gait. As well, the subjects inherently chose a gait pattern with a longer cycle time and spent more time in the double support phase.

Yack et al. [109] mounted an accelerometer over the spine on the upper trunk to measure peak accelerations in the A/P, M/L, and vertical directions during gait. A harmonic analysis was performed on the acceleration data for each stride. The period (fundamental frequency) for each stride was determined using foot switches. Multiples of this fundamental frequency (harmonic coefficients) were then determined using a finite Fourier series. The ratio of summed amplitudes of the acceleration data's even and odd harmonics was calculated for each stride and averaged across 10 strides to obtain an "index of smoothness". Unstable subjects showed a difference from control subjects in A/P and vertical measures; however, no between-group differences were found for the M/L data.

In a study on the dynamic stability of children with and without Down's Syndrome, Buzzi and Ulrich [159] used the Lyapunov exponent (LyE) and approximate entropy (ApEn) along with data acquired with a whole-body marker and camera-based system and a pressure-sensitive mat. Stability at the thigh, shank, and foot were evaluated as the subjects walked on a motorized treadmill at varying speeds. "The LyE is normally used to measure the rate of exponential divergence of trajectories in state space. As nearby points separate, they diverge rapidly and produce instability. The LyE was used to measure the stability of a dynamical system, such as a human during walking, and its dependence on initial conditions. [159]" The authors identified five 'embedded dimensions' (that were not specified) from the segmental angular time series of the gait data. These embedded dimensions were used to calculate the maximum LyE using a time-series-analysis program. "The ApEn was used to assess the complexity of each time series. ApEn is a 'regularity statistic' that quantifies the predictability of fluctuations in a time series. The ApEn was computed using a program written in Matlab software (Mathworks, Natick, MA). [159]"

LyE and ApEn were evaluated such that a zero or negative value for the LyE indicated a periodic system whereas a positive LyE value indicated a non-periodic, or random, system. Similarly, a lower ApEn value would indicate a lower complexity of the system. Therefore, systems that are dynamically stable would result in lower LyE and ApEn values. Data periodicity and predictability were obtained by comparing trials to each other and evaluating the differences [159]. The main drawback found with this approach was that

multiple gait cycles were required to calculate the index. If a subject were to walk on irregular terrain, slight variations in the strides would be expected which would result in higher LyE and ApEn values while the gait may not be necessarily more unstable.

One study conducted by Krebs et al. [186] looked at the foot-COP oscillation-decay rate after a postural perturbation in the A/P direction. A force plate and a force transducer were used to determine static stability of subjects with postural disorders. To administer the postural perturbation test, subjects were positioned on two force plates with their feet 30 cm apart. The subjects tried to maintain their foot positions while meeting the researcher's gentle push at the upper mid spine. When the researcher stopped pushing, the subject tried to maintain balance without moving their feet. A dynamometer synchronized with the force plates recorded the timing, shape, and magnitude of the resistance force.

The body COG was displaced slightly anterior from the neutral position. After the researcher's release ("step input" perturbation), the whole body oscillated about the natural point of equilibrium. The natural COG equilibrium was determined by estimating a horizontal asymptote of the response in Figure 2.18. The measurement of the input *f(t)* (dynamometer-input data) and the output COP (force-plate data) allowed the estimation of the system eigenvalues $(\alpha_k + i\beta_k, k = 1,...,n)$ which could be obtained using the Matlab routine Steiglitz-McBride (STMCB) method. Eigenvalues characterize the dynamic properties of the response, stability, and accuracy of a system. The rate of decay or growth of the signal is proportional to the real part of the eigenvalue, α_k. Negative values for $\alpha_k, k = 1,...,n$ indicate a decay rate while positive values for $\alpha_k, k = 1,...,n$ indicate a growth rate. Assuming a stable system (negative $\alpha_k, k = 1,...,n$ that indicate decay in postural motion), the damping characteristics of the system improves as $\alpha_k, k = 1,...,n$ increases in magnitude. Therefore, as the magnitude of $\alpha_k, k = 1,...,n$ increases, the postural motion has a higher decay rate which means stability is reached faster [186].

Krebs et al. [186] found that COP oscillation dissipation was a practical means to test postural control. The authors also compared postural stability data to gait data (stance

duration, average velocity, base of support) acquired with force plates and a motion analysis system. Gait stability measures showed close consistency with postural COP rate of decay analysis. Unfortunately, the method of observing the COP oscillation rate of decay is not feasible for dynamic gait stability.

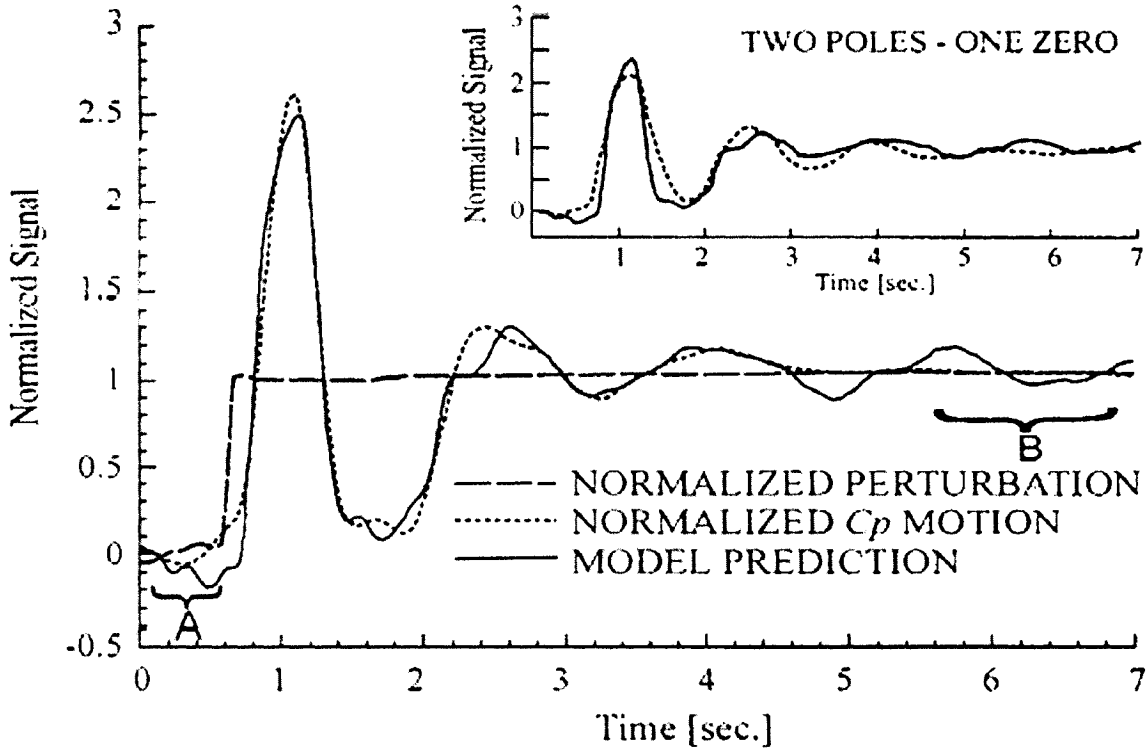

Figure 2.18: Normalized COP motion versus time, step function of the applied force, and predicted motion of the COP [186].

McGraw et al [144] studied gait and postural stability in obese and non-obese boys by comparing ground reaction force frequency information with data obtained from force plates and an optoelectronic system. A Fast Fourier Transform (FFT) was used to quantify frequency composition of the force vectors. Frequency variables included the mean, median, mode, and dispersion of the frequency data. Time in double support, stance, and swing were determined from the video system and postural data were collected from the subjects standing on a force plate. Ground reaction forces in the vertical, M/L, and A/P directions were used for the postural stability assessment. According to the COP motion and force data frequency information of the postural measurements, less stable conditions showed higher

frequency dispersion and a lower mean spectral frequency. Root mean square (RMS) of M/L and A/P COP deviations increased in unstable conditions.

Chang et al. [187] isolated the whole-body moment arm to assess dynamic balance. This moment arm is the COP-COG separation and is proportional to the COG horizontal acceleration. Thus, the moment arm was the primary variable by which horizontal COG acceleration was predicted. This method proved to be very accurate in discriminating between disabled and non-disabled older people. Unfortunately, obtaining COG information requires equipment that would limit the study to a laboratory.

2.5.3 Summary of Stability Measures

The literature provides many possible balance and stability parameters that can be taken into account when establishing a standardized stability index:

- Motion of the foot-COP and body-COG, as well as body sway during quiet standing (Section 2.5.1)
- M/L sway of the body during walking (Section 2.5.2.1)
- Abnormal movements of the COG vertical projection, COG velocity, and vertical COG oscillations (Section 2.5.2.2)
- Base of support parameters such as leading and trailing supporting edges (Section 2.5.2.2)
- Time spent in double support phase (Section 2.5.2.3) as well as stride length and stride time (Section 2.5.2.3)
- A/P COP fluctuations hindering a smooth weight transfer from heel to forefoot [17] (Section 2.5.2.4)

These parameters were all considered to be potential stability index components. The final parameters used in the index and their calculation are discussed later in Section 4.3.8.

Previous research has also considered COG velocity, COG vertical projection [141-143, 155, 177], and torque and state boundaries [135] that are derived from COG data.

However, most unstable gait indicators that cause abnormal COG motion should also be distinguishable via unstable COP behaviour.

In the majority of static and dynamic stability studies, the primary equipment requirements are force plates, markers, and cameras. Although these approaches can result in a valid stability assessment, the subject's mobility can be restricted due to equipment requirements (Figure 2.19). However, the main drawback when dealing with force plates and marker and camera-based systems is that they are typically restricted to a laboratory.

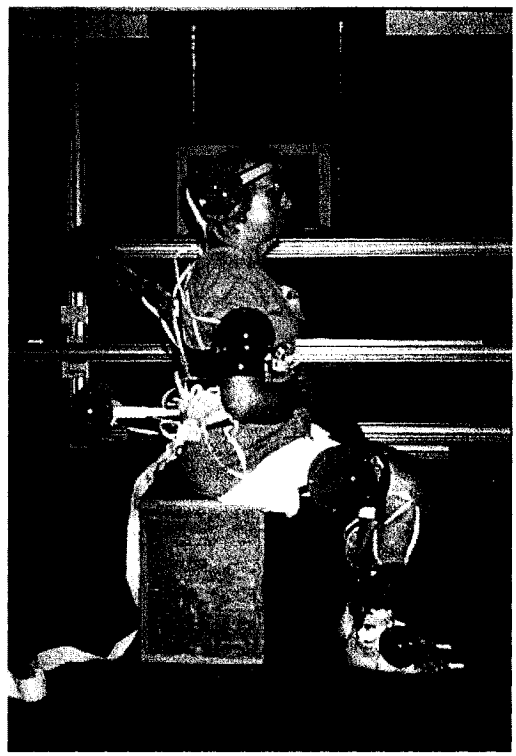

Figure 2.19: An encumbered system used to correlate quadriceps femoris muscle activity with dynamic stability [142].

2.6 Previous Attempts at Developing a Valid Stability Index

The following sections describe previous attempts at creating quantitative dynamic gait stability evaluation systems.

2.6.1 Technique using Floquet Analysis of Mathematically Simulated Instability

Scheiner et al. [188] calculated a computer simulated stability index by using Floquet analysis (explained below) on mathematically generated joint trajectory data. The level of limb motion stability was controlled with the addition of stiffness at the joints using independent linear controllers. Multiple simulations were performed in which the joint stiffness was kept constant for multiple gait cycles and the resulting motion was analyzed using the time-series data. The stability index was determined from simulation where gain at the hip, knee, and ankle joints were varied by a gain multiplier and held constant throughout the walking trial. This mathematically-based method could predict hindered motion due to certain pathologies; however, it would not account for a patient in an unpredictable environment. Since subjects would also be tested on inconsistent and uneven terrain, stride cycle perturbations would not necessarily be caused by unstable gait.

The principle behind Floquet analysis is to construct a differential equation representing a stride that would then be compared to other stride patterns. The slight variations in stride data would be the basis for the stability assessment. In the case of Scheiner's study, at least 40 gait cycles (80 steps) were needed for accurate stability estimation. However, Dingwell et al. [189] also performed a study involving a mathematical stride representation and comparison between strides. Stride-to-stride variability measurements were found to be poor local dynamic stability indicators. Dingwell tried to correlate variability in measured stride components with local dynamic stability measures and statistically significant results were obtained for only four of 24 correlations. This renders the Floquet analysis technique unreliable.

2.6.2 Technique using COG-based Stability Indices

As mentioned earlier in Section 2.5.2.2, Karcnik et al. [155] used COG-based measures to create a "relative kinematic stability index" (RKSI) for kinematic stability and an "absolute velocity index" (AVI) for dynamic stability. In another project led by Karcnik [190], the same RKSI and AVI indices were used to create a wearable/portable system for gait analysis. Their setup relied on goniometers at the hip, knee and ankle of each leg and foot switches

under the heel and toe of each foot. They compared the results of their indices to the 3D stability assessment of a motion analysis system. The main problem in calculating the AVI with goniometers and foot switches was that the head/arms/trunk COG (COG_{HAT}) had to be estimated. When small inaccuracies and fluctuations occurred in the COG_{HAT} calculation, the errors were significantly amplified by the derivative required to calculate the COG_{HAT} velocity. Inaccuracies of the COG_{HAT} velocity and other estimated parameters were the main reason for the inaccurate AVI assessment. The system also had problems during push-off, where a degree of uncertainty was introduced in the calculation of the COG position. Since the angle between the foot and the ground could not be measured, high inaccuracies resulted for RKSI and AVI during the push-off phase. The authors concluded that the correlation coefficients were much higher for the static/kinematic index RKSI than for the dynamic index AVI and that the wearable system is better suited for static/kinematic stability assessment.

2.7 Review of Fuzzy Logic Theory

Fuzzy logic controllers provide a fast and simple way to achieve a definite conclusion based on vague, ambiguous, imprecise, or noisy information [191]. The nature of fuzzy logic is to mimic a person's decision process. Fuzzy logic was initially conceived as a way to sort and manipulate data and has proven to be an excellent choice for control system applications. These controllers are very robust and forgiving of user input and often work when first implemented with little to no tuning. The steps in creating a fuzzy system are:

1. Define the objectives and criteria for the desired system.
2. Define the input and output relationships and choose a minimum number of variables for input to the fuzzy logic system.
3. Create the fuzzy logic membership functions (explained in Section 2.7.2) that define the input and output terms for use in the rule set (explained in Section 2.7.3).
4. Break the system down to a series of rules that define the desired output response for given input conditions. The number and complexity of the rules depends on the number of input parameters and the number of membership functions associated with each parameter.

5. Test the system, evaluate the results, tune the rules and membership functions, and retest until satisfactory results are obtained.

2.7.1 Example of Simple Fuzzy Logic Controller

To illustrate the utility of a fuzzy logic controller, a simple system will be described: a stability index controller based only on gait speed. For faster gait speeds, the index should indicate higher stability. For slower speeds, the index should indicate lower stability. A typical fuzzy logic controller for this situation would monitor the gait speed and adjust the index accordingly.

First, membership functions are established for the only input variable: gait speed. Initial assignment of the number and arrangement of the membership functions is partly arbitrary because these functions can be tuned later. Figure 2.20 shows the initial setup of the three membership functions: 'Poor, 'Medium', and 'Good' that refer to output stability. The function ranges are assigned intuitively but can be easily adjusted later:

- Poor stability for speeds up to 1.5 m/s
- Medium stability for speeds between 1 m/s and 2 m/s
- Good stability for speeds from 1.5 m/s and up

Once the initial conditions are set, the output condition is configured. In this case, the output is the stability index value. Similar to the membership functions, the rule set can be fine-tuned later. The basic rule set for this controller would be the following:

- If gait speed intersects the 'Poor' function, output = 0.1 stability
- If gait speed intersects the 'Medium' function, output = 0.5 stability
- If gait speed intersects the 'Good' function, output = 1.0 stability

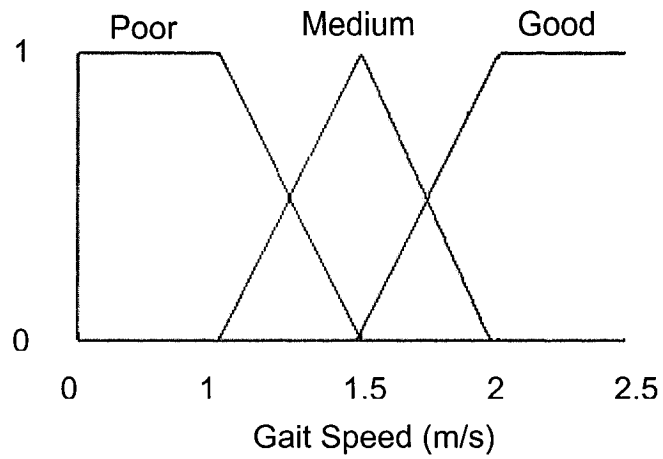

Figure 2.20: Membership functions for single input stability index controller.

After the membership functions and rule set have been configured, the fuzzy logic controller is prepared to accept inputs. Based on a gait speed input, the system will return an appropriate stability value based on the initial conditions. For example, if the gait speed were 1.4 m/s, the input value would intercept both the poor and medium functions (Figure 2.21).

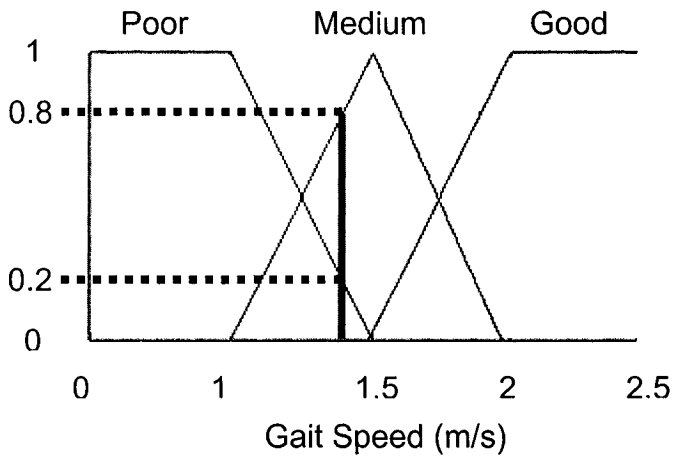

Figure 2.21: Gait speed input for a simple stability index fuzzy logic controller.

According to the rule set, the 'Poor' function leads to an output of 0.1 and the 'Medium' function leads to an output of 0.5. The degree of membership of an input is determined by projecting the input value vertically to the membership functions. In this case, the input speed of 1.4 m/s has a degree of membership with the 'Poor' and 'Medium' functions. The output stability index value can then be calculated (Equation 2.3).

$$\begin{aligned}(m1_{magnitude} \times m1_{membership}) + (m2_{magnitude} \times m2_{membership}) &= output \\ (0.1 \times 0.2) + (0.5 \times 0.8) &= 0.42\end{aligned} \quad \textbf{(2.3)}$$

Equation 2.3 shows the defuzzification calculation of the stability index output. In this equation, *m1* refers to the 'Poor' function where $m1_{magnitude}$ is 1% stability and $m1_{membership}$ is the degree of membership to the 'Poor' function. Similarly, *m2* refers to the corresponding values of the 'Medium' function.

Therefore, for an input gait speed of 1.4 m/s, the fuzzy logic controller would deem the stability as 0.42. This output value can also be adjusted by changing the association between the membership functions and input values or by adjusting the rule set. This is a simplified example and does not apply any defuzzification method described in Section 2.7.4 because only one input variable was used.

2.7.2 Membership Functions

A series of membership functions are created for each input parameter. Membership functions of varying shapes can range from Gaussian curves to single vertical lines, depending on the desired system. Triangular membership functions (Figure 2.22) are typically used for simplicity.

Each input parameter is mapped to membership functions that are created by the user. By convention, the input value is on the horizontal axis while degree of membership is on the vertical axis (Figure 2.22). A degree of membership is determined by selecting an input value and projecting vertically to the membership functions. Depending on the membership function layout, each input may project to more than one function. Similarly, membership functions are also created for the output value and are used for defuzzification (Section 2.7.4).

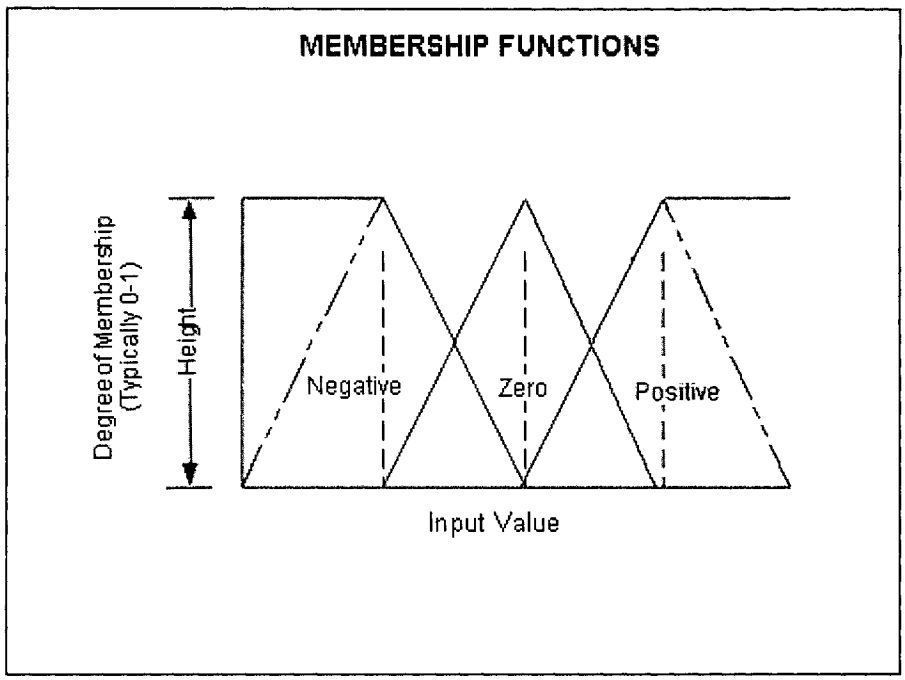

Figure 2.22: A set of generic triangular membership functions [modified from 191].

2.7.3 Fuzzy Rules

The user also creates a set of fuzzy rules that correlate input and output values. As mentioned in Section 2.7.2, one input may have a degree of membership mapped to more than one membership function. Therefore, a fuzzy rule set must consider every combination of membership functions between all input variables. For example, if there are four inputs with three membership functions each, then the rule set must take into account the $3^4 = 81$ possible combinations. Rule set complexity is a direct result of the number of inputs and the total number of membership functions.

The format of each rule is "if X and Y then Z", where X and Y are input conditions and Z is an output condition. This is known as the 'AND' method. The 'OR' method is also commonly used (i.e., "if X or Y then Z"). Selection of either combination method is based on the logical interaction between the variables. The AND method is chosen for unrelated input variables, while the OR method can be used for variables that are related in regards to the output of the system.

2.7.4 Methods of Defuzzification

Once degrees of membership have been assigned to each input, the input values must be combined to obtain a crisp output. This is known as the defuzzification process. Since each input may have a degree of membership to more than one function, there may be a few rules from the rule set that apply to the particular configuration of input values. In Figure 2.23, the rule set uses the 'OR' method and there are three membership functions for each input and output variable. This example also employs the Last of Maximum (LOM) method of defuzzification by obtaining the maximum value of the inputs for each rule and creating a geometric shape by cutting the appropriate output membership function at that height. The shapes created by each rule are combined to form an aggregate shape. Other methods of defuzzification include [191]:

- RCOM (random choice of maximum)
- FOM (first of maximum)
- MOM (middle of maximum)
- COG (center of gravity)
- MeOM (mean of maximum)
- BADD (basic defuzzification distributions)
- GLSD (generalized level set defuzzification)
- ICOG (indexed center of gravity)
- SLIDE (semi-linear defuzzification)
- FM (fuzzy mean)
- WFM (weighted fuzzy mean)
- QM (quality method)
- EQM (extended quality method)
- COA (center of area)
- ECOA (extended center of area)
- CDD (constraint decision defuzzification)
- FCD (fuzzy clustering defuzzification)
- CA (Centroid Average)
- MCA (Maximum Center Average)

The CA and MCA defuzzification techniques are continuous methods and are frequently used in control engineering and process modeling. The RCOM, FOM, MOM, COG, MeOM, BADD, GLSD, ICOG, SLIDE, FM, WFM, QM, EQM, COA, ECOA, CDD, and FCD methods represent discontinuous techniques that are mainly used in decision making and pattern recognition applications [191]. Leekwijck and Kerre [192] also claim

that the maxima methods (RCOM, FOM, MOM, and MeOM) behave well with respect to the more basic defuzzification criteria, and hence are good candidates for fuzzy reasoning systems. The CA method was chosen for the dynamic stability index fuzzy logic controller because of its reported effectiveness for fuzzy reasoning systems and ease of application to the dynamic stability index system [192]. As compared with MCA, CA takes the aggregate shape of all output functions into account while MCA only takes the centre value of the maximum output function. While this makes MCA faster to calculate, CA may provide a more representative result by not eliminating potentially relevant output functions.

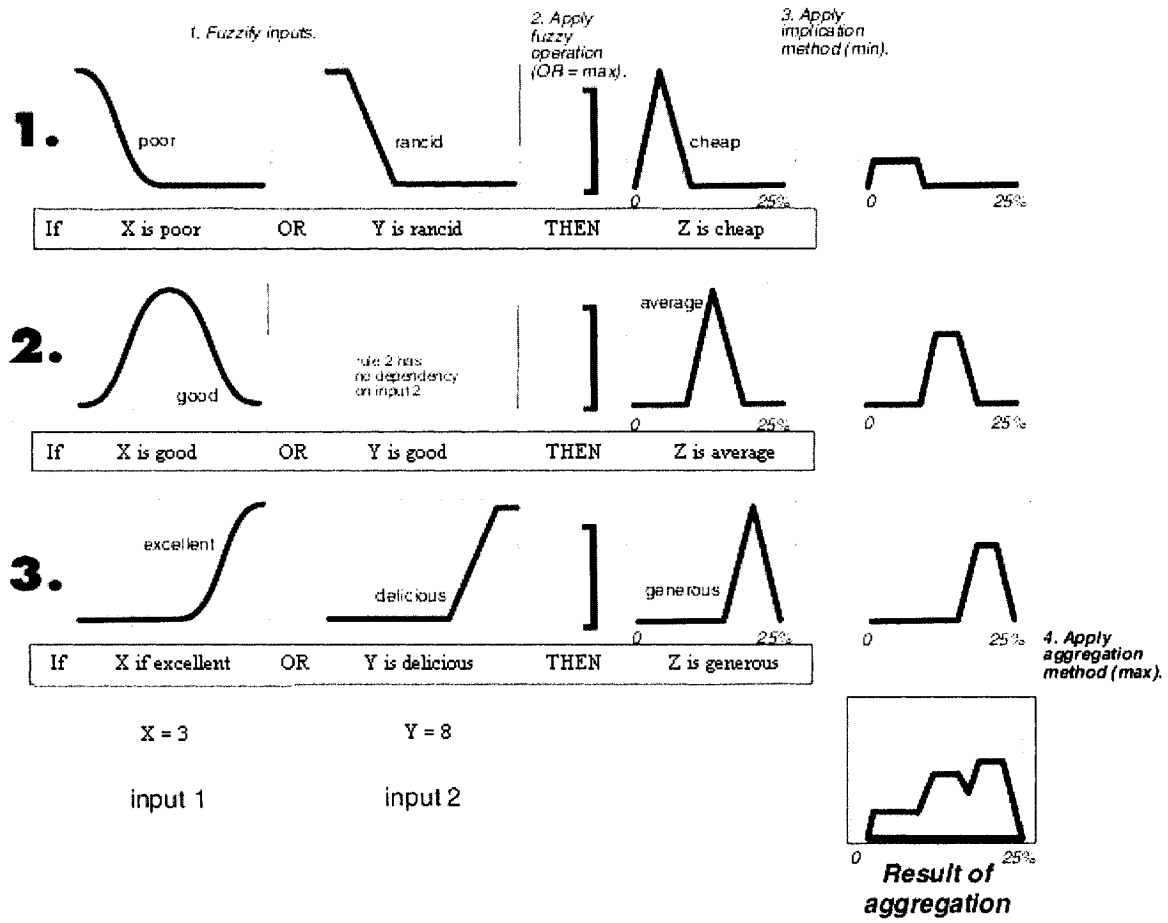

Figure 2.23: Defuzzification example [modified from 193]. After the rules have all been evaluated, an aggregate shape is created.

For the CA method, the centroid of the resultant shape is calculated and the horizontal position of the centroid indicates the crisp output of the fuzzy logic system (Figure 2.24).

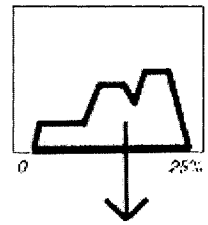

Figure 2.24: Finding the exact horizontal position of the centroid of the aggregated shape yields a crisp output for the fuzzy logic controller [modified from 193].

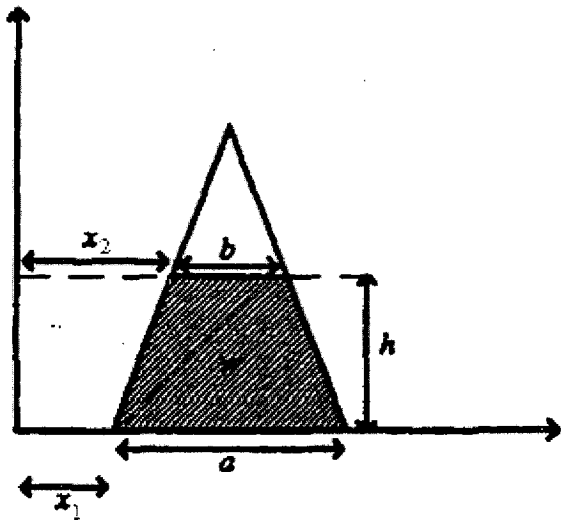

Figure 2.25: A simple output membership function to illustrate the mathematics involved in the centroid method of defuzzification.

Figure 2.25 shows an arbitrary example of an output membership function. To evaluate the mathematical steps involved in taking the centroid in the defuzzification step, two lines must be mathematically defined that go through the corners of *w* and intersect inside the shape (Figure 2.26).

For y_1, the two points on the line are (x_2, h) and $(a+x_1, 0)$:

First, the slope of the line must be defined:

$$m = \frac{0-h}{a+x_1-x_2} = \frac{-h}{a+x_1-x_2}$$

Next, the slope is inserted into the equation of a line:

$$y_1 = mx + b = \frac{-h}{a + x_1 - x_2} x + b$$

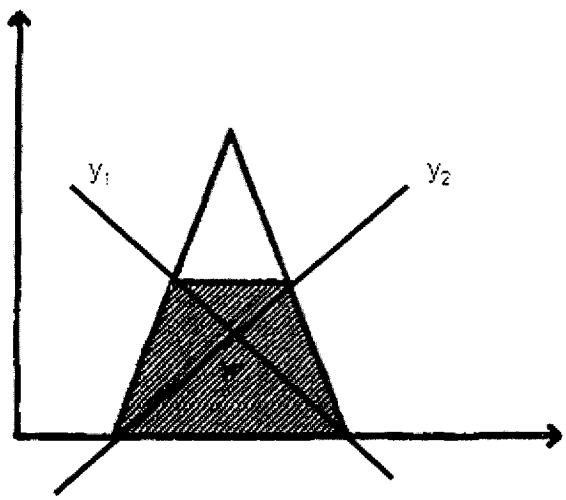

Figure 2.26: To determine the centroid of a shape, two lines must be mathematically defined that go through the corners of the shape and intersect inside.

Then, a point on the line (i.e., (x_2, h)) is used to find the y-intercept, b:

$$h = \frac{-h}{a + x_1 - x_2} x_2 + b$$

$$b = h + \frac{hx_2}{a + x_1 - x_2} = \frac{ha + hx_1}{a + x_1 - x_2}$$

Finally, the equation of y_1 defined as:

$$y_1 = \frac{-h}{a + x_1 - x_2} x + \frac{ha + hx_1}{a + x_1 - x_2}$$

The same manipulation is done with y_2 to arrive at:

$$y_2 = \frac{h}{b + x_2 - x_1} x + \frac{-hx_1}{b + x_2 - x_1}$$

To find the horizontal position of the intersection point, a common x-value can be found by equating the two lines:

$$y_1 = y_2$$

$$\frac{-h}{a+x_1-x_2}x+\frac{ha+hx_1}{a+x_1-x_2}=\frac{h}{b+x_2-x_1}x+\frac{-hx_1}{b+x_2-x_1}$$

$$x\left[\frac{h}{b+x_2-x_1}+\frac{h}{a+x_1-x_2}\right]=\frac{ha+hx_1}{a+x_1-x_2}+\frac{hx_1}{b+x_2-x_1}$$

$$x\left[\frac{ha+hb}{(b+x_2-x_1)(a+x_1-x_2)}\right]=\frac{hab+hax_2+hbx_1}{(a+x_1-x_2)(b+x_2-x_1)}$$

$$x=\frac{hab+hax_2+hbx_1}{ha+hb}$$

Therefore, it is possible to obtain the exact output value of the fuzzy logic controller by manually calculating the horizontal position of the centroid. However, this step is automated when using the Fuzzy Logic Toolbox of Matlab (Section 4.4). The Matlab fuzzy logic controller operates like a black box such that the internal operations are typically hidden from view. The user must adequately describe the inputs and outputs but does not need to define specific equations to this depth.

Chapter 3. Rationale

Stability during locomotion, or dynamic stability, is critical to ensure general safety and a high quality of life. Trans-tibial or trans-femoral amputees, stroke victims, Parkinson's patients, people with traumatic brain injuries, and the elderly population are groups that have chronic balance problems. People who are unstable during locomotion could require physical therapy, pharmaceutical interventions, or ambulatory aids to reduce the risk of falls [195]. Stability evaluation is a crucial step in rehabilitation to evaluate progress and to ensure that correct procedures are being administered [72].

In studies involving stability measurement, gait stability examination tends to be either a clinical observational test or an investigation of kinetic or kinematic gait components measured by force plates or marker and camera-based systems that confine data collection to a laboratory setting. More importantly, stability analysis is ultimately reduced to a subjective evaluation. A dependence on interpretation or reaction time of the assessor is associated with an observational test score or in assessing a qualitative stability parameter. Currently, a validated tool that produces an index of dynamic gait stability does not exist. By establishing a standardized scale, each stability measure would be objective, quantitative, and reliable. Furthermore, by using a portable system, gait stability could be measured in outside environments and would not be confined to a laboratory.

In a clinical setting, observational gait assessment measures are still most frequently used, even though these measures often depend on either the scoring of an evaluator or the reaction time of an assessor when timing the subject on an activity. A common gait stability evaluation technique in research combines force plates (Section 2.4.1) and a camera/marker-based system (Section 2.4.2). Although some stability parameters from these systems may be used in the new stability index, the data acquisition methods themselves are not feasible for a portable system. Accelerometers (Section 2.4.3) were also not included in the present study as they require time to be secured to the subject and to be calibrated. If necessary, accelerometers could be added in the future; however, successful stability index implementation with only one measuring device would create a more efficient system.

A fuzzy logic controller was chosen as the method of combining stability parameters. Fuzzy logic is a fast technique of obtaining a crisp output given precise inputs without requiring any defined transfer functions between the quantities. An artificial neural network (ANN) was another option for the parameter combination task but was not chosen because of its dependence on training data that are not available since there is no gold standard when measuring stability. The rationale for choosing a fuzzy logic controller for this project is detailed in Section 4.4.

3.1 Limitations of Current Gait Stability Measurement Methods and Equipment

Many different methods have been used to assess gait stability. Section 2.5.2.2 describes some previous research that considered COG velocity, COG vertical projection and torque and state boundaries that are all derived from COG data. Unfortunately, total body COG-based information cannot be obtained with a portable system. Therefore, stability parameters from COG were omitted from the current study to minimize equipment requirements and to allow for data collection outside of a laboratory. However, most unstable gait indicators that cause abnormal COG motion should also be distinguishable via unstable COP behaviour that can be observed with a portable pressure measurement system. As a result, this research focuses on the motion of foot-COP.

A number of foot pressure measurement systems are described in Section 2.4.4. The Parotec System (Section 2.4.4.1) and the Pedar-X System (Section 2.4.4.2) can both be made portable but they have a low resolution. Although most optical methods (Section 2.4.4.4) tend to have high spatial resolution and work well for dynamic gait evaluation, they are not portable and would also not be feasible for this study. However, the F-Scan system can be made portable, has a high spatial resolution, and has proven to be a reliable method for dynamic gait analysis.

Although the literature shows that F-Scan has difficulty measuring the exact applied pressure on the sensors when shear forces are involved (Section 2.4.4.7), the stability index would only require a relative pressure distribution as input data. The position and motion of

the COP would be more important than exact pressure values at each cell. Therefore, shear error in the first and last segment of the gait pattern would not be an issue [112]. Therefore, the F-Scan in-shoe pressure measurement system was used for establishing a dynamic stability index of human gait in this research.

Currently, the most common methods of gait analysis in a clinical setting are observational measures. As mentioned above, these can be inexact and rely heavily on interpretation or reaction time of the evaluator. Force plates and camera/marker-based systems are also used for research purposes but also have shortcomings addressed in Section 2.4.5. F-Scan is a portable and accurate system that can obtain foot pressure with a high spatial range. This plantar pressure data can be processed to create a quantitative index of gait stability that could be used for objective gait stability assessment and comparison in clinical and research settings.

3.2 Applications of a Portable Dynamic Gait-Stability Index System

Many people could benefit from knowing their stability level in a non-laboratory environment. People with physical disabilities, patients recovering from surgery or an accident, people working on unstable platforms/boats, and competitive athletes would all benefit from accurate stability measurement in a real-world environment. In a laboratory, recreating uneven terrain is difficult; therefore, assessing dynamic stability with a portable system would be advantageous. In fact, bringing recovering patients outside to evaluate their stability in irregular conditions is common practice during the rehabilitation process. Standard clinical tests exist for simple measurements of balance (Section 2.3); however, these measures cannot provide a quantitative means of comparing dynamic stability between various environments [6].

A dynamic gait stability system could help when fitting patients with a new orthosis or prosthesis and would allow for comparisons between different devices and treatment methods. Clinicians would also be able to assess different alignments or fitting of devices and the impact they have on the patient's stability level.

A stability index could be used to determine the level of recovery as well as help to improve existing performance levels. For athletes that excel at a certain level of instability, such as a discus thrower, an instability threshold could be identified beyond which their athletic performance decreases. By analyzing an athlete's performance and seeing where minor improvements could be made, slight alterations in their training style or even customized footwear may be implemented to increase their capabilities.

Footwear is another area where this type of system may be applicable. By locating periods of gait instability, footwear could be redesigned to improve stability during specific activities. A portable stability analysis system could work on running tracks, skating rinks, or even on ski slopes. The resulting analyses could lead to comfortable customized footwear for a vast array of activities and footwear that increases athletic performance. As well, evaluation of stability on various surfaces could lead to influencing the design of playing surfaces in sports, and floor surfaces in the home and office.

A stability index can also be used when evaluating potentially dangerous activities. Walking on trails and playing certain sports may result in injury for elderly or visually impaired people. Having a stability index associated with these activities could greatly assist in activity planning (i.e., providing better instructions to the patient or changing assistive devices).

Another projected application of this type of system would be to observe gait stability of a person on certain medications to gauge how the medication affects balance. Stability analysis can also lead to a minimum balance measure for activities like driving, where a quick stability measurement could show if a driver is significantly impaired. Although alcohol can be immediately detected with a breathalyser, there is no definite way to quickly assess impairment from other substances like drugs or medication.

It is important to note that potential applications of the stability index that extend outside the scope of level ground walking would only be possible after extensive development and testing to properly correlate stability measures with performance within that specific environment or activity.

3.3 Thesis Objectives

The goal of this research was to develop and clinically validate a quantitative dynamic stability index for human locomotion. The tool had to be easily applied within a research and clinical setting and portable for use on uneven terrain, indoors/outdoors, stairs, and ramps.

The objectives of the research were the following:

1. Obtain valid foot pressure data of human gait with a portable data acquisition system.
2. Properly filter the data to adequately suppress any spike-valued noise that do not represent the applied load of the foot.
3. Divide the data into strides for analysis.
4. Extract the gait stability parameters (Section 4.3) from each stride of the foot pressure data.
5. Develop a fuzzy logic controller to properly combine the stability parameters and produce a single stability index value that reflects the stability of each gait pattern.
6. Validate the stability index in a clinical setting.
    - Simulate four levels of stability and evaluate each level with the developed stability index system.
    - Assess the ability of the stability index to differentiate between induced stability levels.
7. Analyze the results with all stability parameter combinations to determine what stability parameter combination creates the most effective dynamic stability index.

Chapter 4. Methods

To establish a valid stability index system, the requirements, capabilities and limitations of the system had to be determined in regards to equipment and software. This chapter describes the design criteria and necessary equipment for the system. The following sections also review all the raw data manipulation steps involved in obtaining viable stability parameters and the development of a fuzzy logic controller used to arrive at a final stability index. Clinical testing for validation and fine-tuning of the fuzzy logic controller is described in Chapter 5.

4.1 Design Criteria

The proposed stability measurement system should be portable, easy to use, and produce a measure of stability within approximately 20 minutes of collecting a foot pressure trial. The index should assess dynamic stability of forward-progressing gait according to the following criteria:

- Measurement device
  - Does not interfere with gait
  - Measures the stability parameters used to calculate the index
  - Is portable such that it can be used indoors, outdoors, on rough and contoured terrain, and on stairs and ramps
  - Is easy to apply and operate in a clinical and research environment
  - Collects the necessary data within 20 minutes
  - Produces a stability index within 5 minutes of collecting foot pressure data
  - Provides accurate quantitative data
  - Is the only device required to provide all index components
- Index calculation and analysis
  - Combines measurements of stability parameters into a single index value ranging from 0 (good stability) to 1 (poor stability)
  - Directly imports measurement data
  - Automates data analysis and index calculation (i.e., additional user intervention not required)
  - Is easy and efficient to operate

4.2 Equipment

The main equipment used for calculating the dynamic stability index includes the F-Scan Pressure Measurement System including two insoles and a data-logging pack, Microsoft Visual Basic 6.0 (VB6), and Matlab. Memory foam was used to artificially induce instability during clinical testing as part of this research; however, it would not be used for assessing subjects once the system is developed. The foam pieces consisted of 2.5 cm thick medium memory foam adhered on top of 2.5 cm hard memory foam.

4.2.1 F-Scan

The dynamic gait stability index was based on foot pressure data obtained with the F-Scan Pressure Measurement System. F-Scan (Section 2.4.4.7) has sufficient accuracy and reliability to supply the required input data for the dynamic gait stability index model.

The F-Scan raw data file contains a large array of pressure values. A *cell* refers to a single pressure-sensing element. A *frame* is a snapshot of all pressure-sensing elements at one instant in time. One frame of raw data consists of 60 x 21 = 1260 cells. A typical data acquisition trial has approximately 1000 frames of data.

F-Scan stores the pressure value at each cell in N/m^2 and internally calculates the COF per frame. Figure 4.1 shows one frame of raw F-Scan data.

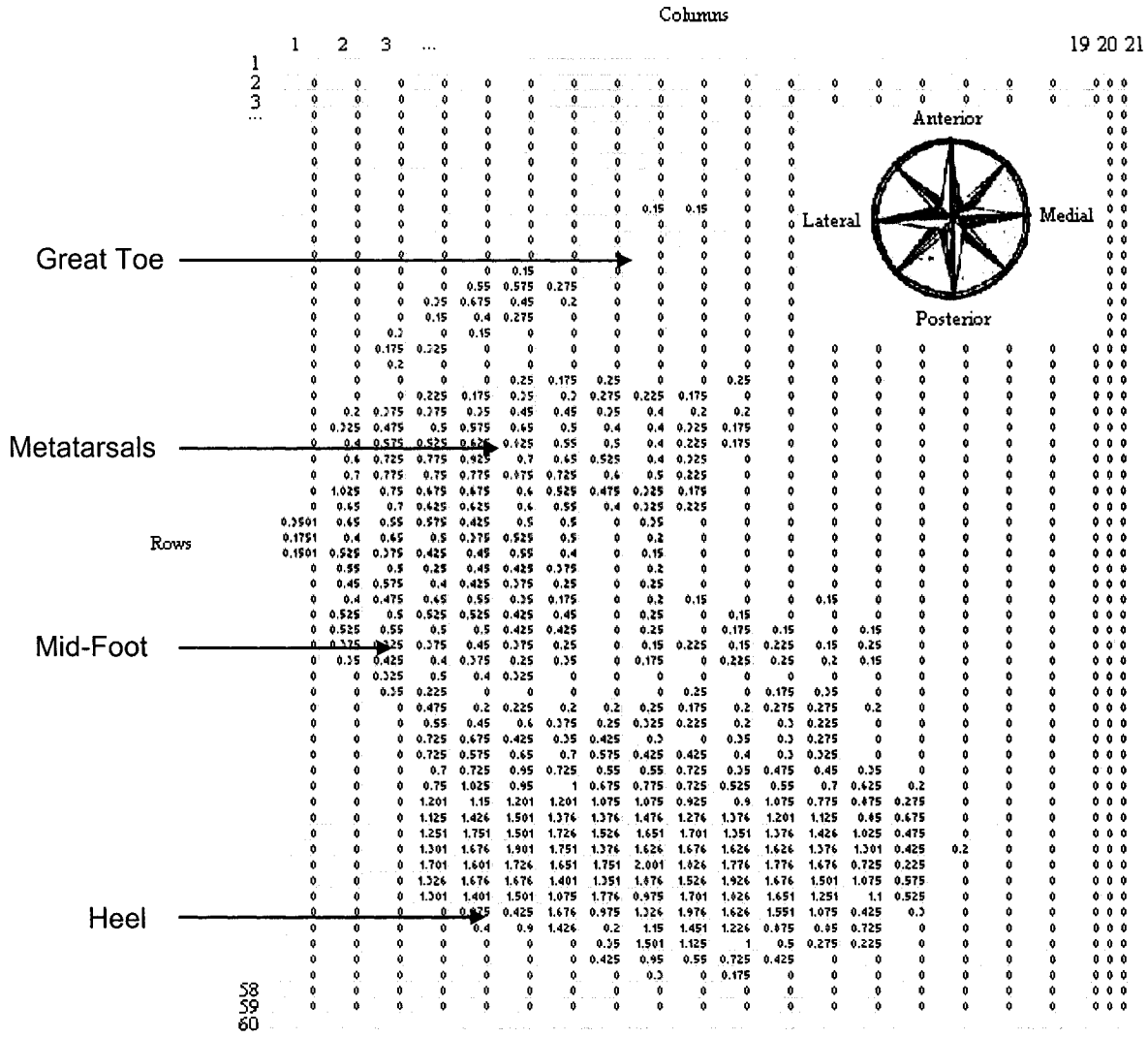

Figure 4.1: One frame of raw F-Scan data showing the instant between foot-strike and mid-stance of the left foot. This image displays the pressure on the toes at the top of the image and on the heel at the bottom of the image. Each cell indicates a pressure reading by a sensing element given in N/m^2.

4.2.2 Index Calculation

Two approaches were investigated for stability parameter calculations: Visual Basic for Applications (VBA) with Microsoft Excel and Visual Basic 6 (VB6). The stability parameter extraction code was initially written in VBA but was later transferred to VB6 to increase efficiency. Excel with VBA enables Visual Basic code to be written using Excel spreadsheet application functions; however, Excel's computational overhead resulted in an excessive index computation time of approximately 40 minutes per data run. Implementation of the

index calculations in VB6 produced an improvement in processing time by a factor of 60. With VB6, the processing time from the F-Scan raw data to the outputted stability parameters is approximately 40 seconds.

A Matlab fuzzy logic controller was used to combine the parameters from VB6 into the stability index value. As explained in Section 2.7, fuzzy logic is a technique to combine quantities without knowing exact transfer functions between the inputs and outputs. This approach is ideal since stability itself is an inexact quantity and it is not currently defined as any specific combination of stability parameters. A fuzzy logic controller would allow for the future fine-tuning of the parameter combination approach to ensure the best response of the index. The full design and operation of fuzzy logic controllers is explained in Section 4.4.

4.3 Stability Index Parameter Measurement

Stability parameters were obtained from the F-Scan system raw data and COF data. The following sections describe some preliminary tests with the F-Scan raw data and also details each stability parameter used in the final stability index.

A preliminary F-Scan data set was created by capturing 5 trials during normal walking and 5 trials with the subjects purposefully creating A/P and M/L deviations. Test data was collected from two subjects. The experimental equipment settings were the same as with the clinical testing (Section 5.2.2). Data from these trials were used in evaluating the preliminary tests discussed in this section.

4.3.1 F-Scan Data File Processing

F-Scan raw pressure and COF values for the entire trial were exported as text files. These data were imported by a VB6 program for analysis and manipulation.

The position on the foot and value of the maximum force (MF) can be extracted by separating the data by frame and searching for the maximum value. This is done with a search algorithm that locates and records the position and value of the cell with the maximum registered pressure within each frame. With F-Scan, since force is proportional to

pressure (by the area of one sensing cell), the maximum pressure position would indicate the maximum force position. In Equation 4.1, force F is proportional to pressure P by a factor of β which is the area of one sensing cell on an F-Scan pressure sensor.

$$F = \beta P \qquad \textbf{(4.1)}$$

The COF data file is a series of COF values and positions for each frame. The difference between the MF and the COF is that the MF is the single cell with the highest pressure value while the COF is the weighted centroid of all the pressure values over the entire foot. The two values both contribute valuable stability information for each stride.

4.3.2 Preliminary Experiments

Once the raw F-Scan data was obtained from the system, the data needed extensive processing to obtain legitimate stability parameters. This section outlines some of the preliminary experiments and processing attempts that were done in an effort to obtain gait stability parameters that could be used for the index. Some methods described in this section attempt to eliminate electronic noise from the F-Scan sensor. This noise consists of discrete spikes, lasting for one or two frames, that register high pressure values at single cells on the sensor. The anatomy of the human foot cannot produce such high pressures in one F-Scan cell without activating neighbouring cells. These spikes should be eliminated prior to obtaining the stability parameters.

4.3.2.1 Data Filtering

One problem with obtaining the maximum force position is that erroneously high-valued data cells could easily be misinterpreted as the maximum force. A single cell can spike to a high value that does not represent the applied load. Sometimes one or more cells on the sensor will also remain active throughout a data acquisition trial which would typically be due to a small crumple in the sensor. When this occurs, the registered pressure by the sensor is much higher than a typical plantar-pressure reading. As well, if the values from two cells are equal, the cell with the higher surrounding values must be identified. A data filter must be applied to correct for this noise.

A low-pass averaging filter can be easily applied in two dimensions and was chosen as one of the filtering methods [120]. The mask shown in Figure 4.2b is applied to the original data (Figure 4.2a) to modify the central cell, as shown in Figure 4.2c. The mask is moved over the entire array of cells to modify all cells of the array except those on the border of the array, and thus generate a new filtered data set. A nine-cell averaging filter results in much smoother data with the high frequencies greatly reduced. To reduce the calculation time, a five-cell average, that omits the corner values, could be used to obtain a new filtering mask (Figure 4.3).

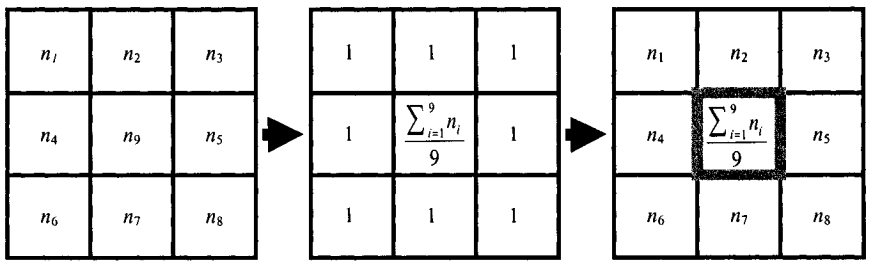

Figure 4.2: Nine-cell filtering algorithm applies a filter mask to the original data values to create a new central cell value: (a) original data (b) filter mask (c) resulting modified central cell. The mask is moved over the entire array of cells to modify all cells of the array except those on the border of the array.

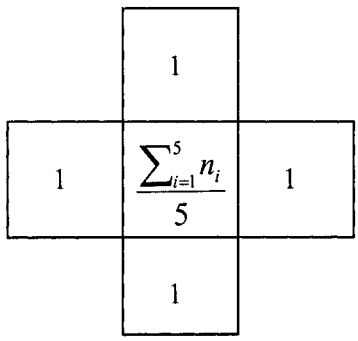

Figure 4.3: Five-cell filtering mask used in an attempt to eliminate high frequency noise from the raw data with a reduced computation time from the nine-cell filtering mask.

Figure 4.4 shows the two filtering methods applied to a sample of F-Scan MF data. According to the graph, the nine-cell averaging filter is much more effective in reducing the high frequency fluctuations in the data, as expected.

A nine-cell median filter, that uses the median of the center cell and eight neighbours, was also considered as a method of modifying the central cell value (Figure 4.5). Median filtering is commonly used in image processing for removal of strong spike-like isolated noise [196].

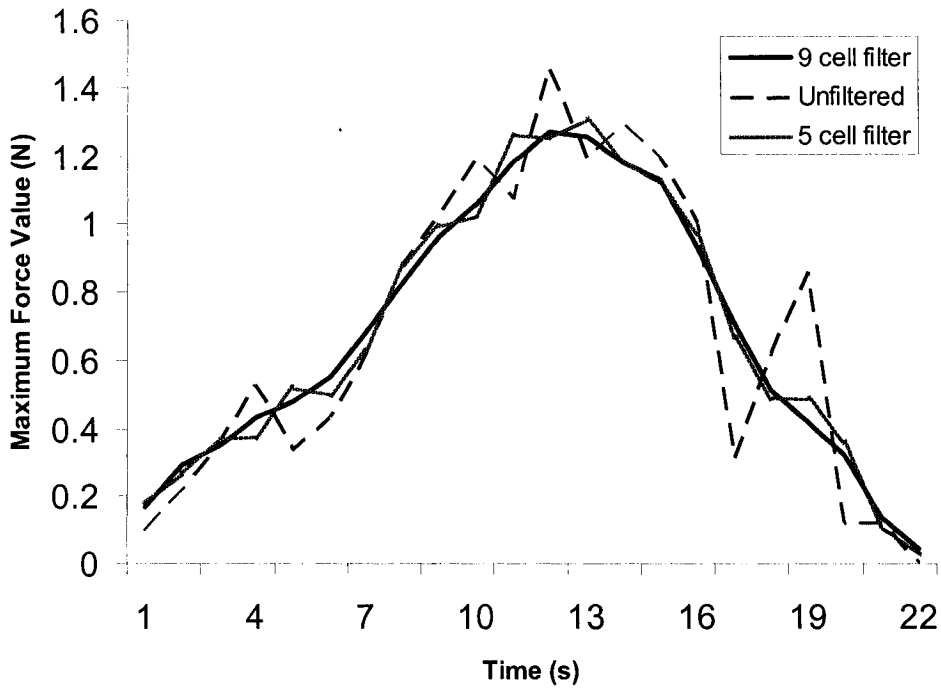

Figure 4.4: Graph comparing MF data obtained with a nine-cell averaging filter, a five-cell averaging filter, and unfiltered data. The intermittent spikes from the unfiltered data are visibly reduced when a nine-cell averaging filter is applied.

The median filter was the better choice for filtering the data because, instead of averaging in the spike-valued error, it completely eliminated the error value when determining the new central cell value. A full data analysis was done to show that the nine-cell median filter was the most effective filtering technique for this application (Section 6.1.1). Based on that analysis, all raw F-Scan data were run through the nine-cell median filter prior to processing.

1	1	1
1	*median* $\{n_1, n_2, \ldots, n_9\}$	1
1	1	1

Figure 4.5: Mask used to apply a median filter to the raw data.

4.3.2.2 Thresholding

Further processing on the filtered data involved thresholding. When the subject's foot is not in contact with the ground, cells may still record pressure values. These readings do not reflect gait stability and mostly occur during foot-strike and push-off, making it difficult to distinguish between strides. A threshold setting in the F-Scan software can eliminate these values before exporting the raw data; however, the internal F-Scan threshold has some limitations. The threshold resolution is not always effective and the threshold will sometimes remove important data or allow too much noise. The F-Scan threshold can be set between 3 and 20 raw units to filter out low-level pressure readings in the sensor areas that are not loaded [197].

To account for the shortcomings of the F-Scan threshold, an additional threshold was implemented in the MF calculation. While calculating the MF for each frame of pressure data, the MF would be assigned a value of zero if below a specified minimum value. The threshold for each trial was determined by slowly incrementing the threshold until strides could be distinguished. MF thresholding results in a filtered data set with distinct strides, a critical step in determining a dynamic stability index.

4.3.2.3 COF Inflection Points

Gait instability could be described as any unnecessary fluctuations in the COF progression. If the COF has an unreasonably high frequency in the A/P or M/L directions, the system should detect this as instability. Concavity shifts in a curve are inflection points where the second

derivative of the curve has a zero crossing and the original data curve switches from concave up to concave down or vice versa (Figure 4.6). According to Figure 2.3, only one concavity shift should occur in the COF path in the stance-phase of healthy gait. It should be noted that Figure 2.3 is not a displacement-time graph, but the general shape would be the same if the horizontal axis were time instead of anterior displacement of the COP on the foot. Additional concavity shifts would indicate extra shifts in location of the subject's weight during stance-phase that would be a sign of instability. Therefore, the number of concavity shifts in the COF position data could be a measure of instability.

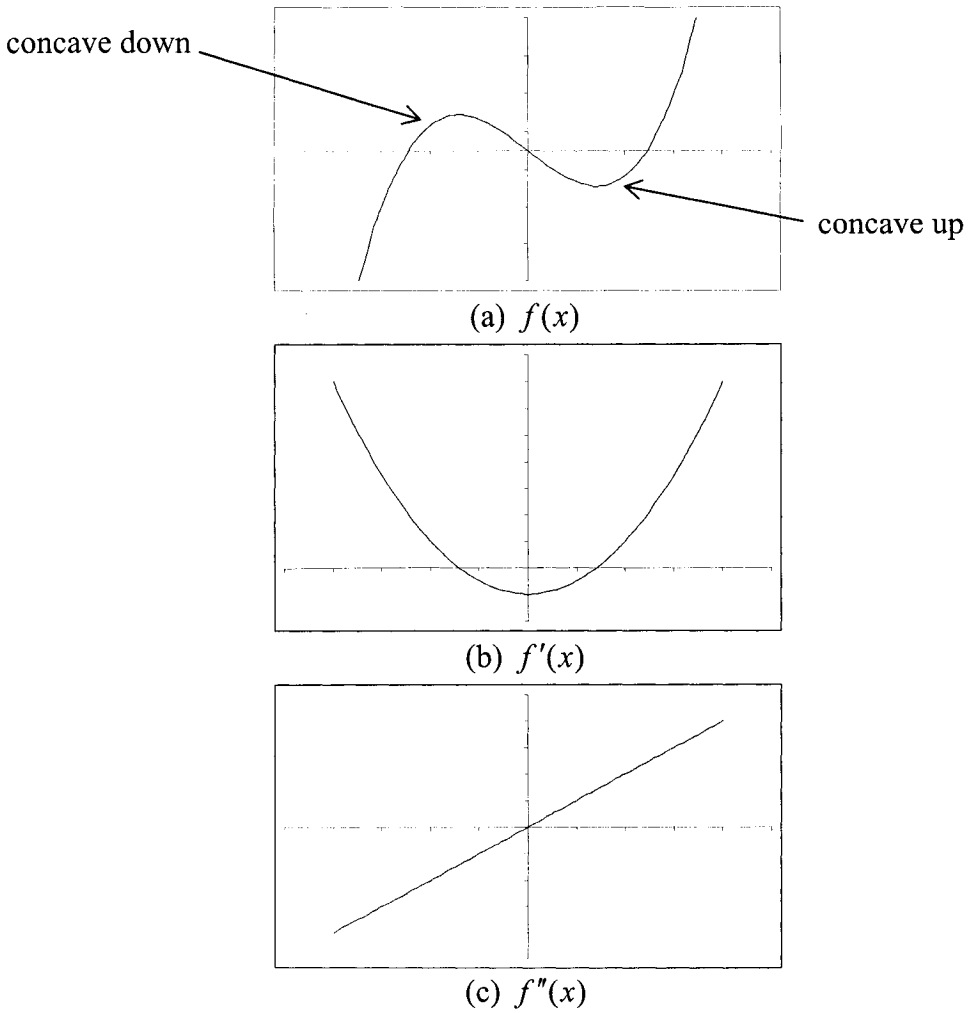

Figure 4.6: An example of a concavity shift and its effect on the first and second derivative: (a) original data (b) first derivative (c) second derivative.

When the second derivative of a curve is zero, an inflection point may be identified without a change in the sign of the first derivative (Figure 4.7). The curve changes from concave down increasing to concave up increasing. This type of inflection point in the raw data can show a point when the COF velocity increased or decreased in magnitude which would indicate points where the subject switched from accelerating to decelerating or vice versa. A high number of inflection points in the COF data would show that the subject repeatedly adjusted their velocity in either the M/L or A/P directions, and this would be considered instability. Therefore, the number of zero crossings of the second derivative should be a good measure of gait stability. The number of inflection points would indicate how often the subject shifted their weight and adjusted their speed during stance-phase.

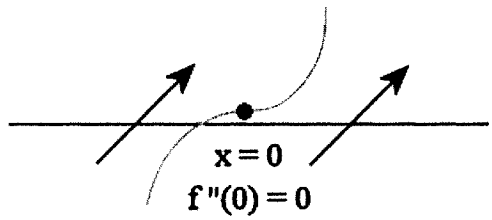

Figure 4.7: An example of an inflection point where the second derivative of the curve is equal to zero yet there is no change in the sign of the first derivative. The curve goes from concave down increasing to concave up increasing.

Figure 4.8 shows that a gradual curve in the data would have a first derivative with a low slope and therefore a low value for the second derivative. Subsequently, a sharper curve would have a high first derivative slope and a high value for a second derivative. Higher second derivative values could represent outliers or artefacts in the data that would have to be removed to analyze the remaining valid stability information.

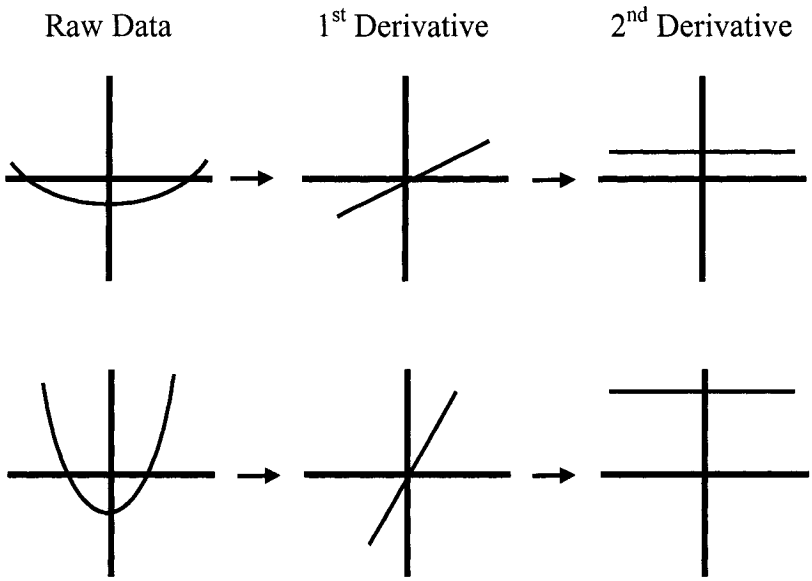

Figure 4.8: Derivatives of different types of curves in raw data; the second derivative value is higher with a sharper curve.

To test this method, test trials of stable gait and unstable gait were processed. Unfortunately, the COF data output by F-Scan was not sufficiently smooth to be processed with the second derivative analysis technique. The second derivative values fluctuated too much to reveal the desired behaviour in the COF position graph (Figure 4.9). The number of second derivative zero crossings for the unstable and stable stride were very similar and could not be adequately differentiated.

When implementing a second derivative-based algorithm, the objectives are to first differentiate instability peaks from noise in the data and then analyze the valid stability data. Therefore, the procedure must be able to first locate the valid stability information. It is assumed that some high frequencies in the data would be too fast to be caused by a human subject and these would have to be eliminated. An effort was made to appropriately filter the high values of second derivative data from test trials; however the technique was too sensitive to noise and the stability data could not be isolated. As a result, F-Scan data concavity shift analysis was abandoned. Another data analysis option was to examine the first derivative of the data which is explored in Sections 4.3.3 and 4.3.4.

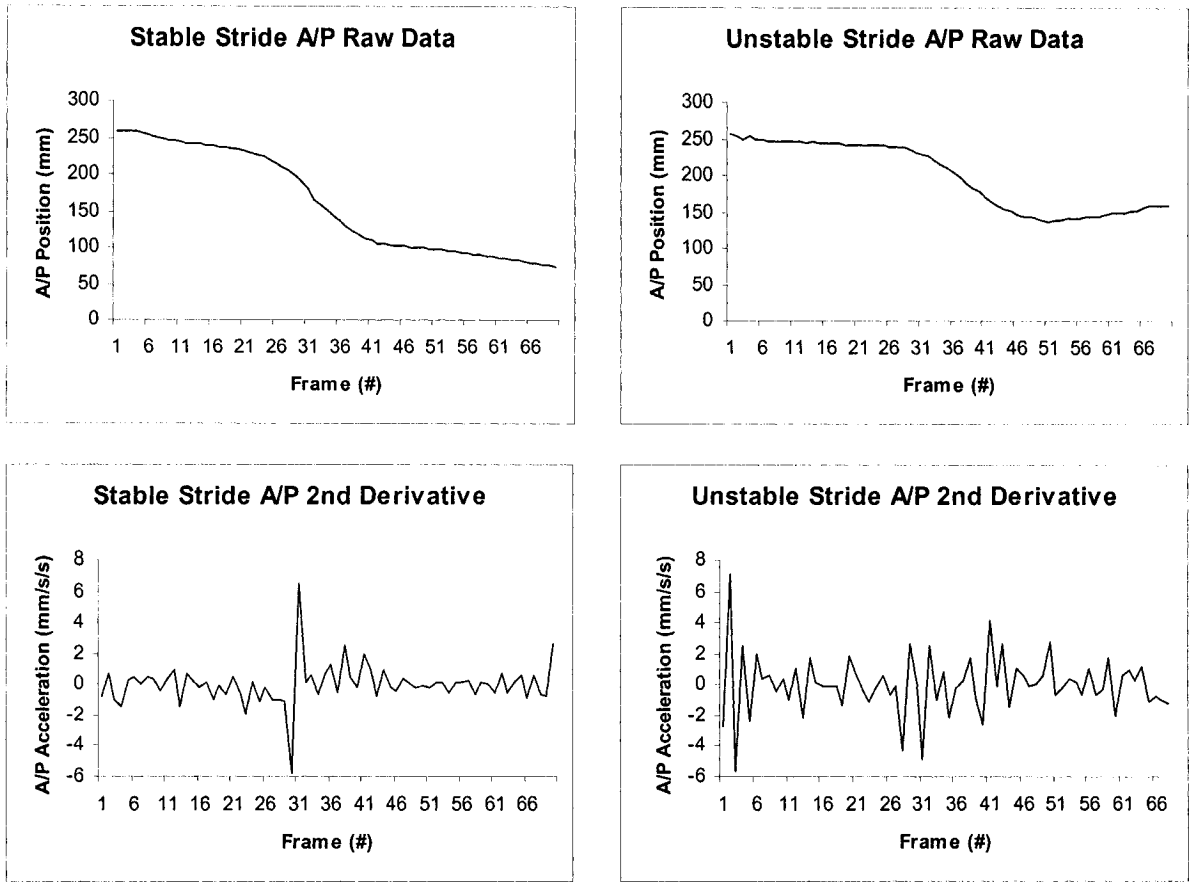

Figure 4.9: Raw data and second derivative graphs of stable and unstable A/P COF motion. The raw data consists of the A/P COF position on the F-Scan sensor insole versus the frame number. Higher row (A/P position) values indicate activity at the heel of the sensor. The second derivative of this data refers to the acceleration of the A/P motion.

4.3.2.4 Frequency Analysis

The Fourier transform is based on the concept that any curve can be represented by a number of sine and cosine functions with varying amplitudes. Equation 4.2 shows the general Fourier series where a_n and b_n are amplitudes of the trigonometric functions.

$$f(x) = \frac{a_0}{2} + a_1\cos(x) + a_2\cos(2x) + a_3\cos(3x) + \ldots + a_n\cos(nx) + b_1\sin(x) + b_2\sin(2x) + b_3\sin(3x) + \ldots + b_n\sin(nx) \quad \textbf{(4.2)}$$

A Fourier transform takes a set of continuous data and translates the set to the frequency domain. The result isolates frequencies that create the original data curve. Performing a Fourier transform on a data set finds the dominant frequencies present in the data (Figure 4.10).

Similar to the concavity analysis, Fourier analysis applied to foot pressure data aims to first distinguish instability peaks from noise in the data and then eliminate the high-valued noise frequencies to analyze the remaining valid stability data.

Ideally, in observing a Fourier transform of COF data, higher frequencies would indicate more perturbations in the COF progression. The test trials of stable and unstable gait were again used to verify if the frequency analysis technique would work. Unfortunately, similar to the concavity analysis, noise associated with the F-Scan COF data was too inconsistent to appropriately remove. The noise and the valid foot pressure data occur at similar frequencies and without knowing the exact values of the noise frequencies, the noise cannot be successfully eliminated without affecting the valid foot pressure data. Therefore, no cut-off frequency can be applied to eliminate noise and the frequency analysis approach was not used.

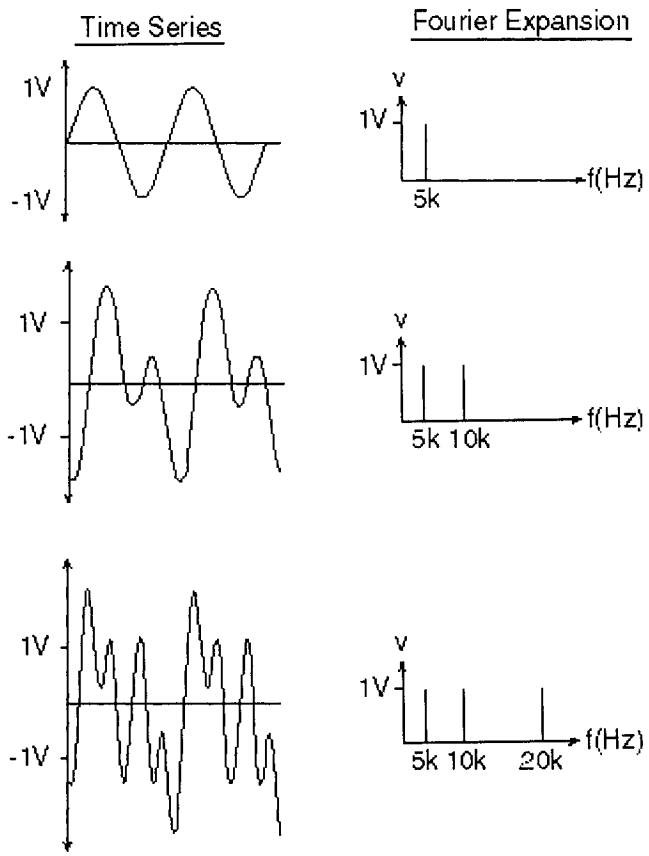

Figure 4.10: Examples of Fourier transforms (modified from [198]).

4.3.3 Anterior/Posterior (A/P) Stability

The A/P stability parameter was the first parameter to be included in the final stability index calculation. During stable gait, the COF should move from the heel to the forefoot without any unnecessary fluctuations. Any backward shifts in COF position are signs of instability. As shown in Figure 4.1, the pressure should move in the negative direction from high row numbers to low row numbers (i.e., from row 60 to row 1 on the F-Scan sensor), and therefore should have a negative slope throughout stance-phase on a graph of position (row number) versus time (Figure 4.11).

Figure 4.11: A/P position of the COF measured during stance phase. A high position value would be at the heel of the sensor and a low value would be at the toe.

A/P stability evaluation used the first derivative of the A/P COF data. A positive slope in the graph of position (row number) versus frame number (Figure 4.11) would indicate hindered forward progression. The number of frames with a positive first derivative is proportional to the amount of time the subject spent moving backwards. The number of samples per stride S was used to normalize the parameter to account for increased deviations as a result of a higher sampling rate. Equation 4.3 shows the calculation of the AP parameter where p is the number of frames with a positive slope.

$$AP = \frac{p}{S} \qquad \textbf{(4.3)}$$

4.3.3.1 A/P Stability Parameter Calculation Pseudocode

The algorithm for obtaining the A/P stability parameter was the following:

- Obtain the A/P position values (row numbers) of the COF for all frames of a data acquisition trial.
- Create *ap_count* as a counting variable
- For each stride (analysis in Section 4.3.7.1):

- Differentiate the A/P position values with respect to time by subtracting each frame's COF A/P position from the preceding frame's value (i.e. $x'(t) = x(t) - x(t-1)$), and divide by the change in time which is 1 frame.
- For each frame:
  - If the first derivative point is positive then increment *ap_count*.
- Divide *ap_count* by the number of samples in the stride to obtain the A/P stability parameter.

4.3.4 Medial/Lateral (M/L) Stability

An M/L stability index parameter was also included in the final stability index. This parameter should accurately measure excess M/L COF motion during stance-phase. M/L stability analysis was slightly different from the A/P analysis because an M/L COF curve was expected to move laterally until mid-stance and return to the medial side of the foot during push-off (Figure 2.3). To analyze this motion, the M/L COF position (i.e. the column number of the F-Scan sensor) was differentiated over an entire stride. The resulting data was then used to look for transitions between positive and negative slopes of the raw M/L COF data (i.e. zero crossing of the first derivative). M/L COF position switches from a positive slope to a negative slope indicate an M/L shift in the COF of the subject. Increased positive/negative slope transitions in M/L COF position data would mean more M/L COF shifts throughout stance-phase and, therefore, increased instability.

A frequency measure of M/L COF shifts would be a good M/L stability index parameter; however, the data contains noise that would need to be removed. To isolate the important stability information, a dynamic (dual) threshold was implemented. The concept of a dynamic (dual) threshold is illustrated in Figure 4.12. Once the threshold is passed, it immediately changes sign (positive to negative or vice versa) to become the second threshold. Therefore, a shift would not be counted if the same sign threshold were repeatedly passed due to low amplitude fluctuation in value.

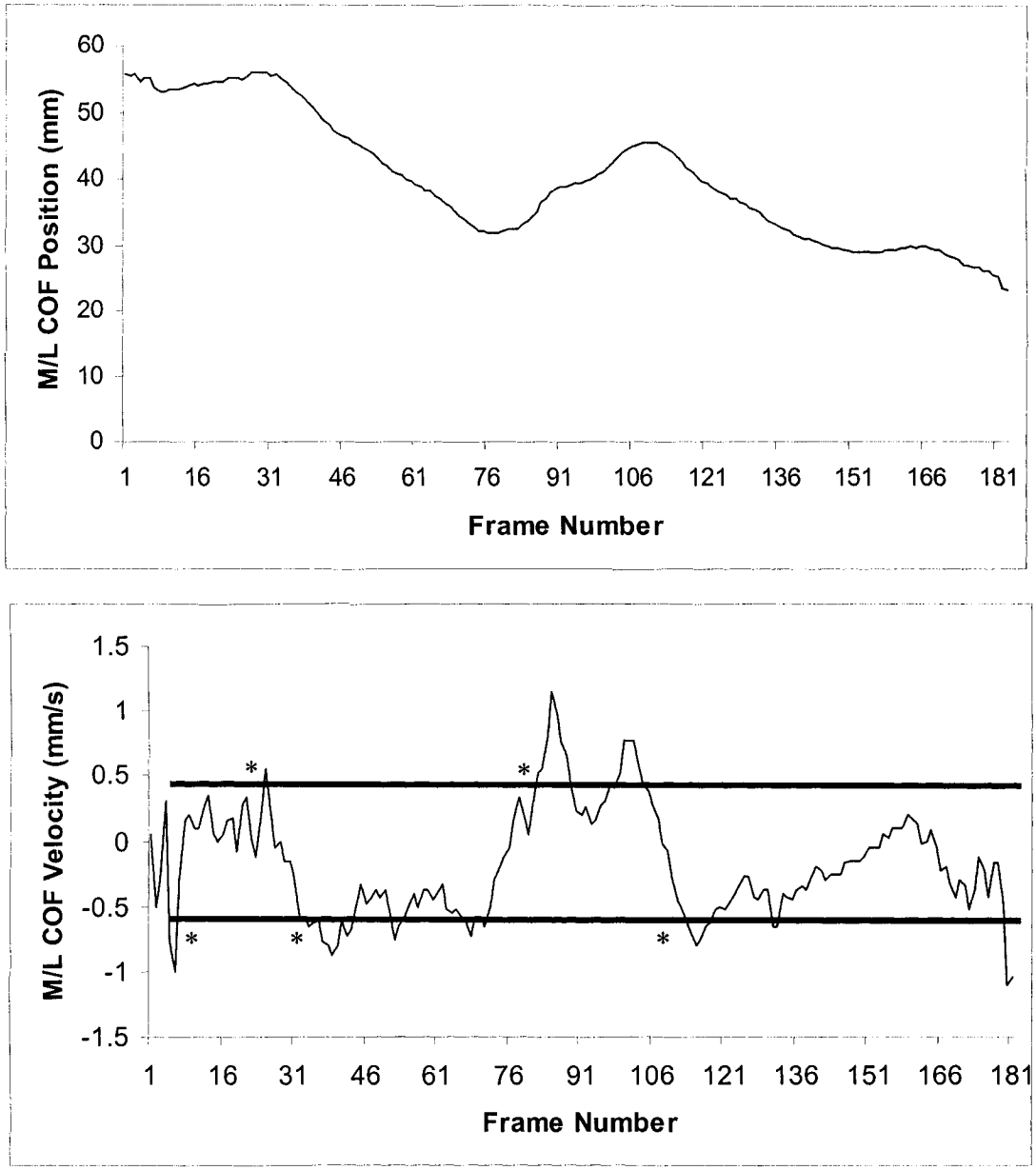

Figure 4.12: M/L position and velocity of an unstable stance-phase. The (*) indicates the counting of a shift due to the M/L COF velocity value exceeding two thresholds of opposite sign at 0.5 and -0.5 M/L COF velocity.

When the COF velocity data in Figure 4.12 has a negative value, then the M/L COF position data is moving in the negative direction. Similarly, when the velocity data has a positive value, then the M/L COF is moving in the positive direction. Therefore, a zero crossing (positive to negative switch) in the velocity-time curve would indicate COF movement from lateral to medial. In Figure 4.12, the threshold triggers when the COF

velocity makes a jump of 1.0 mm/s. Therefore, the subject has to substantially shift their COF in the M/L direction to pass the double threshold. Small amplitude high frequency variations of position seen in the COF velocity graph in Figure 4.12 would not be counted, thereby isolating the subject's actual shifts in COF in the M/L direction. Therefore, the number of times the dynamic dual threshold is passed is an indicator of the number of shifts in COF in the M/L direction.

4.3.4.1 M/L Stability Parameter Calculation Pseudocode

The algorithm for obtaining the M/L stability parameter was the following:

- Obtain the M/L position values (column numbers) of the COF for all frames of a data acquisition trial.
- Create *trigger_count* as a counting variable.
- For each stride (analysis in Section 4.3.7.1):
    - Initialize *trigger_count.*
    - Differentiate the M/L position values with respect to time by subtracting each frame's COF M/L position from the preceding frame's value (i.e. $y'(t) = y(t) - y(t-1)$), and divide by the change in time which is 1 frame.
    - For each frame of the stride:
        - If the first derivative value exceeds the threshold:
            - Increment *trigger_count.*
            - Change the sign of the threshold.
    - The M/L stability parameter is equal to the value of *trigger_count.*

4.3.5 Maximum Lateral Placement of Force

Another stability index parameter was created based on the maximum lateral placement of the COP. Movement of the COP to the lateral side of the foot indicates unsteadiness. Extreme COP lateral placement causes instability and even falls [136, 182]. The F-Scan column data (Figure 4.1) represents the M/L COP position and can be used to assess the lateral movement of the subject's total body centre of gravity and the maximum lateral placement of the COP.

To detect extreme COP lateral placement, a search algorithm was performed on the MF data. Section 4.3.1 describes the method of obtaining the value and row/column position of the maximum registered pressure in each frame of F-Scan data. To find the maximum lateral placement of force, the frame with the furthest lateral MF column value was isolated

and compared to the width of the sensor. The further this value was to the lateral side of the foot, the more unstable the subject. Therefore, the maximum lateral COP placement parameter was the furthest lateral column number that registered a maximum force.

4.3.5.1 Maximum Lateral Position Stability Parameter Calculation Pseudocode

The algorithm for obtaining the maximum lateral position stability parameter was the following:

- Obtain the M/L position values (column numbers) of the MF data for all frames of a full data acquisition trial.
- For each stride (analysis in Section 4.3.7.1):
    - Obtain the maximum lateral position of the MF. This is used as the stability index parameter.

4.3.6 Cell Trigger Frequency

A cell triggering frequency stability parameter was also added to the calculation of the gait stability index. As mentioned earlier, the ideal stance-phase would progress smoothly from heel to fore-foot. As a result, F-Scan cells that come into contact with the foot should only activate once throughout an ideal stance-phase. A cell could be held in the 'ON' position for any number of frames, but once deactivated the cell should not be triggered again. Activating a cell more than once is a sign of abnormal weight shifting, hence an indication of instability. Therefore, the cells that are triggered more than one time during stance-phase can be used as a parameter for the gait stability index. To obtain this index parameter, each frame of filtered and thresholded F-scan data is compared to the previous frame in time. The cells are tagged with an 'ON' or 'OFF' label for each frame. The number of times each cell is triggered throughout a stride is monitored and the cell that is triggered the most often is isolated. The cell triggering frequency parameter also takes into account the number of samples in the stride by dividing the cell trigger frequency by the total number of frames (i.e., normalizing to 100% of stance time). Therefore, the cell triggering frequency stability parameter is the maximum number of times a cell is triggered during a stride divided by the number of frames in the stride. Equation 4.4 defines the cell triggering frequency stability parameter C where T is the maximum number of times a cell is triggered throughout a stride and S is the number of samples in the stride.

$$C = \frac{T}{S} \qquad (4.4)$$

4.3.6.1 Cell Triggering Frequency Stability Parameter Calculation Pseudocode

The algorithm used to obtain the cell triggering frequency stability parameter was the following:

- Obtain the filtered data set for all frames of a full data acquisition trial.
- Create three arrays the size of an F-Scan sensor, *f_array1*, *f_array2*, and *f_array*.
- For each stride (analysis in Section 4.3.7.1):
    - Initialize *f_array1*, *f_array2*, and *f_array* to zero.
    - For each frame:
        - For every cell in the frame, store a value of 1 in the corresponding cell of *f_array2* if the cell has a registered pressure value and a 0 if not.
        - For every cell in the previous frame, store 1 in the corresponding cell of *f_array1* if the cell has a registered pressure value and a 0 if not.
            - For every cell:
                - If *f_array2* – *f_array1* = 1 then the cell was just activated:
                    - Add 1 to the corresponding element in *f_array*.
    - After going through each frame of the stride, the maximum value of *f_array* is divided by the number of frames in the stride to obtain the cell triggering frequency stability parameter.

4.3.7 Stride Parameters

Stride time (ST) and double support time (DST) are known to have a direct correlation to gait stability (Section 2.5.2.3). Therefore, these parameters were used in the gait stability index. ST is the time from heel-strike to heel-strike of one foot. DST is the time when both feet are in contact with the ground, or the amount of time spent in the double support phase. Both ST and DST should increase as gait stability decreases. These parameters can be extracted after the F-Scan data is divided into strides. According to Ochi et al. [199], when dealing with stroke patients, the typical ST is 2.22 ± 0.92 s and DST is 1.15 ± 0.38 s.

The stride division algorithm searches through the data and stores consecutive frames with a registered maximum force (according to the F-Scan and software-based threshold

described in Section 4.3.2). A maximum force is not registered for the frames when the foot is not in contact with the ground (i.e., swing phase). Therefore, each series of consecutive frames with a registered maximum force is considered to be stance-phase. The number of frames in a stride would consist of the entire stance-phase (frames with a registered maximum force) as well as the following swing-phase (frames with zeros until the following registered maximum force). The number of frames in the stride is divided by the sampling rate to calculate ST. The F-Scan data of the left and right foot are also compared with respect to time such that the overlap between left and right strides reveal when both feet are in contact with the ground. The number of frames in a stride where both feet register a maximum force, divided by the sampling rate yields DST.

4.3.7.1 Stride Time Stability Parameter Calculation Pseudocode

The algorithm for obtaining the ST stability parameter was the following:

- Obtain the filtered MF data for a full data acquisition trial.
- Create *start_frame*, *end_frame*, and *st_count* as a counting variables.
- For each frame:
    - Register the first frame number of the stride in *start_frame*.
    - *st_count* is equal to start frame of the stride (initially frame 1).
    - Repeat until the frame has no registered maximum force:
        - If the frame has a registered maximum force:
            - Increment *st_count*.
    - {Now *st_count* is equal to the frame number at the end of push off.}
    - Repeat until the frame has a registered maximum force:
        - If the frame has no registered maximum force:
            - Increment *st_count*.
    - {Now *st_count* is equal to the frame number at the start of the following heel strike.}
    - *end_frame* = *st_count*
    - *st_count* = *end_frame* – *start_frame*
    - Register these variables with the stride and repeat for the following stride.

- Once all the strides have been stored (at end of file), for each stride:
    - Divide the number of frames in the stride by the sampling rate to obtain the ST.

4.3.7.2 Double Support Time Stability Parameter Calculation Pseudocode

The algorithm for obtaining the DST stability parameter was the following:

- Obtain the filtered MF data for the left and right foot of a full data acquisition trial.
- Create *dst_count* as a counting variable.

- For each stride (analysis in Section 4.3.7.1):
  - Initialize *dst_count*.
  - From the start frame to the end frame of the stride:
    - If there is a registered maximum force in both the left and right foot data of the frame, then increment *dst_count*.
  - *dst_count* is divided by the sampling rate to obtain the DST.

4.3.8 Summary of Stability Index Parameters

Given the F-Scan system capabilities and limitations, six gait stability parameters were chosen as input for the dynamic stability index (Table 4.1); A/P, M/L, maximum lateral position, cell triggering frequency, ST and DST. The A/P and M/L parameters, defined in Sections 4.3.3 and 4.3.4, are associated with abnormal weight shifting in the A/P and M/L directions. The maximum lateral placement of force, described in Section 4.3.5, identifies the most lateral position of maximum force during stance-phase. Another parameter is based on the F-Scan cell triggering frequency (Section 4.3.6). Finally, ST and DST are temporal gait measures that have been used in many studies in determining stability (Section 4.3.7).

Table 4.1: Overview of parameters used in dynamic gait stability index.

Stability Index Parameter	Method	Rationale
A/P Parameter	**Source**: first derivative of COF A/P position (F-Scan COF row data)	Posterior COP motion during gait is an indication of instability (i.e., perturbations in A/P curve).
	Processing: Number of frames with a positive first derivative value (posterior motion) divided by total number of frames in the stride.	
M/L Parameter	**Source**: first derivative of COF M/L position (F-Scan COF column data)	Excessive M/L COP perturbations are a sign of gait instability (i.e., perturbations in M/L curve).
	Processing: The M/L parameter detected and counted significant M/L shifts in the COF position data.	
Maximum Lateral Position	**Source:** Median and averaging filtered MF position column data	Excessive lateral placement of the COP causes unstable gait. This parameter correlates well with gait instability.
	Processing: Frame where the MF is at its most lateral position.	

Cell Triggering Frequency	**Source:** Filtered F-Scan pressure data	An ideal stride would only activate each cell once. Reactivation of a cell during one stride is a sign of abnormal weight shifting.
	Processing: The maximum number of times that a cell is triggered, divided by the number of frames in the stride.	
Stride Time (ST)	**Source:** Filtered MF values	ST is a well-known measure of gait stability.
	Processing: The number of samples in a stride is divided by the sampling rate to find ST.	
Double Support Time (DST)	**Source:** Filtered MF values	DST is a well-known measure of gait stability.
	Processing: The left and right stride data are compared to each other and the number of overlapping frames is divided by the sampling rate.	

4.4 Fuzzy Logic Controller

Once the stability parameters have been isolated and calculated, the values must be combined to achieve a final index. The fuzzy logic controller was the tool selected for combining the dynamic stability index parameters. An artificial neural network (ANN) is another option for the parameter combination. An ANN is a data modeling tool that can capture and represent complex input/output relationships. A typical ANN requires a desired output in order to 'learn' the weights and system coefficients. The goal of an ANN is to create a model that correctly maps the inputs to the output using historical or 'training' data so that the model can be used to produce the outputs for any new inputs [200]. The ideal application of an ANN is for pattern recognition or data classification [201]. However, in the case of a dynamic stability index, the output is unknown. The purpose of the combination technique is to establish the output index. The effectiveness of an ANN is directly related to the training data provided. Since a clear relationship between input and output is difficult to determine in order to create the training data sets, ANN was not used for this research.

Fuzzy logic controllers, on the other hand, can be customized according to the expected input values and they can also be established with no initial data. Fuzzy controllers are versatile and can be programmed to deal with any type of application. The main strength of a fuzzy logic controller is the ability to relate quantities that do not have a clear

mathematical connection, such as stability index parameters. As well, by using a fuzzy logic controller, the combination technique can be finely adjusted in the future. An alternative method would be to sum a normalized value of each of the parameters. However, even though neither method immediately guarantees a good result, the fuzzy logic model has a lot more control over the combination methods with its rules and membership functions, and it would be easier to adjust in the future.

4.4.1 Fuzzy Logic Controller used for the Stability Index

This section outlines the fuzzy logic controller built in this thesis to generate the stability index.

4.4.1.1 Membership Functions

The stability index platform is built with four triangular membership functions for each parameter and is illustrated in Figure 4.13:

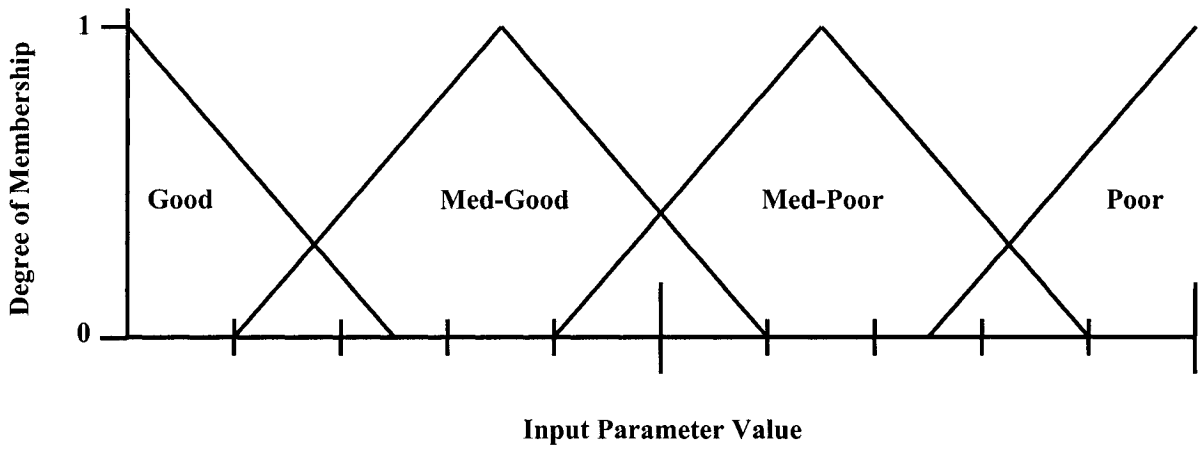

Figure 4.13: Layout of four evenly-spaced triangular membership functions used for each input parameter.

Ranges for the A/P, M/L, Cell Triggering Frequency and Maximum Lateral Position parameters were established by retrieving the upper limit of the variables from clinical testing trials (Chapter 5) in an attempt to span the range of all possible values. These parameters were constructed for this research project and, as a result, their limits would not be documented in previous research studies. The upper limits of ST and DST used the worst

case scenario for stroke patients from the literature (Section 4.3.7). The membership functions were spread evenly over the range of the input variables (Table 4.2).

Table 4.2: Stability parameter ranges and membership functions used in the stability index fuzzy-logic controller.

Parameter	Good	Med-Good	Med-Poor	Poor	Measure
A/P	0 – 0.1	0.04 – 0.24	0.16 – 0.36	0.3 – 0.4	$AP = \frac{p}{S}$
M/L	0 – 0.025	0.01 – 0.06	0.04 – 0.09	0.075 – 0.1	Number of significant M/L shifts in COP
Maximum Lateral Position	0 – 3.25	1.3 – 7.8	5.2 – 11.7	9.75 – 13	Furthest lateral position of the COP
Cell Triggering Frequency	0 – 21.25	8.5 – 51	34 – 76.5	63.75 – 85	Maximum number of times any cell is retriggered throughout one stride
Stride Time (s)	0 – 1.02	0.41 – 2.44	1.62 – 3.65	3.05 – 5.08	Time from foot strike to following foot strike of the same foot
Double Support (s)	0 – 0.66	0.26 – 1.57	1.05 – 2.36	1.97 – 3.28	Time with both feet in contact with the ground

The number of membership functions was increased to six for the output parameter to increase the sensitivity of the controller (Figure 4.14).

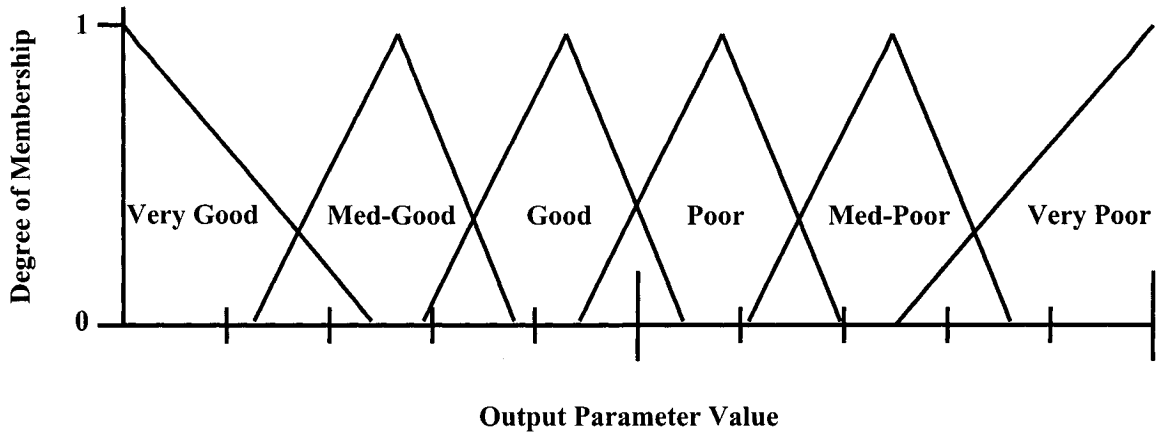

Figure 4.14: Six membership functions used for the stability index output parameter to increase the sensitivity of the controller.

4.4.1.2 Fuzzy Rule Set

Once the membership functions had been created for each input and output variable, the next step was to create the rule set. The AND method was chosen for this step because each input was assumed to be unrelated. As a result, a rule needed to be made for each possible combination of input parameters. With six input variables and four membership functions each, the number of rules would be 4^6= 4096 rules for the fuzzy logic controller. Since all stability parameter combinations were evaluated (57 combinations in total); there were 14,576 rules that needed to be created. Assigning each rule individually would be incredibly time-consuming, so an algorithm was created to automatically create the rule set. The algorithm evenly distributes the output conditions across all the possible combinations of the input parameters.

The first step of the algorithm was to order the input parameters. This was done by analyzing the stability parameters produced by trials of test data created by the researcher. The input parameters were preliminarily ranked according to a visual inspection of the results as follows: A/P, M/L, DST, ST, Cell Triggering Frequency, and Maximum Lateral Position. The ordering of the parameters acts as a weighting scheme. Next, the inputs were arranged in nested 'for' loops (Figure 4.15). The number of rules for each condition of the A/P parameter (Input 1) was calculated as '**a**'. In the case of the six parameter combination, this value would be 4^5=1024. Then, the number of different output conditions for each

condition of the A/P parameter was calculated as '**b**'. Figure 4.15 shows that **b**=3 as there would be three output conditions for each condition of the A/P parameter. The rationale behind overlapping the output conditions across the four conditions of input 1 is to increase the influence of the lower ordered parameters. Finally, the output conditions are assigned accordingly.

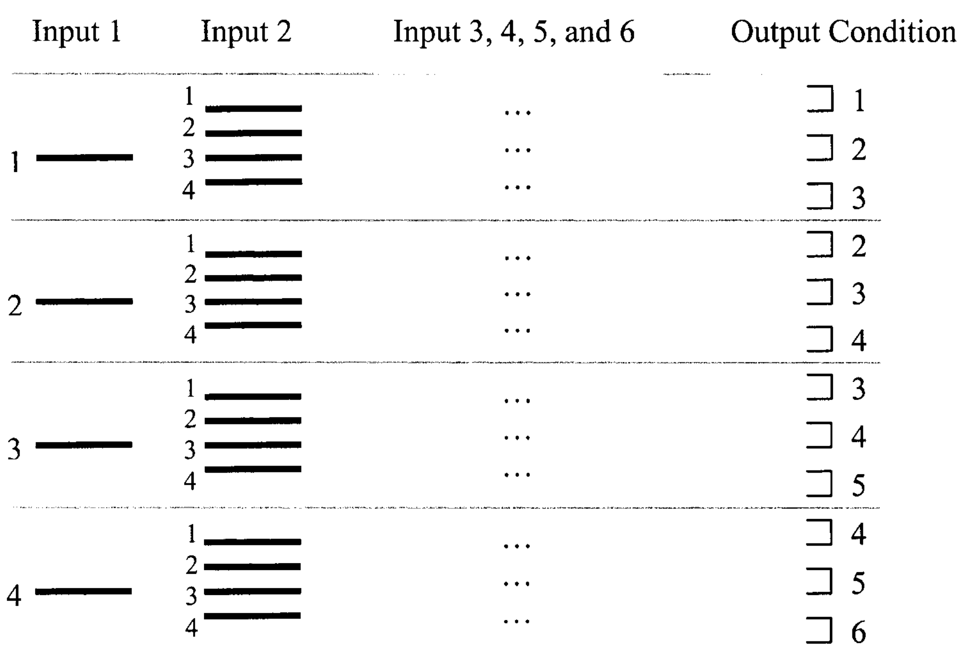

Figure 4.15: Diagram of the layout of input and output conditions for creating the rule set for a fuzzy logic controller with four input conditions and six output conditions.

The pseudocode for the rule set assignment algorithm is the following:

- Order the input parameters
- Let **a** = the number of rules needed for each condition (membership function) of the first input (4^5=1024 rules for each condition of the first input)
- Let **b** = the number of different output conditions (membership functions) for each condition of the first input (6 output conditions – 4 input conditions + 1 = 3)
- Find out if '**b**' is evenly divisible by '**a**'; if not, then let **c** = the remainder
- Let **d** = the number of rules with the same output condition in a row (1024/3 = 341)
- While cycling through all possible combinations of input functions:
  - Assign the output condition '**d**' times
    - Check for extra times with '**c**'
  - Go to next output condition

4.4.1.3 Defuzzification

After the membership functions and the rule set were created, the final step was the defuzzification of the controller. The default centroid method of defuzzification from the Matlab Fuzzy Logic Toolbox was used to arrive at a stability index output. This method was fully described earlier in Section 2.7.4.

Chapter 5. Clinical Testing

The stability index was clinically tested with unstable human gait to evaluate gait stability assessment effectiveness of the developed system. Ethical clearance on patients with unstable gait, such as those in the process of rehabilitation, was difficult to obtain given the lack of prior stability index validation. Instead of evaluating the pathological gait of stroke and amputee patients, as was originally planned, clinical testing was performed on healthy individuals whose gait was purposely impaired to induce instability. This study was approved by the research ethics bodies at the University of Ottawa, The Ottawa Hospital Rehabilitation Centre, and the University of Waterloo (See Appendix A).

5.1 Purpose

The purpose of the clinical testing was to confirm that the gait stability index can correctly classify various levels of gait stability from foot-pressure and stride data acquired by the F-Scan pressure-measurement system.

5.2 Methods

5.2.1 Subjects

A convenience sample of fifteen subjects was recruited from the staff of The Ottawa Hospital Rehabilitation Centre, Ottawa, Canada and the community. All subjects were healthy able-bodied adults with no history of back/neck pain or balance disorders. The subjects read an information sheet and completed a consent form before participating in the study. Nine male and six female subjects agreed to participate. The average weight of the participants was 69.21 ± 11.77 kg, the average height was 1.67 ± 0.09 m, and the average age was 33.53 ± 11.85 years.

5.2.2 Data Collection

All data collection trials were performed in the Gait and Motion Analysis (GAMA) laboratory at The Ottawa Hospital Rehabilitation Centre. Subject demographic data was collected on a data sheet (age, gender, height, and weight). The F-Scan system was used for

all plantar pressure measurements. F-Scan pressure sensitive insoles were trimmed to fit inside the shoes of each subject. Once the insoles were properly placed inside the subject's shoes, all wires were secured with a belt strap to eliminate any interference with a comfortable gait pattern. Finally, the system was calibrated for the subject's weight using the F-Scan software. All walking trials were performed over an 8 m area and the subjects walked at their natural cadence.

Each subject was evaluated at four levels of stability:

1. walking on flat level ground
2. walking on a 50 mm-thick combination of medium and hard memory foam
3. walking on the same foam with eyes closed
4. walking on the same foam with eyes closed after being spun five to fifteen times at approximately one revolution per two seconds while seated in a chair

Pressure data was recorded during mid-gait (i.e. only while the subject was walking) to eliminate abnormal pressures that may have resulted from gait initiation or termination. The F-Scan data acquisition trials lasted 7.12 seconds while recording 1000 frames of data at a sampling rate of 140 Hz. Each subject performed five trials for each stability level (a total of 20 trials per subject), at a self-selected walking pace. Subjects were allowed to rest between trials, if necessary, which was mainly done during the trials involving dizziness. A minimum of two people always ran the protocol to adequately ensure subject safety (i.e., one person could spot the subject).

5.2.3 Data Processing

The raw F-Scan data files were exported from the F-Scan software into a custom designed Microsoft Visual Basic 6.0 (VB6) program to extract the six stability parameters for each trial. The VB6 program was used to:

- Store the 1000 raw data frames from the left and right foot (2000 frames in total).
- Filter the raw data to remove any spike-like noise that may have been registered by the F-Scan pressure sensor.

- Divide the filtered data into strides.
- Calculate the six stability parameters (Section 4.3.8) for each stride.
- Output the stability parameters into an ASCII data file.

The filtering stage of the VB6 program had two options: a median filter and an averaging filter. To determine the better filtering method, two full data sets were analyzed. The averaging filter would smooth data by averaging noise, while the median filter would choose the median of a nine-cell array in an attempt to eliminate noise. The median filter proved to be the better filtering technique because it eliminated any effect of spike-valued noise by taking the median value (Section 6.1.1).

Another custom designed program was written in Matlab using Simulink and the Matlab Fuzzy Logic Toolbox. This program was designed to import the VB6 ASCII data file and use a fuzzy logic controller (Section 4.4) to combine the six stability parameters of each foot to obtain a left and right index value. The program also calculated index values for all 57 combinations of five, four, three, and two stability parameters. The gait stability indices were then output to another ASCII data file that was imported into Microsoft Excel.

The final gait stability index is an average of the left and right indices. Gait analysis of the left and right side individually has some advantages since specific problems with either side can be located and addressed specifically. However, the rationale behind taking the average of the left and right strides is for the stability index to account for people who may have an affected side. If a person only has one affected side in their gait pattern, they should have a better score on the index than someone with two affected legs.

5.2.4 Data Analysis

Once imported into Excel, the average index value for each subject was arranged to show how the four stability levels of each subject were analyzed by each stability parameter combination (Appendix B). Since the indices should increase from stability level one to four (stable to unstable), the optimal combination of parameters was based on the most consistently large increase over the stability levels for each subject. Figure 5.1, Figure 5.2,

Figure 5.3, and Figure 5.4 show graphs from subject 4 of the difference in index value between the four stability levels for each of the 57 stability parameter combinations. The graphs show the change in index readings from stability level 2 to 1, level 3 to 2, and level 4 to 3.

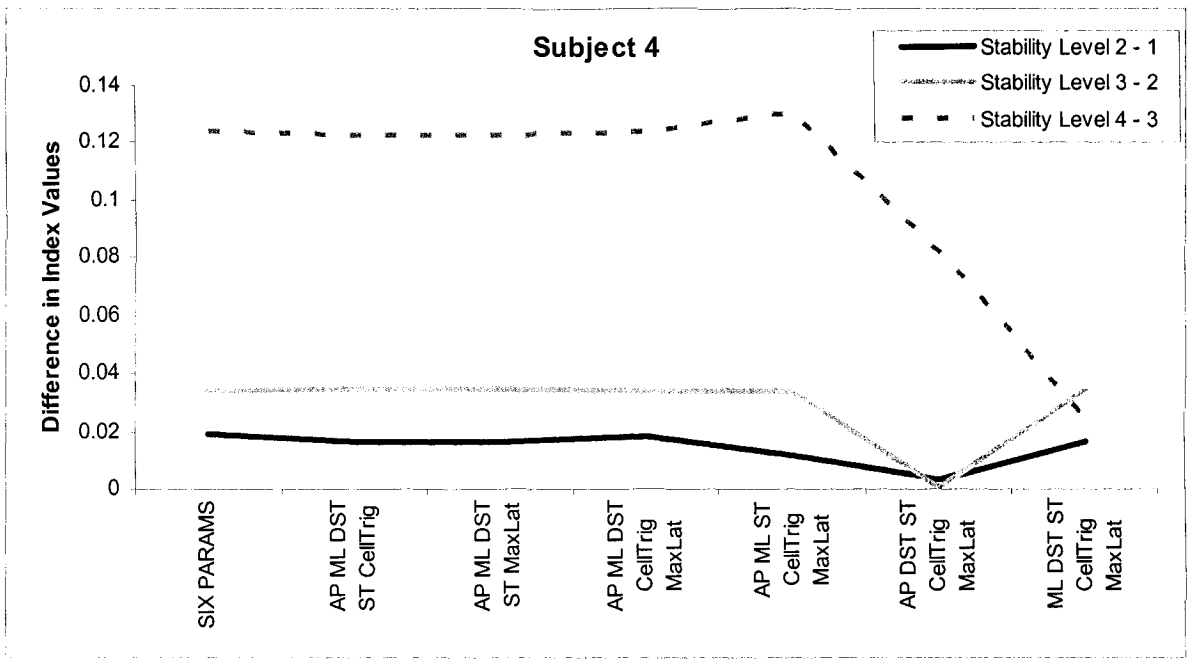

Figure 5.1: Change in index value over the four stability levels for indices of six and five-parameter combinations for subject 4. The abbreviations for the parameter combinations are: *SIX PARAMS* = the index with all six parameters included, *AP*=A/P, *ML* = M/L, *CellTrig* = Cell Triggering Frequency, *MaxLat* = Maximum Lateral Position, *ST* = Stride Time, and *DST* = Double Support Time.

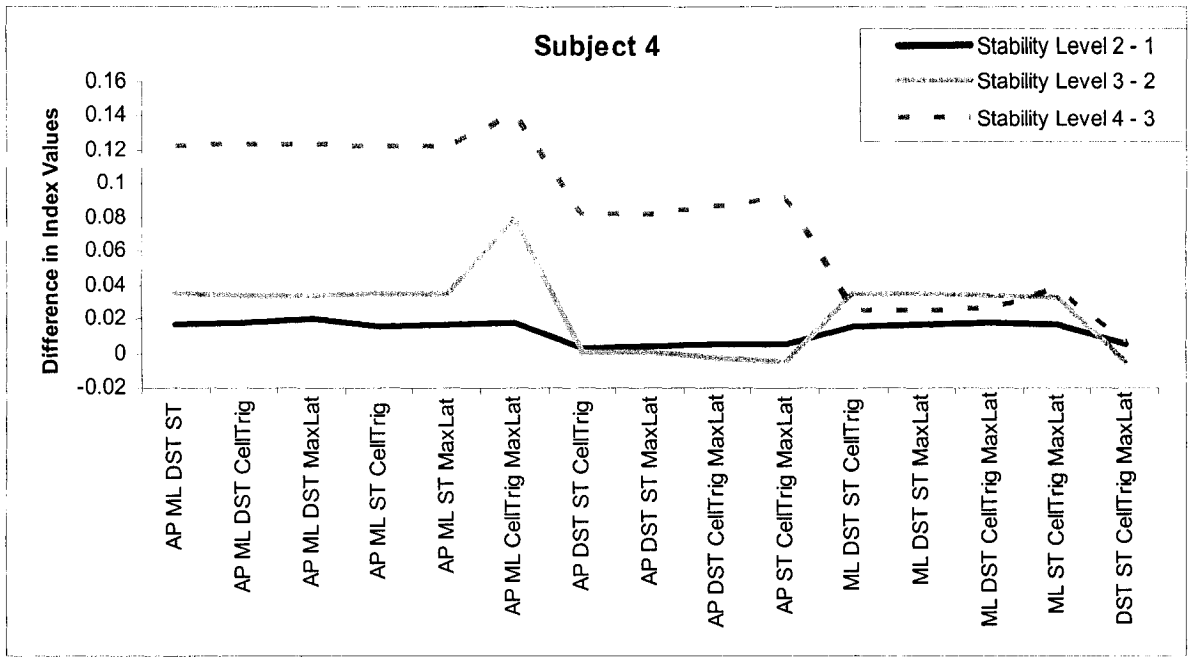

Figure 5.2: Change in index value over the four stability levels for indices of four-parameter combinations for subject 4.

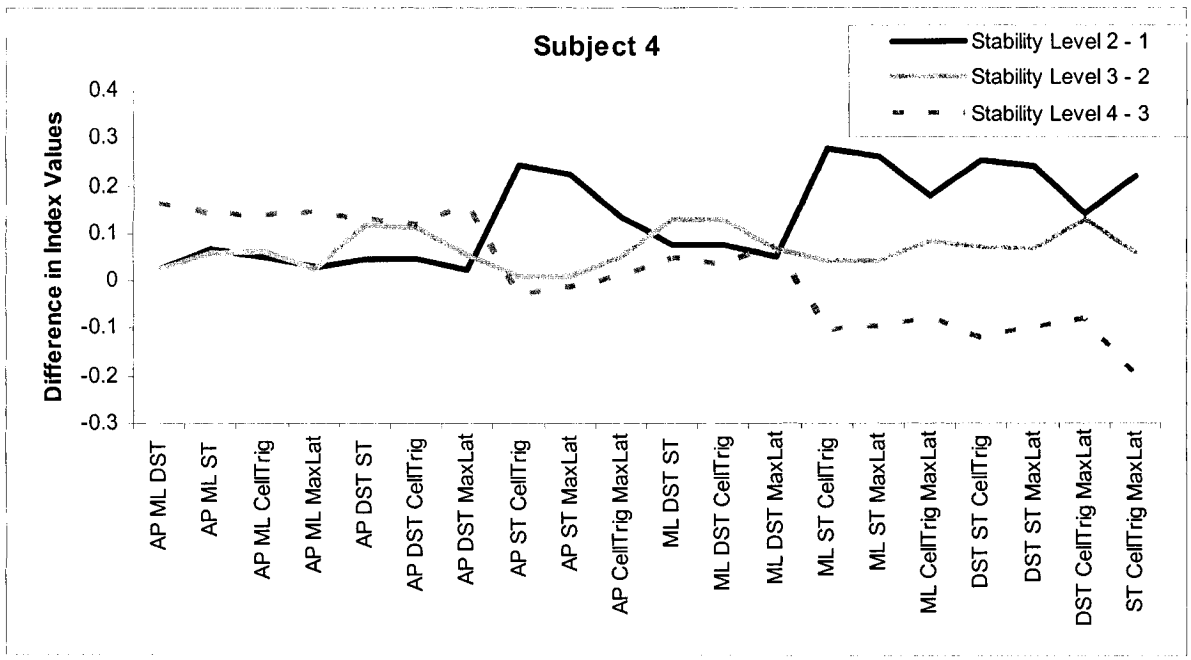

Figure 5.3: Change in index value over the four stability levels for three-parameter combinations for subject 4.

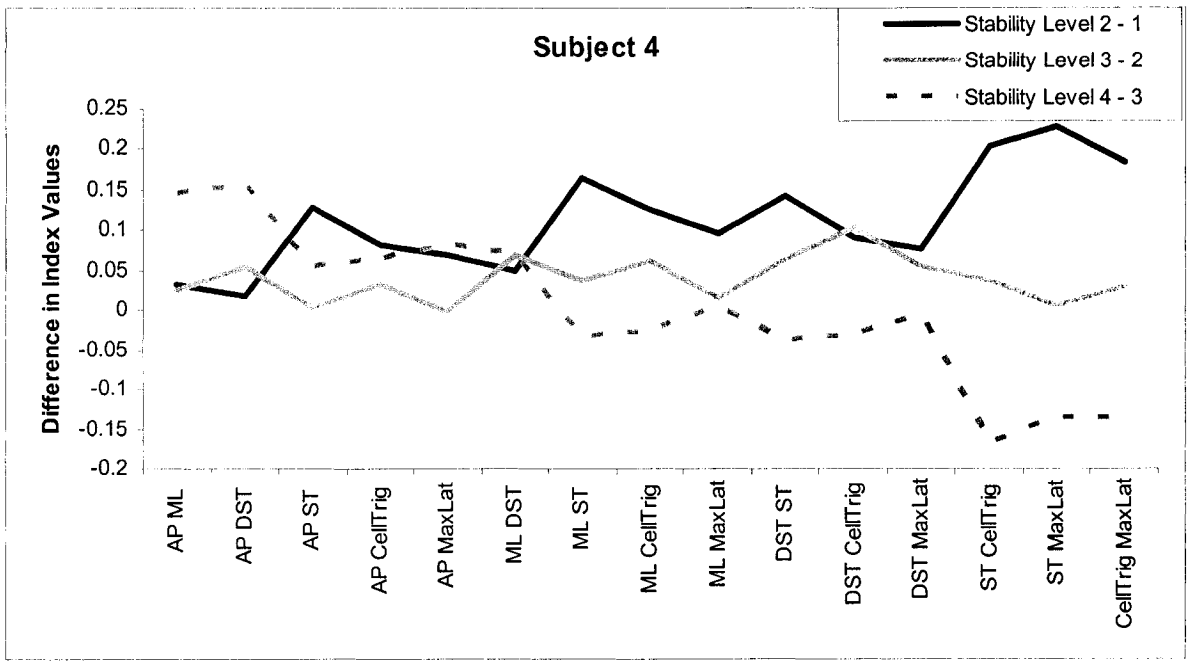

Figure 5.4: Change in index value over the four stability levels for two-parameter combinations for subject 4.

The best stability parameter combination would provide consistent index values and the three comparison lines on the graphs should follow a similar pattern. Visual inspection of the data shows that the final index should have at least four parameters because the combinations of three or two parameters displayed an erratic behaviour, indicating that they would not consistently analyze the stability of a subject. Two and three-parameter combinations showed no consistent relationship between the stability levels and showed no observable trends. Upon further analysis of Figure 5.5, when the A/P and M/L parameters are omitted from the index, the change in index value seems to decrease over the stability levels. This means that the indices lacking the A/P and M/L parameters show a smaller difference between the stability levels. Therefore, the final index should have at least four parameters and should include the A/P and M/L parameters.

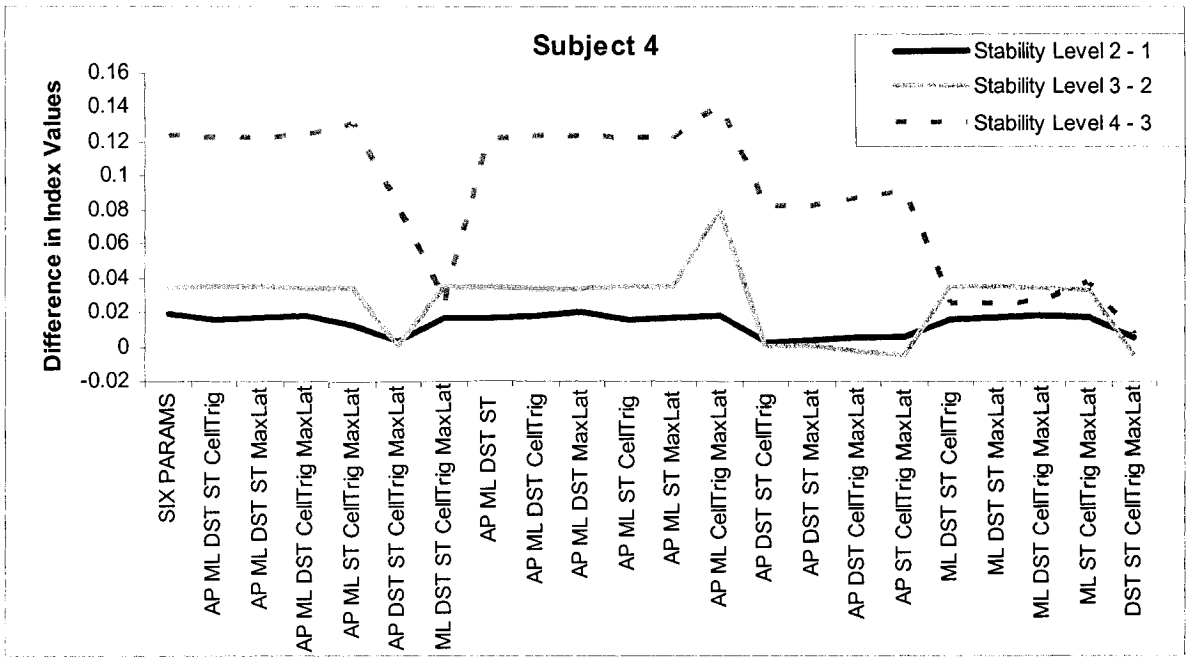

Figure 5.5: Change in index value over the four stability levels for the 22 index combinations with at least four parameters for subject 4.

An analysis of standard deviations (SD) was used to justify omitting certain parameter combinations. The standard deviation of the change in index readings showed how much the jump in stability level would vary around a mean value. The less it varied, the more consistently it should be able to analyze stability. Analysis included all parameter combinations (57 indices), the combinations with at least four parameters (22 indices), and the combinations with at least four parameters that include A/P and M/L (11 indices). This analysis was done across all subjects and found that the standard deviation improved by 74.64% ± 22.75%, going from the full data set to only the four parameter combinations that included A/P and M/L.

The next step in deciding the most effective combination of stability parameters was to rank the indices according to the difference between the most stable and least stable test conditions for each subject (Table 5.1). A bigger difference indicated a more effective index. As well, the index should have a consistently large difference across subjects. Results were ranked from 1 to 11, with 1 being the biggest difference. The parameter combination rankings for each subject were summed to generate a total ranking score. The best index

would have the lowest total ranking across subjects (Table 6.2 and Table 6.3). This is discussed in the next chapter, Chapter 6.

Table 5.1: Ranking the difference between first and last stability level for subject 10.

Parameter Combination	*1*	*2*	*3*	*4*	*Difference (4-1)*	*Index Rank*
AP ML CellTrig MaxLat	0.118	0.322	0.213	0.429	0.311	1
AP ML ST CellTrig MaxLat	0.118	0.254	0.207	0.412	0.294	2
AP ML ST MaxLat	0.118	0.254	0.206	0.392	0.275	3
AP ML ST CellTrig	0.118	0.254	0.207	0.392	0.274	4
AP ML DST CellTrig MaxLat	0.118	0.254	0.207	0.383	0.265	5
AP ML DST ST	0.117	0.254	0.205	0.376	0.259	6
AP ML DST ST MaxLat	0.118	0.254	0.206	0.376	0.259	7
AP ML DST ST CellTrig	0.118	0.254	0.207	0.376	0.258	8
SIX PARAMS	0.117	0.254	0.204	0.373	0.255	9
AP ML DST CellTrig	0.118	0.253	0.207	0.373	0.254	10
AP ML DST MaxLat	0.117	0.254	0.206	0.372	0.254	11

Chapter 6. Results

6.1 Results of Preliminary Tests

Preliminary tests involved the analysis of the concavity shifts of the COF progression curve (Section 4.3.2.3) and a frequency analysis of the COF progression curve (Section 4.3.2.4). As mentioned earlier, these analyses did not produce viable results. The COF curve contained noise that could not be adequately removed to isolate the pertinent stability data. Another preliminary test dealt with the filtering method. To select between the median and average filtering technique, final stability index results were obtained for two data sets and compared in the following section.

6.1.1 Median versus Averaging Filter

Proper data filtering was essential for dividing the F-Scan data into strides (Section 4.3.2). The full data analysis tables comparing median and averaging filter results can be seen in Appendix C. However, a comparison table of the differences in index values between the data obtained with the averaging filter and the data obtained with median filter can be seen in Table 6.1. According to this table, the two filtering methods varied by an average of approximately 0.7%. As well, a comparison with the averaging filter values (Table C.2) shows an average percent difference of approximately 3%. Therefore, values obtained by the two methods were not substantially different.

Table 6.1: Differences in index values calculated by subtracting the data set obtained from median filtering from the data set obtained from average filtering. This table shows a small average difference in index values (0.7%) between the two methods.

	Stability Level					
	1	2	3	4	Average	
	0.0059	0.0066	0.0079	0.0082	0.0072	AVG
SIX PARAMS	0.0262	0.0508	0.0195	0.0689	0.0414	SD
	0.0053	0.0061	0.0080	0.0101	0.0074	AVG
AP ML DST ST CellTrig	0.0285	0.0513	0.0212	0.0360	0.0342	SD
	0.0064	0.0101	0.0034	0.0060	0.0065	AVG
AP ML DST ST MaxLat	0.0274	0.0485	0.0233	0.0425	0.0354	SD
	0.0065	0.0104	0.0054	0.0067	0.0072	AVG
AP ML DST CellTrig MaxLat	0.0276	0.0503	0.0266	0.0439	0.0371	SD
	0.0039	0.0138	0.0070	0.0038	0.0071	AVG
AP ML ST CellTrig MaxLat	0.0242	0.0590	0.0291	0.0499	0.0405	SD
	0.0125	0.0066	0.0042	0.0183	0.0104	AVG
AP DST ST CellTrig MaxLat	0.0447	0.0223	0.0179	0.0270	0.0280	SD
	0.0100	0.0129	0.0026	0.0124	0.0095	AVG
ML DST ST CellTrig MaxLat	0.0357	0.0486	0.0263	0.0332	0.0359	SD
	0.0053	0.0079	0.0079	0.0096	0.0077	AVG
AP ML DST ST	0.0285	0.0541	0.0204	0.0368	0.0349	SD
	0.0054	0.0058	0.0073	0.0107	0.0073	AVG
AP ML DST CellTrig	0.0286	0.0514	0.0201	0.0366	0.0342	SD
	0.0065	0.0096	0.0029	0.0066	0.0064	AVG
AP ML DST MaxLat	0.0275	0.0479	0.0223	0.0430	0.0352	SD
	0.0032	0.0067	0.0105	0.0098	0.0075	AVG
AP ML ST CellTrig	0.0248	0.0534	0.0238	0.0377	0.0350	SD
	0.0043	0.0107	0.0061	0.0033	0.0061	AVG
AP ML ST MaxLat	0.0237	0.0505	0.0263	0.0501	0.0377	SD
	0.0032	0.0130	0.0018	0.0058	0.0060	AVG
AP ML CellTrig MaxLat	0.0331	0.0674	0.0314	0.0501	0.0455	SD
	0.0074	0.0041	0.0049	0.0071	0.0059	AVG
AP DST ST CellTrig	0.0289	0.0252	0.0157	0.0174	0.0218	SD
	0.0085	0.0049	0.0026	0.0156	0.0079	AVG
AP DST ST MaxLat	0.0286	0.0167	0.0156	0.0187	0.0199	SD
	0.0126	0.0065	0.0043	0.0177	0.0103	AVG
AP DST CellTrig MaxLat	0.0447	0.0222	0.0180	0.0265	0.0279	SD
	0.0132	0.0034	0.0020	0.0156	0.0085	AVG
AP ST CellTrig MaxLat	0.0410	0.0242	0.0197	0.0233	0.0271	SD
	0.0097	0.0112	0.0014	0.0092	0.0079	AVG
ML DST ST CellTrig	0.0354	0.0486	0.0175	0.0237	0.0313	SD
	0.0099	0.0127	0.0025	0.0107	0.0089	AVG
ML DST ST MaxLat	0.0351	0.0478	0.0261	0.0242	0.0333	SD
	0.0102	0.0131	0.0023	0.0126	0.0096	AVG
ML DST CellTrig MaxLat	0.0358	0.0491	0.0255	0.0333	0.0359	SD
	0.0056	0.0108	0.0031	0.0092	0.0072	AVG
ML ST CellTrig MaxLat	0.0292	0.0520	0.0308	0.0343	0.0366	SD
	0.0122	0.0047	0.0021	0.0204	0.0099	AVG
DST ST CellTrig MaxLat	0.0428	0.0238	0.0291	0.0437	0.0348	SD

To further compare the filtering methods, indices produced by the two data sets were ranked by the difference between the best and worst stability levels of each subject, as described in Section 5.2.4. Table 6.2 and Table 6.3 show the ranked indices from the data obtained with an averaging filter and a median filter, respectively. As mentioned earlier, the selected gait stability index should show the largest difference between best and worst stability levels over all subjects. According to the results, the most effective index was obtained with the median filter and used the A/P, M/L, Cell Triggering Frequency and Maximum Lateral Position parameters. This particular index had the lowest total (37), thereby having the most consistently lowest (best) rank (i.e., a rank of 1). In contrast, the averaging filter produced a lowest total of 46 but also isolated the same parameter combination as being the most effective. This confirmed that the index with the A/P, M/L, Cell Triggering Frequency, and Maximum Lateral Position parameters was the most effective parameter combination, and also suggests that the median filter was the better method of filtering erroneous spike-like noise from the raw data.

Table 6.2: Ranking of data obtained with an averaging filter.

Subjects	AP ML CellTrig MaxLat	AP ML ST CellTrig MaxLat	AP ML ST CellTrig	AP ML DST ST CellTrig	AP ML DST ST	AP ML ST MaxLat	SIX PARAMS	AP ML DST ST MaxLat	AP ML DST CellTrig	AP ML DST CellTrig MaxLat	AP ML DST MaxLat
1	1	3	7	4	7	9	11	5	6	2	9
2	1	4	3	8	6	2	5	6	10	10	9
3	11	1	3	3	10	7	6	7	5	2	9
4	1	2	10	10	7	7	4	7	5	6	3
5	2	1	11	9	7	4	3	5	10	8	6
6	9	6	2	2	2	6	5	6	1	9	9
7	1	3	5	4	6	8	10	9	7	2	11
8	1	10	3	4	2	7	6	7	4	10	7
9	2	6	1	3	3	6	11	8	5	8	8
10	2	1	6	6	3	4	8	4	10	10	9
11	1	2	3	7	7	3	5	7	11	6	10
12	1	2	2	6	9	4	5	9	7	7	11
13	1	9	3	3	2	7	6	7	3	9	11
14	1	7	7	7	2	2	2	2	7	7	2
15	11	2	2	2	5	5	1	5	8	8	10
TOTAL	**46**	**59**	**68**	**78**	**78**	**81**	**88**	**94**	**99**	**104**	**124**
Rank	**1**	**2**	**3**	**4**	**4**	**6**	**7**	**8**	**9**	**10**	**11**

Table 6.3: Ranking of data obtained with a median filter.

Subjects	AP ML CellTrig MaxLat	AP ML ST CellTrig MaxLat	AP ML DST ST	AP ML ST CellTrig	AP ML ST MaxLat	AP ML DST ST MaxLat	AP ML DST ST CellTrig	SIX PARAMS	AP ML DST CellTrig MaxLat	AP ML DST CellTrig	AP ML DST MaxLat
1	1	2	6	6	6	2	2	11	5	9	9
2	1	4	6	3	2	6	8	5	9	9	11
3	1	8	6	3	10	10	3	5	7	2	9
4	1	5	7	10	7	7	10	3	6	4	2
5	2	1	3	11	7	3	9	5	8	10	6
6	11	6	4	2	8	8	2	5	6	1	8
7	1	3	7	5	8	9	4	10	2	6	11
8	1	2	4	9	6	6	9	4	2	9	6
9	2	3	9	4	1	6	10	5	8	10	6
10	1	2	6	4	3	7	8	9	5	10	11
11	1	2	5	3	3	5	5	8	9	11	10
12	1	4	5	2	3	8	6	11	10	7	9
13	1	10	2	3	6	6	3	8	10	3	9
14	1	7	2	7	2	2	7	2	7	7	2
15	11	8	1	8	8	1	1	4	5	7	5
TOTAL	**37**	**67**	**73**	**80**	**80**	**86**	**87**	**95**	**99**	**105**	**114**
Rank	**1**	**2**	**3**	**4**	**4**	**6**	**7**	**8**	**9**	**10**	**11**

Table 6.4 shows the means and standard deviations of the index values for each parameter combination, across all trials, for all subjects. The standard deviations were consistent between stability levels. The average standard deviation value was 0.143 (SD = 0.016). The range standard deviations increased from stability level 1 (average = 0.138) to stability level 4 (average = 0.156). This result is reasonable since increased variability is expected as a person becomes more unstable. When averaged across all subjects, the index that combines A/P, M/L, Cell Triggering Frequency, and Maximum Lateral Position had the largest increase in average index value between stability levels. The full set of stability index

values for each subject is given in Appendix D. The within subject standard deviations were much smaller than the between subjects results. From Table D.1, the average of the standard deviation values was 0.070 (SD = 0.047).

Table 6.4: Average stability index values across all subjects for each parameter combination. The standard deviations are in parentheses.

Parameter Combination	Stability Level			
	1	2	3	4
SIX PARAMS	0.227 (0.131)	0.273 (0.151)	0.262 (0.118)	0.401 (0.152)
AP ML DST ST CellTrig	0.224 (0.136)	0.273 (0.159)	0.269 (0.117)	0.409 (0.151)
AP ML DST ST MaxLat	0.227 (0.131)	0.272 (0.140)	0.266 (0.116)	0.402 (0.154)
AP ML DST CellTrig MaxLat	0.227 (0.131)	0.273 (0.142)	0.269 (0.116)	0.402 (0.154)
AP ML ST CellTrig MaxLat	0.232 (0.138)	0.275 (0.142)	0.272 (0.118)	0.426 (0.178)
AP ML DST ST	0.227 (0.131)	0.273 (0.142)	0.269 (0.116)	0.402 (0.154)
AP ML DST CellTrig	0.235 (0.141)	0.281 (0.150)	0.272 (0.134)	0.414 (0.154)
AP ML DST MaxLat	0.235 (0.140)	0.281 (0.145)	0.270 (0.128)	0.422 (0.139)
AP ML ST CellTrig	0.237 (0.144)	0.283 (0.150)	0.277 (0.138)	0.437 (0.152)
AP ML ST MaxLat	0.237 (0.144)	0.283 (0.145)	0.277 (0.133)	0.431 (0.153)
AP ML CellTrig MaxLat	0.245 (0.151)	0.314 (0.176)	0.322 (0.163)	0.485 (0.175)

6.2 Results of Stability Index Evaluation

The average values and standard deviations over all subjects of stability parameter values can be seen in Table 6.5. Table 6.6 shows the stability parameter values normalized to the range of each variable. The graph in Figure 6.1 demonstrates how most of the variables tended to increase with each stability level for all subjects. This graph shows values of each stability parameter averaged over all subjects for each stability level. Both ST and DST did not vary much between stability levels. The jump from the second to the third stability level showed little change in A/P, M/L, and Cell Triggering Frequency and showed a negative change in Maximum Lateral Position.

According to the data analysis in Section 5.2.4, the most effective index was the combination of A/P, M/L, Cell Triggering Frequency, and Maximum Lateral Position parameters. Figure 6.2 shows the performance of this index, as well as the combination of all six parameters, for all 15 subjects individually. According to these graphs, the index value indicated that there was a consistent drop in stability from level 1 to 4 for most subjects

(increase in index value) which meant that their stability decreased from the most to the least stable levels. Stability levels 2 and 3 displayed some inconsistencies that were largely due to an issue with the testing procedures that is discussed in Section 7.1.

Both the index of parameters A/P, M/L, Cell Triggering Frequency, and Maximum Lateral Position and the six parameters index maintained the same pattern through all subjects. The values of both indices coincided throughout all index measurements. Even though the data did not always display the expected behaviour of an increase in instability over every stability level, they did coincide in most values throughout all stability levels over all subjects.

Table 6.5: Summary of stability parameter averages and standard deviations over all subjects for each stability condition.

Stability Parameter	Stability Level				
	1	2	3	4	
AP	0.193	0.214	0.215	0.428	AVG
	0.159	0.163	0.162	0.225	SD
ML	0.387	0.478	0.486	0.544	AVG
	0.278	0.229	0.281	0.250	SD
DST (s)	0.166	0.163	0.184	0.237	AVG
	0.135	0.088	0.144	0.160	SD
ST (s)	1.101	1.161	1.193	1.234	AVG
	0.189	0.190	0.285	0.258	SD
CellTrig	0.400	0.445	0.458	0.548	AVG
	0.177	0.221	0.273	0.244	SD
MaxLat	0.069	0.220	0.170	0.311	AVG
	0.242	0.238	0.237	0.209	SD

Table 6.6: Summary of stability parameter averages and standard deviations over all subjects for each stability condition normalized to the range of each variable.

Stability Parameter	Stability Level				
	1	2	3	4	
AP	0.193	0.214	0.215	0.428	AVG
	0.159	0.163	0.162	0.225	SD
ML	0.387	0.478	0.486	0.544	AVG
	0.278	0.229	0.281	0.250	SD
DST	0.056	0.055	0.063	0.082	AVG
	0.052	0.034	0.055	0.062	SD
ST	0.197	0.212	0.220	0.228	AVG
	0.047	0.047	0.070	0.066	SD
CellTrig	0.400	0.445	0.458	0.548	AVG
	0.177	0.221	0.273	0.244	SD
MaxLat	0.069	0.220	0.170	0.311	AVG
	0.242	0.238	0.237	0.209	SD

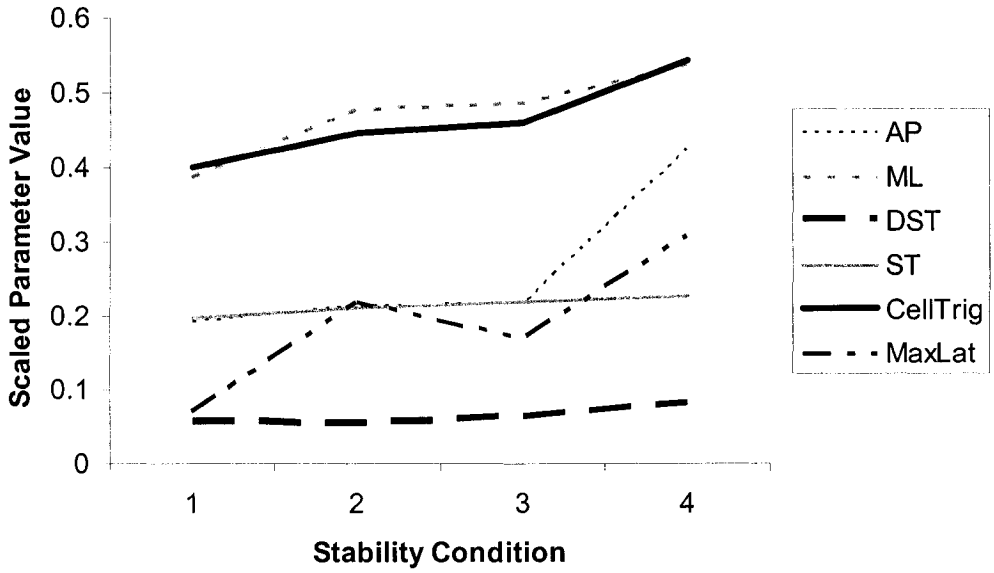

Figure 6.1: Stability parameter values, scaled from 0 to 1, versus stability condition. These values were obtained by averaging over all 15 subjects for each stability condition.

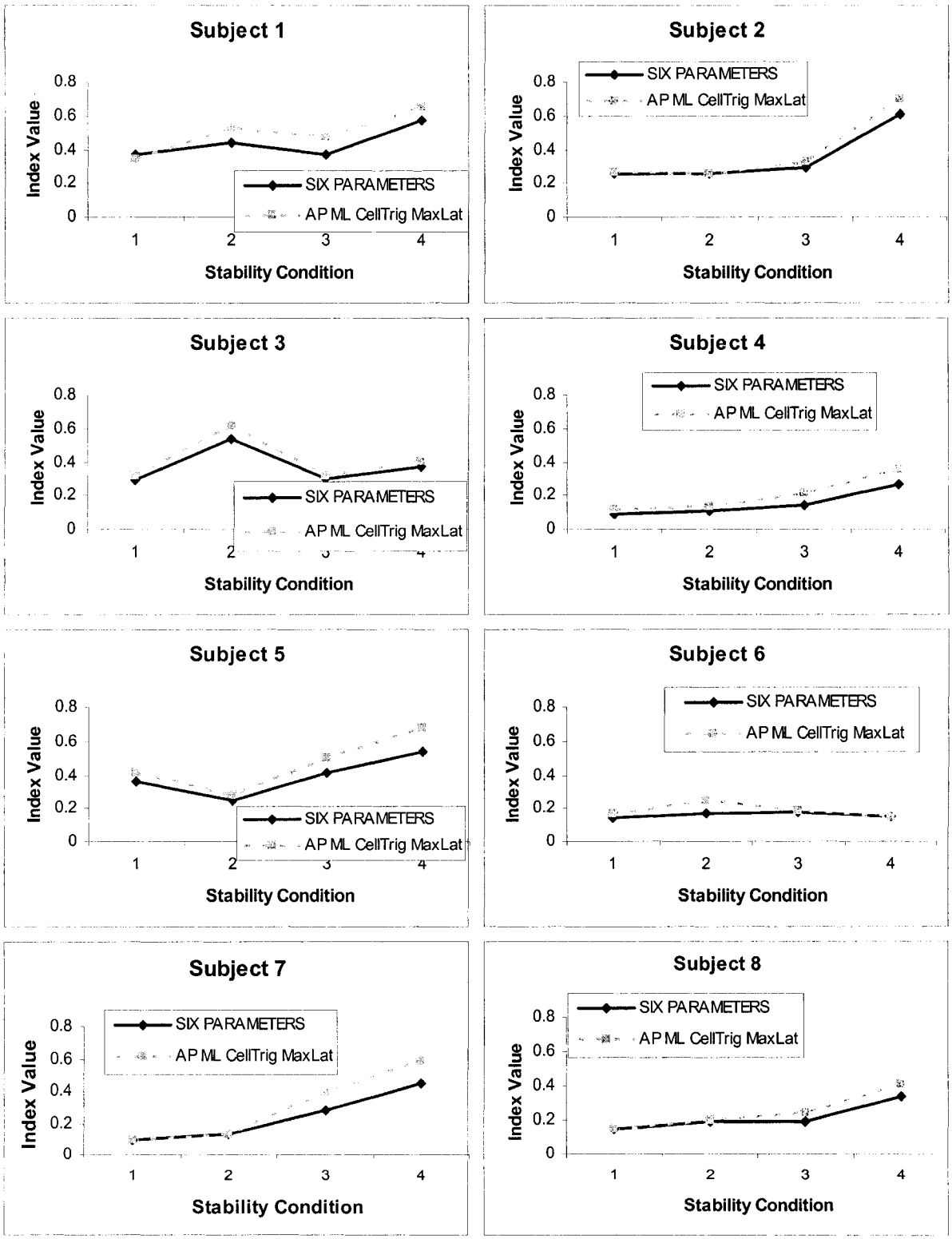
Subject 1
Index Value
0.8
0.6
0.4
0.2
0
1
2
3
4
Stability Condition
SIX PARAMETERS
AP ML CellTrig MaxLat
Subject 2
Index Value
0.8
0.6
0.4
0.2
0
1
2
3
4
Stability Condition
SIX PARAMETERS
AP ML CellTrig MaxLat
Subject 3
Index Value
0.8
0.6
0.4
0.2
0
1
2
Stability Condition
SIX PARAMETERS
AP ML CellTrig MaxLat
Subject 4
Index Value
0.8
0.6
0.4
0.2
0
1
2
3
4
Stability Condition
SIX PARAMETERS
AP ML CellTrig MaxLat
Subject 5
Index Value
0.8
0.6
0.4
0.2
0
1
2
3
4
Stability Condition
SIX PARAMETERS
AP ML CellTrig MaxLat
Subject 6
Index Value
0.8
0.6
0.4
0.2
0
1
2
3
4
Stability Condition
SIX PARAMETERS
AP ML CellTrig MaxLat
Subject 7
Index Value
0.8
0.6
0.4
0.2
0
1
2
3
4
Stability Condition
SIX PARAMETERS
AP ML CellTrig MaxLat
Subject 8
Index Value
0.8
0.6
0.4
0.2
0
1
2
3
4
Stability Condition
SIX PARAMETERS
AP ML CellTrig MaxLat

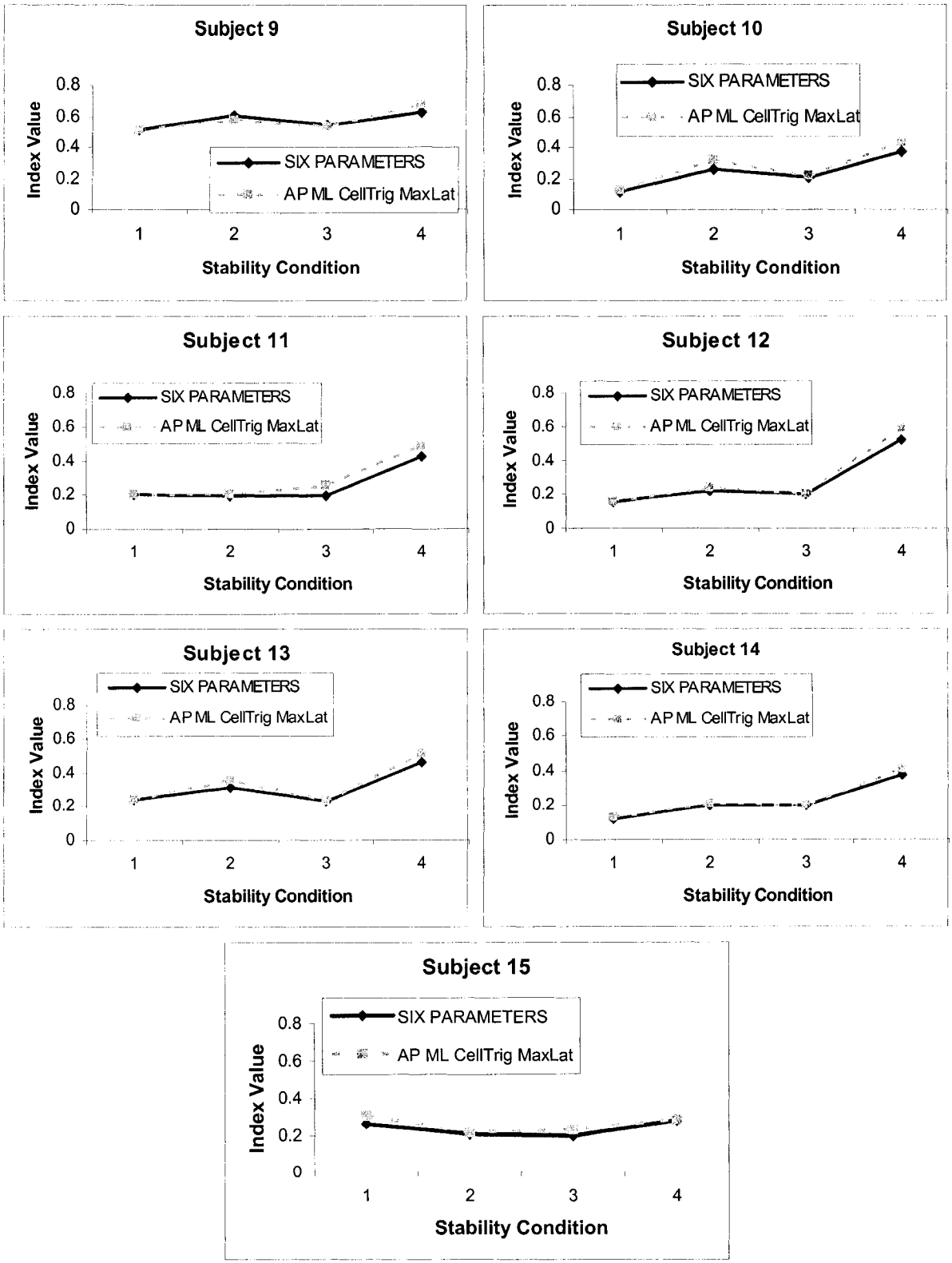

Figure 6.2: Graphs of the index combining A/P, M/L, Cell Triggering Frequency, and Maximum Lateral Position, as well as the index with all six parameters. The graphs show the performance of the indices over the four stability conditions for all 15 subjects.

Both indices, "A/P, M/L, Cell Triggering Frequency, and Maximum Lateral Position" and the "six parameters index" correctly identified the difference between the least and most stable conditions for 93.3% of the subjects. Graphs of subjects 2, 4, 7, 8, and 14 displayed the ideal behaviour (40.0% of subjects) where the stability index results were properly ordered for all four stability levels. Subjects 1, 3, 9, 10, 12, and 13 all had good results for their most and least stable trials. However, their second and third stability readings indicate that they were more stable with their eyes closed on foam than with their eyes open on foam (53.3% of subjects). This may be attributed to the testing procedure, where the "walking on foam" trials may not necessarily have produced greater instability (Section 7.1), or a learning effect between trials for conditions 2 and 3. Subjects 5 and 15 were the only people whose most stable trials did not produce the lowest reading and the least stable levels of subjects 6 and 15 were also not evaluated as least stable by the indices. These inconsistencies in data are difficult to pinpoint due to the fact that there is no gold standard for stability comparisons.

Chapter 7. Discussion

The goal of this research was to develop and clinically validate a quantitative, dynamic stability index for human locomotion. The tool was designed to be easily applied within a research and clinical setting and to be portable for use on uneven terrain, indoors/outdoors, stairs, and ramps. After an extensive literature review of gait stability assessment methods, the F-Scan Pressure Measurement System was selected as the platform for establishing a dynamic gait stability index. The gait stability parameters used for gait assessment were also evaluated and six stability parameters were selected for the index calculation.

One very important step in arriving at a valid stability index was adequately filtering the raw data. The two methods for filtering the data were an averaging filter and a median filter. The two resulting data sets only differed by an average of 0.7% (Section 5.2.4). The median filter was selected over the averaging filter by ranking the indices that were created by each filtering method. Both methods indicated the same parameter combination as the best index; however, the final index created by the median filter was a more consistently effective index in properly ranking the stability levels for each subject. This was expected because a median filter eliminates spike-like noise instead of averaging the high values. Averaging data with such spikes can artificially increase the average result. The median filter is therefore much better suited for this application.

Another crucial step was dividing the data into strides. There were constant problems associated with the automated stride division algorithm. The filtering and threshold algorithms would not remove every erroneous pressure reading (i.e., crumples in the sensor or spike-valued error) when the foot was not in contact with the ground. When these problems occurred, the F-Scan data would be manually screened frame by frame to adjust any cells that were not sensing correctly. This was a viable solution given the small population tested; however, a more effective stride division algorithm would need to be developed for future applications of the stability index.

The six stability input parameters were selected based on previous gait studies and because they were all attainable with foot pressure data. As well, the six parameters should be able to locate the main deficiencies in an unstable gait pattern. Even if someone tried to compensate, for example, by slowing down their gait in order to minimize A/P fluctuations in the COP, the parameters would adjust accordingly. The A/P fluctuations may be reduced but the stride time parameter would increase. Therefore, the system should still be able to identify the problem in the gait pattern and calculate an appropriate index.

Fuzzy logic was the final step in the creation of the index. The rationale of the fuzzy logic controller was to have a technique of combining all the stability parameters without defining any functions. A fuzzy logic controller was a good way to obtain an index given exact inputs without needing training data. This method worked well for obtaining a stability index value and also allows for future adjustment of the combination method by tuning the membership functions or the controller's rule set (Sections 2.7.2 and 2.7.3). This added control over the influence of each input parameter and made fuzzy logic a much better option than simply normalizing and averaging the parameters. Improvements can be made in the rule set by optimizing the algorithm that automatically assigns the rules. There is a possibility that the effect of some parameters may be artificially increased or decreased if the weighting scheme is incorrect. However, fine-tuning the controller can only be done once the stability parameter extraction algorithm is finalized with a larger sample of test data.

The stability index system was validated by testing healthy subjects over a range of stability-varying tasks. The least and most stable stability levels were successfully differentiated by the index; however, the stability index values could not always correctly classify the middle levels of stability (walking on foam with eyes open and walking on foam with eyes closed). This could have been a problem with the index, but is more likely an issue with the testing procedure. Figure 6.1 shows that each individual parameter did not show much difference between the second and third stability levels. It seems to indicate that the index itself may still be suitable. The subjects may have been able to adapt to the foam and therefore did not become more unstable. Since the all trials were conducted in the same order, a learning effect may have reduced differences between the eyes closed and eyes open

trials on foam. This problem could be corrected by administering the tests in a random order, and should be done for any future testing.

All parameters showed an increase from the most to least stable conditions. The similarities between the second and third stability levels were particularly visible with the Maximum Lateral Position parameter. ST and DST also show some similarities and were not included in the most effective index according to the data analysis. Since ST and DST were configured to account for the clinically documented worst-case scenario, the upper limit was probably set too high for the healthy subjects in the study (i.e., even the most unstable task did not approach the ST and DST values for highly unstable stroke patients). These parameters still showed a consistent increase through the stability levels; however, they minimally affect the index since they only varied over a fraction of their full range. This can be corrected by either altering the range of these parameters or testing a population with significantly worse gait. Unfortunately, due to a lack of preliminary testing, ethical clearance could not be obtained to test the system with the pathological gait of stroke and amputee patients. As a result, the system was only tested with induced gait instability to simulate disability in healthy subjects. However, it is quite possible that the gait of healthy subjects that are dizzy, blindfolded and walking on foam may not compare to the impaired gait of a patient who has just had a stroke. The ranges of the ST and DST variables were not altered to fit the range of the healthy subjects because the index should be applicable to clinical patients. By prematurely eliminating part of the range, the index may not be as effective when dealing with stroke or amputee patients in the future. Therefore, the ranges of the variables should only be altered once data is collected with pathological gait.

The stability indices were able to classify most induced instability levels. The best index was identified as the combination of the A/P, M/L, Cell Triggering Frequency and Maximum Lateral Position parameters; however, the combination of all six parameters was also considered. As mentioned earlier, the reason for the exclusion of ST and DST are likely due to the method of inducing instability in healthy subjects. Therefore, it would be beneficial to maintain all six stability parameters in the index calculation pending further clinical testing. There were some problems with the second and third stability levels, but in

general the indices were able to properly classify the index values into the appropriate stability levels. The indices were able to properly order all four stability levels for 40.0% of subjects, while 53.3% of the subjects had the second and third stability levels reversed as mentioned earlier. The indices correctly identified the difference between the least and most stable conditions for 93.3% of the subjects. The reason for the discrepancies in the data is difficult to determine. Altering the fuzzy logic controller rule set and membership functions would be another method of adjusting the calculated stability indices. However, more test data is needed to identify if the result lies in the simulated instability conditions, with the subjects' adaptation or approach to the anticipated instability in the walking tasks, in the selection of parameters used in the stability index or in the method of calculation of the stability index itself.

7.1 Limitations

The major limitation with this study was the lack of a gold standard for measuring stability. With no absolute comparison, the accuracy of the calculated indices could not be directly measured. As well, with no gold standard there was no way to accurately characterize each stability level used in the testing. The only assertion that could be made was that the stability of a person should decrease over the four simulated instability levels. Therefore, stability index values could not be compared across all subjects. The stability values could only be analyzed for each person individually (i.e., four data points at a time) which resulted in a much smaller data set that could be used to compare each stability parameter combination.

Another problem was that the four distinct stability levels did not always create measurable differences in gait stability. Stability levels two and three were based on walking on foam with eyes open and eyes closed. During testing, subjects could have learned to adapt to the foam, and since there was only a slight difference in the outcome data for the trials, these two stability levels were possibly not as different as anticipated. As mentioned above, subjects may also have anticipated instability and therefore walked more cautiously with eyes closed than when open. As a result, the main comparison for each stability index was the best and worst stability level. Future gait trials should be performed in random order to eliminate the possibility of subjects adapting to the simulated instability condition. Another

approach would be to create instability conditions that would not be known to the subjects themselves even when they begin each trial.

Clinical testing was also affected by variability. Subjects were asked to walk at their comfortable pace, however the speed at which they chose to walk would unavoidably affect their stability. If a subject were to try to walk faster while dizzy, they would likely be more unstable than someone who slowed down to stabilize themselves. The walking speed of the subjects was not measured since the ST parameter should change accordingly and adjust the index. However, due to the low reaction of this parameter, the speed chosen by the subjects may have been a source of variability that was not fully accounted for. As well, subjects were made dizzy by spinning them until they asked to stop. However, some subjects may have been able to handle more spins, and as a result, would have had much worse stability readings for the least stable trial. Conversely, some subjects may not have liked the dizzy feeling and stopped after fewer spins that would have given them a much more stable gait pattern for their least stable condition.

Another limitation of the study was the test population. There was a lack of preliminary testing since the gait stability index system was also created in this study. Therefore, ethical clearance could not be obtained for testing stroke and amputee patients with pathological gait. The induced instability of healthy subjects proved that the index works and can differentiate between certain levels of instability. However, a much better comparison would be to observe the gait of patients periodically throughout their rehabilitation. Clinical observational measures could be taken at the same time as the stability index measures to provide a much more accurate gauge of the sensitivity of the system.

7.2 Future Work

The dynamic gait stability index is a system that can be used as an accurate and quantitative measurement of gait stability in a clinical setting. However, further testing is necessary to ensure its accuracy and reliability.

7.2.1 Future Clinical Testing

Stroke and amputee patients with pathological gait exhibit more perturbations in plantar pressure and stability than induced instability in healthy subjects. Although the clinical testing validated the dynamic gait stability index system, it would be useful to obtain clinical data using the appropriate subject base and testing them periodically throughout their rehabilitation. Having plantar pressure data from stroke and amputee patients would allow for the further development of the stability index and would confirm its effectiveness on the intended population.

7.2.2 Future Technical Work

Dividing the strides of the subject's gait is a crucial step in calculating an accurate stability index. Currently, the stride division algorithm has some flaws where small crumples in the sensor still cause considerable errors. Further development of the stride division and filtering algorithms is necessary to completely eliminate these problems.

The fuzzy logic controller is another aspect of the system that could be fine tuned. The system has been set up so that the combination method can be easily reconfigured. The rule set and membership functions can be altered to make minor adjustments to the final output of the system. However, before tuning the fuzzy logic controller, a larger sample of test data is necessary to finalize the stability parameter extraction algorithm.

Finally, to be able to create a commercially viable system, the code should be integrated into one system. Currently, the system is run on two platforms: the stability parameter extraction is done with VB6 and the fuzzy logic controller is written in Matlab. A more user-friendly interface that incorporates the entire system might be necessary to create a finished product.

Chapter 8. Conclusions

The purpose of this study was to design and validate a system that obtains a quantitative index through the dynamic plantar pressure analysis of human gait. This system can be made portable and provides a fast and easy method to obtain an objective gait stability measurement.

The system was validated by inducing instability in healthy subjects to create four distinct levels of gait stability. Testing revealed that the index can successfully differentiate between the four levels of simulated instability. The indices were able to properly order all four stability levels for 40.0% of subjects. For 53.3% of the subjects, the second and third stability levels were reversed, possibly due to walking adaptations made during multiple-trial testing. The indices correctly identified the difference between the least and most stable conditions for 93.3% of the subjects. Future testing of the system should involve periodically testing patients throughout their rehabilitation and comparing stability index results with clinically observational measures.

Six stability parameters were chosen based on a thorough literature review and were isolated by the index. The parameters quantitatively measure various aspects of gait that may indicate instability. These parameters were combined using a fuzzy logic controller to produce a singe index that proved to be a viable combination method. All combinations of stability parameters were ranked based on their ability to distinguish between stability levels. The most effective index was the A/P, M/L, Cell Triggering Frequency, and Maximum Lateral Position parameters. ST and DST were the two parameters omitted by the data analysis as they did not seem to vary sufficiently with the stability levels. However, the reason behind the low response of these parameters is believed to be a result of testing only healthy subjects. The induced instability did not adequately hinder the speed of the subjects. Therefore, all six parameters should be used to calculate the index until further clinical testing can be done with the appropriate population.

Chapter 9. References

[1] Sabata D, Pynoos J. Home Environmental Modification: Preventing Falls at Home. http://www.homemods.org/folders/presentation%20archive/Fall.prev.dc.pdf [verified September 21, 2006].

[2] Falls and Hip Fractures Among Older Adults. http://www.cdc.gov/ncipc/factsheets/falls.htm [verified March 1, 2006].

[3] Report on Injuries in America – 2003. http://www.nsc.org/nsm/research.htm [verified March 1, 2006].

[4] Merriam-Webster On-Line Dictionary. http://www.m-w.com/dictionary.htm [verified March 1, 2006].

[5] Considine GD, Kulik PH. "Van Nostrand's Scientific Encyclopedia – Ninth Edition – Volume 2," Wiley-Interscience John Wiley & Sons Inc., New York, 2002.

[6] Yim-Chiplis PK, Talbot LA. Defining and measuring balance in adults. *Biological Research for Nursing*, Apr 2000; 1 (4): 321-331.

[7] University of Glasgow – Institute of Biomedical and Life Sciences. www.gla.ac.uk/ibls/ fab/glossary/anterior.html [verified March 1, 2006].

[8] Dalhousie University – Department of Mechanical Engineering. www.me.dal.ca/ ~dp_03_8/rev2.html [verified March 1, 2006].

[9] Ellis W, Kishner S, Laborde JM. E-Medicine – Instant Access to the Minds of Medicine - http://www.emedicine.com/orthoped/topic633.htm [verified March 1, 2006].

[10] Morton SM, Bastian AJ. Relative contributions of balance and voluntary leg-coordination deficits to cerebellar gait ataxia. *Journal of Neurophysiology*, 2003; 89: 1844-1856.

[11] Pribut SM. Dr. Stephen M. Pribut's Sport Pages. www.drpribut.com/sports/spgait.html [verified March 1, 2006].

[12] Redmond A, Lumb PSB, Landorf K. Effect of cast and non-cast foot orthoses on plantar pressure and force during normal gait, *Journal of the American Podiatric Medical Association*, 2000; 90 (9): 441-449.

[13] Steenwyk - Custom Shoes & Orthotics – Pronation and Supination. http://www.steenwyk.com/pronsup.htm [verified March 1, 2006].

[14] Sports Medicine Health Topics. http://www.med.umich.edu/1libr/sma/sma_pronatio_art.htm [verified March 1, 2006].

[15] Whittle MW, "Gait Analysis – An Introduction," Butterworth-Heinemann, Oxford, 1996.

[16] Smith BT, Coiro DJ, Finson R, Betz RR, McCarthy J. Evaluation of force-sensing resistors for gait event detection to trigger electrical stimulation to improve walking in the child with cerebral palsy. *IEEE Transactions on Neural Systems and Rehabilitation Engineering*, 2002; 10 (1): 22-29.

[17] Silva F, Tenreiro Machado JA. Controllability analysis of biped walking robots. *Proceedings of 6th International Workshop on Advanced Motion Control*, 2000: 595-600.

[18] Nevill AJ, Pepper MG, Whiting M. In-shoe foot pressure measurement system utilizing piezoelectric film transducers. *Medical and Biological Engineering and Computing*, 1995; 33 (1): 76-81.

[19] Bowen TR, Miller F, Castagno P, Richards J, Lipton G. A method of dynamic foot-pressure measurement for the evaluation of pediatric orthopaedic foot deformities, *Journal of Pediatric Orthopaedics*, 1998; 18 (6): 789-793.

[20] Liu XC, Thometz JG, Tassone C, Barker B, Lyon R. Dynamic plantar pressure measurement for the normal subject: Free-mapping model for the analysis of pediatric foot deformities, *Journal of Pediatric Orthopaedics*, 2005; 25 (1): 103-106.

[21] Clinician's Corner – Basic Anatomic Terms. http://www.footmaxx.com/clinicians/anatomic.html [verified March 1, 2006].

[22] Urry S. Plantar pressure-measurement sensors. *Measurement Science and Technology*, 1999; 10: R16-R32.

[23] Bryant AR, Tinley PT, Singer KP. Normal values of plantar pressure measurements determined using the EMED-SF system, *Journal of the American Podiatric Medical Association*, 2000; 90 (6): 295-299.

[24] Olrin MN, McPoil TG. Plantar pressure assessment, *Physical Therapy*, 2000; 80: 399-409.

[25] Lavery LA, Vela SA, Fieischli JG, Armstrong DG, Lavery DC. Reducing plantar pressure in the neuropathic foot, *Diabetes Care*, 1997; 20: 1706-1710.

[26] Mechanical Engineering Research. http://mech.skku.ac.kr/sub3_2_8.html [verified March 1, 2006].

[27] Segal A, Rohr E, Orendurff M, Shofer J, O'Brien M, Sangeorzan B. The effect of walking speed on peak plantar pressure, *Foot and Ankle International*, 2004; 25 (12): 926-33.

[28] Bennett PJ, Duplock LR. Pressure distribution beneath the human foot, *Journal of the American Podiatric Medical Association*, 1993; 83 (12): 674-678.

[29] Quesada PM, Rash GS. Simultaneous pedar and S-Scan plantar pressure measurement during walking, *Gait and Posture*, 1997; 5 (2): 164-165.

[30] Zhu H, Harris GF, Wertsch JJ, Tompkins WJ, Webster JG. A microprocessor-based data-acquisition system for measuring plantar pressures from ambulatory subjects, *IEEE Transactions on Biomedical Engineering*, 1991; 38 (7): 710-714.

[31] Zequra ML, Solomonidis SE, Vega F, Rondon LM. Study of the plantar pressure distribution on the sole of the foot of normal and diabetic subjects in the early stages by using a hydrocell pressure sensor, *Proceedings of the 25th Annual International Conference of the IEEE EMBS*, 2003: 1874-1877.

[32] Weijers RE, Walenkamp GHIM, van Mameren H, Kessels AGH. The relationship of the position of the metatarsal heads and peak plantar pressure, *Foot and Ankle International*, 2003; 24 (4): 349-353.

[33] Dayton P, Goldman FD, Barton E. Compartment pressure in the foot, *Journal of the American Podiatric Medical Association*, 1990; 80 (10): 521-525.

[34] Brown M, Rudicel S, Esquenazi A. Measurement of dynamic pressure at the shoe-foot interface during normal walking with various foot orthoses using the FSCAN system, *Foot and Ankle International*, 1996; 17 (3): 152-156.

[35] Bryant A, Singer K, Tinley P. Comparison of the reliability of plantar pressure measurements using the two-step and midgait methods of data collection, *Foot and Ankle International*, 1999; 20 (10): 646-650.

[36] Anemaet WK, Moffa-Trotter ME. Functional tools for assessing balance and gait impairments. *Topics in Geriatric Rehabilitation*, 1999; 15 (1): 66-83.

[37] Lin SI, Lin RM. Sensorimotor and balance function in older adults with lumber nerve root compression. *Clinical Orthopaedics and Related Research*, 2002; 394: 146-153.

[38] Baloh RW. Disequilibrium and gait disorders in older people. *Reviews in Clinical Gerontology*, 2002; 12: 21-30.

[39] Gerdhem P, Ringsberg KAM, Akesson K, Obrant KJ. Clinical history and biologic age predicted falls better than objective functional tests. *Journal of Clinical Epidemiology*, 2005; 58: 226-232.

[40] Sullivan EV, Rosenbloom MJ, Pfefferbaum A. Balance and gait deficits in schizophrenia compounded by the comorbidity of alcoholism. *American Journal of Psychiatry*, 2004; 161 (4): 751-755.

[41] Bueno-Cavanillas A, Padilla-Ruiz F, Jimenez-Moleon JJ, Peinado-Alonso CA, Galvez-Vargas R. Risk factors in falls among the elderly according to extrinsic and intrinsic precipitating causes. *European Journal of Epidemiology*, 2000; 16: 849-859.

[42] Sullivan EV, Rosenbloom MJ, Lim KO, Pfefferbaum A. Longitudinal changes in cognition, gait, and balance in abstinent and relapsed alcoholic men: Relationships to changes in brain structure. *Neuropsychology*, 2000; 14 (2): 178-188.

[43] Hill K, Schwarz J, Flicker L, Carroll S. Falls among healthy, community-dwelling, older women: a prospective study of frequency, circumstances, consequences and prediction accuracy. *Australian and New Zealand Journal of Public Health*, Feb 1999; 23 (1): 41-48.

[44] Magliozzi Giorgetti M, Harris BA, Jette A. Reliability of clinical balance outcome measures in the elderly. *Physiotherapy Research International*, 1998; 3 (4): 274-283.

[45] Topp R, Mikesky A, Wigglesworth J, Holt Jr. W, Edwards JE. The effect of a 12-week dynamic resistance strength training program on gait velocity and balance of older adults. *The Gerontologist*, 1993; 33 (4): 501-506.

[46] Dickstein R, Zaslanski R, Heffes Y, Mizrachi E, Shabtai EL, Abulaffio N. Somatosensory evoked potentials of the posterior tibial nerve in hemiparetic patients: Relation to stance balance and walking ability. *American Journal of Physical Medicine and Rehabilitation,* 1997; 78: 1125-1128.

[47] Sjostrom H, Allum JHJ, Carpenter M, Adkin A, Honegger F, Ettlin T. Trunk sway measures of postural stability during clinical balance tests in patients with chronic whiplash injury symptoms. *Spine*, 2003; 28: 1725-1734.

[48] Fiolkowski P, Brunt D, Bishop M, Woo R. Does postural instability affect the initiation of human gait? *Neuroscience Letters*, 2002; 323: 167-170.

[49] Herdman SJ, Schubert MC, Tusa RJ. Strategies for balance rehabilitation – Fall risk and treatment. *Annals New York Academy of Sciences*, 2001: 394-412.

[50] Stalenhoef PA, Diederiks JPM, Knottnerus JA, Kester ADM, Crebolder HFJM. A risk model for the prediction of recurrent falls in community-dwelling elderly: A prospective cohort study. *Journal of Clinical Epidemiology*, 2002; 55: 1088-1094.

[51] Herman T, Giladi N, Gurevich T, Hausdorff JM. Gait instability and fractal dynamics of older adults with a "cautious" gait: why do certain older adults walk fearfully? *Gait and Posture*, 2005; 21: 178-185.

[52] Baloh RW. Disequilibrium and gait disorders in older people, *Reviews in Clinical Gerontology*, 1996; 6: 41-48.

[53] Levo H, Blomstedt G, Pyykko I. Postural stability after vestibular Schwannoma surgery. *Annals of Otology, Rhinology and Laryngology* , 2004; 113: 994-999.

[54] Zelczak TA. The Neurologic Examination. http://www.opt.pacificu.edu/ce/catalog/COPE9462/Neuro_Zelczak.html [verified March 1, 2006].

[55] Duckrow RB, Abu-Hasaballah K, Whipple R, Wolfson L. Stance perturbation-evoked potentials in old people with poor gait and balance. *Clinical Neurophysiology*, 1999; 110: 2026-2032.

[56] Shimada H, Uchiyama Y, Kakurai S. Specific effects of balance and gait exercises on physical function among the frail elderly. *Clinical Rehabilitation*, 2003; 17: 472-479.

[57] Mak MK, Ng PL. Mediolateral sway in single-leg stance is the best discriminator of balance performance for tai-chi practitioners. *American Journal of Physical Medicine and Rehabilitation*, 2003; 84: 683-686.

[58] Adkin AL, Frank JS, Jog MS. Fear of falling and postural control in Parkinson's Disease. *Movement Disorders*, 2003; 18 (5): 496-502.

[59] Lim LIIK, van Wegen EEH, de Goede CJT, Jones D, Rochester L, Hetherington V, Nieuwboer A, Willems AM, Kwakkel G. Measuring gait and gait-related activities in Parkinson's patients own home environment: a reliability, responsiveness and feasibility study. *Parkinsonism and Related Disorders*, 2005; 11: 19-24.

[60] Li F, Harmer P, Fisher KJ, Mcauley E. Tai Chi: Improving functional balance and predicting subsequent falls in older persons. *Official Journal of the American College of Sports Medicine*, 2004; 2046-2052.

[61] Lindemann U, Muche R, Becker C. Improving balance by improving motor skills. *Zeitschrift für Gerontologie und Geriatrie*, 2004; 37: 20-26.

[62] Roberts-Warrior D, Overby A, Jankovic J, Olson S, Lai EC, Krauss JK, Grossman R. Postural control in Parkinson's disease after unilateral posteroventral pallidotomy. *Brain*, 2000; 123: 2141-2149.

[63] Cattaneo D, De Nuzzo C, Fascia T, Macalli M, Pisoni I, Cardini R. Risks of falls in subjects with Multiple Sclerosis. *American Journal of Physical Medicine and Rehabilitation*, 2002; 83: 864-867.

[64] Dite W, Temple VA. A clinical test of stepping and change of direction to identify multiple falling older adults. *American Journal of Physical Medicine and Rehabilitation*, Nov 2002; 83: 1566-1571.

[65] Hughes MA, Duncan PW, Rose DK, Chandler JM, Studenski SA. The relationship of postural sway to sensorimotor function, functional performance, and disability in the elderly, *American Journal of Physical Medicine and Rehabilitation,* June 1996; 77: 567-572.

[66] Duncan PW, Weiner D, Chandler J, Studensnski S. Dunctional reach: a new clinical measure of balance. *Journal of Gerontology*, 1990; 45: M192-M197.

[67] Wernick-Robinson M, Krebs DE, Giorgetti MM. Functional reach: Does it really measure dynamic balance? *American Journal of Physical Medicine and Rehabilitation*, 1999; 80: 262-269.

[68] Basford JR, Chou LS, Kaufman KR, Brey RH, Walker A, Malec JF, Moessner AM, Brown AW. An assessment of gait and balance deficits after traumatic brain injury. *American Journal of Physical Medicine and Rehabilitation,* 2003; 84: 343-349.

[69] Bruyere O, Wuidart MA, Palma ED, Gourlay M, Ethgen O, Richy F, Reginster JY. Controller whole-body vibration to decrease fall risk and improve health-related quality of life of nursing home residents. *American Journal of Physical Medicine and Rehabilitation,* 2005; 86: 303-307.

[70] Najafi B, Aminian K, Loew F, Blanc Y, Robert PA. Measurement of stand-sit and sit-stand transitions using a miniature gyroscope and its application in fall risk evaluation in the elderly. *IEEE Transactions on Biomedical Engineering*, 2002; 49 (8): 843-851.

[71] Hasan S, Lichtenstein MJ, Shiavi RG. Effect of loss of balance on biomechanics platform measures of sway: Influence of stance and a method for adjustment. *Journal of Biomechanics*, 1990; 23 (8): 783-789.

[72] Berg K, Norman KE. Functional assessment of balance and gait. *Clinics in Geriatric Medicine*, 1996; 12 (4): 705-723.

[73] Corna S, Nardone A, Prestinari A, Galante M, Grasso M, Schieppati M. Comparison of Cawthorne-Cooksey exercises and sinusoidal support surface translations to improve balance in patients with unilateral vestibular deficit. *American Journal of Physical Medicine and Rehabilitation,* 2003; 84: 1173-1184.

[74] Thomas M, Jankovic J, Suteerawattananon M, Wankadia S, Salomi Caroline K, Dat Vuong K, Protas E. Clinical gait and balance scale (GABS): validation and utilization. *Journal of the Neurological Sciences*, 2004; 217: 89-99.

[75] Hall CD, Schubert MC, Herdman SJ. Prediction of fall risk reduction as measured by dynamic gait index in individuals with unilateral vestibular hypofunction. *Otology & Neurology*, 2004; 25: 746-751.

[76] Shumway-Cook A, Baldwin M, Polissar NL, Gruber W. Predicting the probability for falls in community-dwelling older adults. *Physical Therapy*, 1997; 77: 812-819.

[77] Whitney SL, Hudak MT, Marchetti GF. The dynamic gait index relates to self-reported fall history in individuals with vestibular dysfunction. *Journal of Vestibular Research*, 2000; 10: 99-105.

[78] Whitney SL, Wrisley DM. The influence of footwear on timed balance scores of the modified clinical test of sensory interaction and balance. *American Journal of Physical Medicine and Rehabilitation,* 2004; 85: 439-443.

[79] McConvey J, Bennet SE. Reliability of the Dynamic Gait Index in individuals with Multiple Sclerosis, *American Journal of Physical Medicine and Rehabilitation,* 2005; 86: 130-133.

[80] Badke MB, Shea TA, Miedaner JA, Grove CR. Outcomes after rehabilitation for adults with balance dysfunction, *American Journal of Physical Medicine and Rehabilitation,* 2004; 85: 227-233.

[81] Boulgarides LK, McGinty SM, Willett JA, Barnes CW. Use of clinical and impairment-based tests to predict falls by community-dwelling older adults. *Physical Therapy*, 2003; 83 (4): 328-339.

[82] Wrisley DM, Marchetti GF, Kuharsky DK, Whitney SL. Reliability, internal consistency, and validity of data obtained with the functional gait assessment. *Physical Therapy*, 2004; 84 (10): 906-918.

[83] Mao HF, Hsueh IP, Tang PF, Sheu CF, Hsieh CL. Analysis and comparison of the psychometric properties of three balance measures for stroke patients. *Stroke*, 2002; 33: 1022-1027.

[84] Cole B, Finch E, Gowland C, Mayo N, "Physical Rehabilitation Outcome Measures," Canadian Physiotherapy Association, Toronto, Ontario, 1994.

[85] Podsiadlo D, Richardson S. The Timed "Up and Go": A test of basic functional mobility for frail elderly persons. *Journal of the American Geriatrics Society*, 1991; 39: 142-148.

[86] Laufer Y. Effects of one-point and four-point canes on balance and weight distribution in patients with hemiparesis. *Clinical Rehabilitation*, 2002; 16: 141-148.

[87] Berg KO, Kairy D. Balance interventions to prevent falls. *Generations*, Winter 2002/2003; 26 (4): 75-78.

[88] Melzer I, Benjuya N, Kaplanski J. Postural stability in the elderly: a comparison between fallers and non-fallers. *Age and Aging*, 2004; 33 (6): 602-607.

[89] Butcher SJ, Meshke JM, Sheppard MS. Reduction in functional balance, coordination, and mobility measures among patients with stable chronic obstructive pulmonary disease. *Journal of Cardiopulmonary Rehabilitation*, 2004; 24: 274-280.

[90] Cohen HS, Kimball KT. Decreased ataxia and improved balance after vestibular rehabilitation. *Otolaryngology - Head and Neck Surgery*, 2004; 130: 418-425.

[91] Salbach NM, Mayo NE, Higgins J, Ahmed S, Finch LE, Richards CL. Responsiveness and predictability of gait speed and other disability measures in acute stroke. *American Journal of Physical Medicine and Rehabilitation,* 2001; 82: 1204-1212.

[92] Geiger RA, Allen JB, O'keefe J, Hicks RR. Balance and mobility following stroke: effects of physical therapy interventions with and without biofeedback/force plate training. *Physical Therapy*, 2001; 81 (4): 995-1005.

[93] Liston RA, Brouwer BJ. Reliability and validity of measures obtained from stroke patients using the Balance Master. *American Journal of Physical Medicine and Rehabilitation,* 1996; 77 (5): 425-430.

[94] Trader SE, Newton RA, Cromwell RL. Balance abilities of homebound older adults classified as fallers and nonfallers. *Journal of Geriatric Physical Therapy*, 2003; 26 (3): 3-8.

[95] Lim LIIK, van Wegen EEH, de Goede CJT, Jones D, Rochester L, Hetherington V, Nieuwboer A, Willems AM, Kwakkel G. Measureing gait and gait-related activities in Parkinson's patients own home environment: a reliability, responsiveness and feasibility study. *Parkinsonism and Related Disorders*, 2005; 11: 19-24.

[96] Rosengren KS, McAuley E. Gait adjustments in older adults: Activity and efficacy influences. *Psychology and Aging*, 1998; 13 (3): 375-386.

[97] Lord SE, Halligan PW, Wade DT. Visual gait analysis: the development of a clinical assessment and scale. *Clinical Rehabilitation*, 1998; 12: 107-119.

[98] Pomeroy VM, Evans B, Falconer M, Jones D, Hill E, Giakas G. An exploration of the effects of weighted garments on balance and gait of stroke patients with residual disability. *Clinical Rehabilitation*, 2001; 15: 390-397.

[99] Rochester L, Hetherington V, Jones D, Nieuwboer A, Willems AM, Kwakkel G, Van Wegen E. Attending to the task: Interference effects of functional tasks on waking in Parkinson's Disease and the roles of cognition, depression, fatigue and balance. *American Journal of Physical Medicine and Rehabilitation,* 2004; 85: 1578-1585.

[100] Garland SJ, Willems DA, Ivanova TD, Miller KJ. Recovery of standing balance and functional mobility after stroke, *American Journal of Physical Medicine and Rehabilitation,* 2003; 84: 1753-1759.

[101] Timonen L, Rantanen T, Ryynanen OP, Taimela S, Timonen TE, Sulkava R. A randomized controlled trial of rehabilitation after hospitalization in frail older women: effects on strength, balance and mobility. *Scandinavian Journal of Medicine and Science in Sports*, 2002; 12: 186-192.

[102] Hahn ME, Chou LS. Age-related reduction in sagittal place center of mass motion during obstacle crossing. *Journal of Biomechanics*, 2004; 37: 837-844.

[103] Duarte E, Marco E, Muniesa JM, Belmonte R, Diaz P, Tejero M, Escalada F. Trunk control test as a functional predictor in stroke patients. *Journal of Rehabilitation Medicine*, 2002; 34: 267-272.

[104] Finch E, Brooks D, Stratford PW, Mayo NE. "Physical Rehabilitation Outcome Measures, Second Edition – A Guide to Enhanced Clinical Decision Making." Canadian Physiotherapy Association, Toronto, Ontario, 2002.

[105] Department of Environmental Health – University of Cincinnati. http://www.eh.uc.edu/lowbackstresslab/FORCEPLATETRIAL.htm [verified March 1, 2006].

[106] University of Washington – Computer Science and Engineering. http://www.cs.washington.edu/homes/zoran/mocap/ [verified March 1, 2006].

[107] Janz KF. Validation of the CSA accelerometer for assessing children's physical activity. *Medicine and Science in Sports and Exercise*, 1994; 26 (3): 369-375.

[108] Moe-Nilssen R, Helbostad JL, Talcott JB, Toennessen FE. Balance and gait in children with dyslexia. *Experimental Brain Research*, 2003; 150: 237-244.

[109] Yack HJ, Berger RC. Dynamic stability in the elderly: Identifying a possible measure. *Journal of Gerontology*, 1993; 48 (5) M225-M230.

[110] Viksraitis S, Norkus T, Astrauskas T, Kaikaris V, Rimdeika R, Averkina S. Free musculocutaneous and muscle flaps for foot reconstruction: a clinical and gait analysis study. *European Journal of Plastic Surgery*, 2000; 23 (11): 111-116.

[111] Orlin MN, McPoil TG. Plantar Pressure Assessment. *Physical Therapy*, 2000; 80 (4): 399-409.

[112] Schaff PS. An overview of foot pressure measurement systems. *Clinics in Podiatric Medicine and Surgery*, 1993; 10 (3): 403-415.

[113] Davis BL, Cothren RM, Quesada P, Hanson SB, Perry JE. Frequency content of normal and diabetic plantar pressure profiles: Implications for the selection of transducer sizes, *Journal of Biomechanics*, 1996; 29 (7): 979-983.

[114] Novel – Product Information. http://www.novel.de/productinfo/systems-pedar.htm [verified March 1, 2006].

[115] Birke JA, Foto JG, Pfiefer LA. Effect of orthosis material hardness on walking pressure in high-risk diabetes patients. *Journal of Prosthetics and Orthotics*, 1999; 11 (2): 43-49.

[116] Nevill AJ, Pepper MG, Whiting M. In-shoe foot pressure measurement system utilizing piezoelectric film transducers. *Medical and Biological Engineering and Computing*, 1995; 33 (1): 76-81.

[117] Chodera J. Pedobarograph – apparatus for visual display of pressures beneath contacting surfaces of irregular shapes, CZS patent 10451430D, 1960.

[118] Betts RP, Duckworth T. A device for measuring plantar foot pressures under the sole of the foot, *Engineering Medicine*, 1978; 7: 223-228.

[119] Arcan M, Brull A. A fundamental characteristic of the human body and foot, the foot-ground pressure pattern. *Journal of Biomechanics*, 1976; 9: 453-457.

[120] Stilson T. Force Sensing Resistors http://ccrma.stanford.edu/CCRMA/Courses/252/sensors/node8.html [verified March 1, 2006].

[121] Force-sensitive resistor. http://www.sensorwiki.org/index.php/Force-sensitive_resistor_(FSR) [verified March 1, 2006].

[122] Sumiya T, Suzuki Y, Kasahara T, Ogata H. Sensing stability and dynamic response of the F-Scan in-shoe sensing system: A technical note. *Journal of Rehabilitation Research and Development*, June 1998; 35 (2): 192-200.

[123] Tekscan - Untethered In-Shoe Plantar Pressure/Force Measurement. http://www.tekscan.com/medical/system_mobile.html [verified March 1, 2006].

[124] Harris GF, Wertsch JJ. Procedures for gait analysis. *Archives of Physical Medicine and Rehabilitation*, 1994; 75: 216-225.

[125] Chen B, Bates BT. Comparison of F-Scan in-sole and AMTI force plate system in measuring vertical ground reaction force during gait. *Physiotherapy Theory and Practice*, 2000; 16: 43-53.

[126] Han TR, Paik NJ, Im MS. Quantification of the path of the center of pressure (COP) using an F-Scan in-shoe transducer. *Gait and Posture*, 1999; 10: 248-254.

[127] Lord M, Reynolds DP, Hughes JR. Foot pressure measurement: A review of clinical findings. *Journal of Biomedical Engineering*, 1986; 8 (4): 283-294.

[128] Turnbull Gi, Charteris J, Wall JC. Deficiencies in standing weight shifts by ambulant hemiplegic subjects. *American Journal of Physical Medicine and Rehabilitation,* 1996; 77: 356-362.

[129] de Haart M, Geurts AC, Huidekoper SC, Fasotti L, van Limbeek J. Recovery of standing balance in postacute stroke patients: A rehabilitation cohort study. *American Journal of Physical Medicine and Rehabilitation,* 2004; 85: 886-895.

[130] Rose J, Wolff DR, Jones VK, Bloch DA, Oehlert JW, Gamble JG. Postural balance in children with cerebral palsy. *Developmental Medicine & Child Neurology*, 2002; 44: 58-63.

[131] Wagenaar RC, Holt KG, Kubo M, Ho CL. Gait risk factors for falls in older adults: A dynamic perspective. *Generations*, Winter 2002/2003; 26 (4): 28-32.

[132] Ferdjallah M, Harris GF, Smith P, Wertsch JJ. Analysis of postural control synergies during quiet standing in healthy children and children with cerebral palsy. *Clinical Biomechanics*, 2002; 17: 203-210.

[133] Seifer CM, Parry SW. Monitoring devices for falls and syncope. *Clinics in Geriatric Medicine*, 2002; 18: 295-306.

[134] Ringsberg K, Gerdhem P, Johansson J, Obrant KJ. Is there a relationship between balance, gait performance and muscular strength in 75-year-old women? *Age and Ageing*, 1999; 28: 289-293.

[135] Patton JL, Pai YC, Lee WA. Evaluation of a model that determines the stability limits of dynamic balance. *Gait & Posture*, 1999; 9 (1): 38-49.

[136] Bauby CE, Kuo AD. Active control of lateral balance in human walking. *Journal of Biomechanics*, 2000; 33: 1433-1440.

[137] Honeycutt PH, Ramsey P. Factors contributing to falls in elderly men living in the community. *Geriatric Nursing*, 2002; 23 (5): 250-256.

[138] Raymakers JA, Samson MM, Verhaar HJJ. The assessment of body sway and the choice of the stability parameter(s). *Gait and Posture*, 2005; 21: 48-58.

[139] Simoneau GG, Krebs DE. Whole-body momentum during gait: A preliminary study of non-fallers and frequent fallers, *Journal of Applied Biomechanics*, 2000; 16: 1-13.

[140] Riley PO, Mann RW, Hodge WA. Modeling of the biomechanics of posture and balance. *Journal of Biomechanics*, 1990; 23 (5): 503-506.

[141] Krebs DE, Jette AM, Assmann SF. Moderate exercise improves gait stability in disabled elders. *American Journal of Physical Medicine and Rehabilitation,* 1998; 79: 1489-1495.

[142] Krebs DE, Jette AM, Assmann SF. Moderate exercise improves gait stability in disabled elders. *American Journal of Physical Medicine and Rehabilitation,* 1998; 79: 1489-1495.

[143] Tucker CA, Ramirez J, Krebs DE, Riley PO. Center of gravity dynamic stability in normal and vestibulopathic gait. *Gait and Posture*, 1998; 8: 117-123.

[144] McGraw B, McClenaghan BA, Williams HG, Dickerson J, Ward DS. Gait and postural stability in obese and non-obese pre-pubertal Boys. *Archive of Physical Medical Rehabilitation*, 2000; 81: 484-489.

[145] Hallemans A, Aerts P, Otten B, De Deyn PP, De Clercq DD. Mechanical energy in toddler gait – A trade-off between economy and stability? *The Journal of Experimental Biology*, 2004; 207: 2417-2431.

[146] Yoshino K, Motoshige T, Araki T, Matsuoka K. Effect of prolonged free-walking fatigue on gait and physiological rhythm. *Journal of Biomechanics*, 2004; 37: 1271-1280.

[147] Hahn ME, Chou LS. Can motion of individual body segments identify dynamic instability in the elderly? *Clinical Biomechanics*, 2003; 18: 737-744.

[148] Sorensen KL, Hollands MA, Patla AE. The effects of human ankle muscle vibration on posture and balance during adaptive locomotion. *Experimental Brain Research*, 2002; 143: 24-34.

[149] McGibbon CA, Krebs DE, Puniello MS. Mechanical energy analysis identifies compensatory strategies in disabled elders' gait. *Journal of Biomechanics*, 2001; 34: 481-490.

[150] Macht Sliwinski M, Sisto SA, Batavia M, Chen B, Forrest GF. Dynamic stability during walking following unilateral total hip arthroplasty. *Gait and Posture*, 2004; 19: 141-147.

[151] Oddsson LIE, Wall III C, McPartland MD, Krebs DE, Tucker CA. Recovery from perturbations during paced walking. *Gait and Posture*, 2004; 19: 24-34.

[152] Bhatt T, Wening JD, Pai YC. Influence of gait speed on stability: recovery from anterior slips and compensatory stepping. *Gait and Posture*, 2005; 21: 146-156.

[153] Martin M, Shinberg M, Kuchibhatla M, Ray L, Carollo JJ, Schenkman ML. Gait initiation in community-dwelling adults with Parkinson disease: Comparison with older and younger adults without the disease. *Physical Therapy*, 2002; 82 (6): 566-577.

[154] Oates AR, Patla AR, Frank JS, Greig MA. Control of dynamic stability during gait termination on a slippery surface. *Journal of Neurophysiology*, 2005; 93: 64-70.

[155] Karcnik T, Krajl A. Stability and velocity in incomplete spinal cord injured subject gaits. *Artificial Organs*, 1999; 23 (5): 421-423.

[156] Karcnik T. Stability in legged locomotion. *Biological Cybernetics*, 2004; 90: 51-58.

[157] Gok H, Ergin S, Yavuzer G. Kinetic and kinematic characteristics of gait in patients with medial knee arthrosis. *Acta Orthopaedica Scandinavica*, 2002; 73 (6): 647-652.

[158] Endo H, Mitani S, Senda M, Kawai A, McCown C, Umeda M, Miyakawa T, Inoue H. Three-dimensional gait analysis of adults with hip dysplasia after rotational acetabular osteotomy. *Journal of Orthopaedic Science*, 2003; 8: 762-771.

[159] Buzzi UH, Ulrich BD. Dynamic stability of gait cycles as a function of speed and system constraints. *Motor Control*, 2004; 8: 241-254.

[160] Ledebt A, Bril B. Acquisition of upper body stability during walking in toddlers. *Developmental Psychobiology*, 2000; 36: 311-324.

[161] Lee LW, Kerrigan DC. Identification of kinetic differences between fallers and non-fallers in the elderly. *American Journal of Physical Medicine and Rehabilitation*, 1999; 78(3):242-246.

[162] Bronstein AM, Guerraz M. Visual-vestibular control of posture and gait: physiological mechanisms and disorders. *Current Opinion in Neurology*, 1999; 12 (1): 5-11.

[163] Morris M, Iansek R, Matyas T, Summers J. Abnormalities in the stride length-cadence relation in pakinsonian gait. *Movement Disorders*, 1998; 13: 61-69.

[164] Zijlstra W, Rutgers AWF, Van Weerden TW. Voluntary and involuntary adaptation of gait in Parkinson's disease. *Gait Posture*, 1998; 7: 53-63.

[165] Kubo T, Kamakura H, Hirokawa Y, Yamamoto K, Imai T, Hirasaki E. 3D analysis of human locomotion before and after caloric stimulation. *Acta Oto-Laryngologica (Stockholm)*, 1997; 117: 143-148.

[166] Alexander NB, Mollo JM, Giordani B, Ashton-Miller JA, Schultz AB, Grunawalt JA, Foster NL. Maintenance of balance, gait patterns, and obstacle clearance in Alzheimer's disease. *Neurology*, 1995; 45 (5): 908-914.

[167] White R, Agouris I, Selbie RD, Kirkpatrick M. The variability of force platform data in normal and cerebral palsy gait. *Clinical Biomechanics*, 1999; 14: 185-192.

[168] Bonan IV, Yelnik AP, Colle FM, Michaud C, Normand E, Panigot B, Roth P, Guichard JP, Vicaut E. Reliance on visual information after stroke. Part II: Effectiveness of a balance rehabilitation program with visual cue deprivation after stroke: A randomized controlled trial. *American Journal of Physical Medicine and Rehabilitation,* 2004; 85: 274-278.

[169] Shkuratova N, Morris ME, Huxham F. Effects of age in balance control during walking. *American Journal of Physical Medicine and Rehabilitation,* 2004; 85: 582-588.

[170] Lenke LG, Engsberg JR, Ross SA, Reitenbach A, Blanke K, Bridwell KH. Prospective dynamic functional evaluation of gait and spinal balance following spinal fusion in adolescent idiopathic scoliosis. *Spine*, 2001; 26: E330-E337.

[171] Draganich LF, Kuo CE. The effects of walking speed on obstacle crossing in healthy young and healthy older adults. *Journal of Biomechanics*, 2004; 37: 889-896.

[172] Kim CM, Eng JJ. Magnitude and pattern of 3D kinematic and kinetic gait profiles in persons with stroke: relationship to walking speed. *Gait and Posture*, 2004, 20: 140-146.

[173] Chou LS, Kaufman KR, Hahn ME, Brey RH. Medio-lateral motion of the center of mass during obstacle crossing distinguishes elderly individuals with imbalance. *Gait and Posture*, 2003; 18: 125-133.

[174] Helbostad JL, Moe-Nilssen R. The effect of gait speed on lateral balance control during walking healthy elderly. *Gait and Posture*, 2003; 18: 27-36.

[175] Kavanagh JJ, Barrett RS, Morrison S. Upper body accelerations during walking in healthy young and elderly men. *Gait and Posture*, 2004; 20: 291- 298.

[176] Chou LS, Kaufman KR, Walker-Rabatin AN, Brey RH, Basford JR. Dynamic instability during obstacle crossing following traumatic brain injury. *Gait and Posture*, 2004; 20: 245-254.

[177] Kaya BK, Krebs DE, Riley PO. Dynamic stability in elders: Momentum control in locomotor ADL. *The Journals of Gerontology*, 1998; 53A (2); M126-M134.

[178] Bauer JA, Cauraugh JH, Tillman MD. An insole pressure measurement system: repeatability of postural data. *Foot and Ankle International*, 2000; 21 (3): 221-226.

[179] Lay AN, Hass CJ, Webb Smith D, Gregor RJ. Characterization of a system for studying human gait during slope walking. *Journal of Applied Biomechanics*, 2005; 21: 153-166.

[180] Bartolic A, Pirtosek Z, Rozman J, Ribaric S. Postural stability of Parkinson's Disease patients is improved by decreasing rigidity. *European Journal of Neurology*, 2005; 12: 156-159.

[181] Hass CJ, Gregor RJ, Waddell DE, Oliver A, Smith DW, Fleming RP, Wolf SL. The influence of Tai Chi training on the center of pressure trajectory during gait initiation in older adults. *American Journal of Physical Medicine and Rehabilitation,* 2004; 85: 1593-1598.

[182] Cueman Hudson C, Krebs DE. Frontal plane dynamic stability and coordination in subjects with cerebellar degeneration. *Experimental Brain Research*, 2000; 132: 103-113.

[183] Bateni H, Olney SJ. Kinematic and Kinetic Variations of Below-Knee Amputee Gait. http://www.oandp.org/jpo/library/2002_01_002.asp [verified March 1, 2006].

[184] Bellew JW, Fenter PC, Chelette B, Moore R, Loreno D. Effects of a short-term dynamic balance training program in healthy older women, *Journal of Geriatric Physical Therapy*, 2005; 28 (1): 4-27.

[185] Gefen A, Megido-Ravid M, Itzchak Y, Arcan M. Analysis of muscular fatigue and foot stability during high-heeled gait. *Gait and Posture*, 2002; 15: 56-63.

[186] Krebs DE, McGibbon CA, Goldvasser D. Analysis of postural perturbation responses. *IEEE Transactions on Neural Systems and Rehabilitation Engineering*, 2001; 9 (1): 76-80.

[187] Chang H, Krebs DE. Dynamic balance control in elders: gait initiation assessment as a screening tool. *American Journal of Physical Medicine and Rehabilitation,* May 1999; 80: 490-494.

[188] Scheiner A, Ferencz DC, Chizeck HJ. Quantitative measurement of stability in human gait through computer simulation and Floquet analysis. *IEEE-EMBC and CMBEC Theme 6: Physiological Systems/Modelling and Identification*, 1997; 1489-1490.

[189] Dingwell JB, Cusumano JP, Cavanagh PR, Sternad D. Local dynamic stability versus kinematic variability of continuous overground and treadmill walking. *Journal of Biomechanical Engineering*, 2001; 123: 27-32.

[190] Karcnik T, Watanabe T, Futami R, Hoshiyama N. Wearable data collection system for on-line gait stability analysis. *Neuromodulation*, 2004; 7 (3): 223-229.

[191] Encoder – The Newsletter of the Seattle Robotics Society – Fuzzy Logic Tutorial. http://www.seattlerobotics.org/encoder/mar98/fuz/flindex.html [verified March 15, 2006].

[192] Leekwijck WV, Kerre EE. Defuzzification: criteria and classification, *Fuzzy Sets and Systems*, 1999, 108 (2): 159-178.

[193] ProTyS – Defuzzification Methods. http://www.protys.cz/fuzzyDesigner_features_defuzzification.php [verified March 1, 2006].

[194] Mathworks – Fuzzy Logic Toolbox – Dinner for Two. http://www.mathworks.com/access/helpdesk/help/toolbox/fuzzy/fp684.html [verified March 1, 2006].

[195] Rubenstein LZ, Josephson KR. The epidemiology of falls and syncope. *Clinics in Geriatric Medicine*, 2002; 18: 141-158.

[196] Median Filtering. http://www.dca.fee.unicamp.br/dipcourse/html-dip/c9/s3/front-page.html [verified March 1, 2006].

[197] F-Scan Software help file – Noise Threshold [verified March 15, 2006].

[198] DataQ Instruments. http://www.dataq.com/images/article_images/an11fig1.gif [verified March 1, 2006].

[199] Ochi, F, Esquenazi A, Hirai B, Talaty M. Temporal-spatial feature of gait after brain injury, *Journal of Head Trauma Rehabilitation*, 1999; 14 (2): 105-115.

[200] NeuroSolutions – What is a Neural Network? http://www.nd.com/neurosolutions/products/ns/whatisNN.html [verified March 1, 2006].

[201] Stergiou C. What is a Neural Network? http://www.doc.ic.ac.uk/~nd/surprise_96/journal/vol1/cs11/article1.html [verified March 1, 2006].

Appendix A

This appendix includes the letters obtained from the Ethics Review Boards of the University of Ottawa, the University of Waterloo, and The Rehabilitation Centre allowing for the testing of human subjects for this research project.

Université d'Ottawa University of Ottawa

December 16, 2005

Edward Lemaire
Rehabilitation Centre of Ottawa
Ottawa Hospital
505 Smyth Road
Ottawa, ON K1H 8M2

Ajoy Biswas
304 Beedle Drive
Ames, IA USA 50010

Jonathan Kofman
Department of Systems Design Engineering
University of Waterloo
Waterloo, ON N2L 3G2

RE: Dynamic Gait Stability Index for Physical Rehabilitation – Pilot Test (file H 10-05-10)

Dear Doctors Lemaire and Kofman and Mr. Biswas,

You will find enclosed the Health Sciences and Science REB ethical clearance for the abovementioned study.

During the course of the study, any modifications to the protocol or forms may not be initiated without prior written approval from the REB. You must also promptly report to the REB all adverse events or experiences encountered by participants.

This certificate of ethical clearance is valid until December 16, 2006. Please submit an annual status report to the Protocol Officer in December, 2006 to either close the file or request a renewal of ethics approval. This document can be found at:
http://we19.uottawa.ca/services/rgess/Ethics/Application_Form.asp

A copy of this approval will be sent to research services, if necessary.

If you have any questions, you may contact the undersigned at the number 562-5387.

Sincerely yours,

Rita D'Alessandro
Protocol Officer for Ethics in Research
For Dr. Daniel Lagarce, Chair of the Health Sciences and Science REB

Université d'Ottawa University of Ottawa

HEALTH SCIENCES AND SCIENCE RESEARCH ETHICS BOARD

CERTIFICATE OF ETHICAL APPROVAL

This is to certify that the University of Ottawa Health Sciences and Science Research Ethics Board has examined the application for ethical approval of the research project entitled **Dynamic Gait Stability Index for Physical Rehabilitation – Pilot Test (file H 10-05-10)** submitted by Ajoy Biswas and supervised by Edward Lemaire of the Ottawa Hospital and Jonathan Kofman of the University of Waterloo. The Board found that this research project met appropriate ethical standards as outlined in the Tri-Council Policy Statement and in the Procedures of the University of Ottawa Research Ethics Boards, and accordingly gave it a Category 1a (approval). This certification is valid one year from the date indicated below.

December 16, 2005
Date

Rita D'Alessandro
Protocol Officer for Ethics in Research
For Dr. Daniel Lagarec, Chair of the
Health Sciences and Science REB

UNIVERSITY OF WATERLOO

OFFICE OF RESEARCH ETHICS

Notification of Full Ethics Clearance of Application to Conduct Research with Human Participants

---

Principal/Co-Investigator: Dr. Edward Lemaire — **Department:** University of Ottawa, Faculty of Medicine
Faculty Supervisor: Dr. Jonathan Kofman — **Department:** Systems Design Engineering
Student Investigator: Ajoy Biswas — **Department:** University of Ottawa, Mechanical Engineering

ORE File #: 12480

Project Title: Dynamic Gait Stability Index for Physical Rehabilitation - Pilot Study - Revised

---

This certificate provides confirmation that the additional information/revised materials requested for the above project have been reviewed and are considered acceptable in accordance with the University of Waterloo's Guidelines for Research with Human Participants and the Tri-Council Policy Statement: Ethical Conduct for Research Involving Humans. Thus, the provisional ethics clearance status has been removed and the project now has received full ethics clearance. This clearance is valid for a period of four years from the date shown below and is subject to an annual ethics review process (see Note 2). A new application must be submitted for on-going projects continuing beyond four years.

Note 1: This project must be conducted in accordance with the description in the application and revised materials for which full ethics clearance has been granted. All subsequent modifications to the application must be submitted for prior ethics review using ORE Form 104 and must not be initiated until notification of ethics clearance has been received.

Note 2: All ongoing research projects must undergo annual ethics review. ORE Form 105 is used for this purpose and must be submitted by the Faculty Investigator/Supervisor (FI/FS) when requested by the ORE. Researchers must submit a Form 105 at the conclusion of the project if it continues for less than a year.

Note 3: FIs and FSs also are reminded that they must immediately report to the ORE (using ORE Form 106) any events related to the procedures used that adversely affected the participants and the steps taken to deal with these.

ADDITIONAL COMMENTS:

see comments in attached email message

Susan E. Sykes, Ph.D., C.Psych.
Director, Office of Research Ethics
OR
Susanne Santi, M. Math
Manager, Research Ethics

12/20/05
Date

Duplicate Return
DEC 20 2005
Office of Research Ethics

The Ottawa Hospital | L'Hôpital d'Ottawa

The Rehabilitation Centre | Le Centre de réadaptation

505 Smyth
Ottawa, Ontario
K1H 8M2

Tel./Tél.:
(613) 737-7350

Fax/Télécopieur:
(613) 737-9638

17 November 2005

Ajoy Biswas
Mechanical Engineering
University of Ottawa

Dear Ajoy,

Thank you for your prompt reply to our last review. You appear to have satisfactorily addressed all of our remaining concerns, and so it gives me pleasure to inform you that your research project entitled **"Dynamic gait stability index for physical rehabilitation – pilot test"** has been granted final approval by The Rehabilitation Centre (TRC). TRC approval indicates that you have met all Research Ethics Board (REB) and Institute for Rehabilitation Research and Development (IRRD) conditions for acceptance. Your research project may now commence.

Principal Investigators are required to submit a progress report on an annual basis to the Chair of the Research Ethics Board. You and Dr. Lemaire will be notified in ten months as to when this is due. You are also expected to provide notification of the termination of your project. As well, any modifications to the protocol or adverse events must be reported immediately to the Chair of the Research Ethics Board. You can request forms for these reporting requirements by emailing djackson@ottawahospital.on.ca or by calling TRC extension 75577.

Congratulations and good luck with your project!

Sincerely,

David Jackson, PhD
Chair,
Research Ethics Board
The Rehabilitation Centre

Ecopy: Dr. Jamie MacDougall
Dr. Edward Lemaire
Cc: REB file

Appendix B

Once imported into Microsoft Excel, the average index value for each subject was arranged to show how the four stability levels of each subject were analyzed by each stability parameter combination.

Table B.1: Stability index values for each subject at every stability condition for all stability parameter combinations. These values were all obtained by processing data that was initially filtered with a nine-cell median filter.

	Level	Subject														
		1	2	3	4	5	6	7	8	9	10	11	12	13	14	15
SIX PARAMS	1	0.372	0.259	0.288	0.090	0.359	0.142	0.089	0.146	0.510	0.117	0.200	0.155	0.233	0.123	0.264
	2	0.437	0.251	0.533	0.109	0.242	0.171	0.132	0.189	0.601	0.254	0.190	0.218	0.308	0.200	0.206
	3	0.368	0.294	0.301	0.144	0.414	0.179	0.281	0.194	0.540	0.204	0.194	0.200	0.233	0.200	0.198
	4	0.568	0.606	0.365	0.267	0.540	0.151	0.444	0.341	0.629	0.373	0.420	0.518	0.460	0.368	0.281
AP ML DST ST CellTrig	1	0.326	0.260	0.287	0.094	0.360	0.138	0.089	0.148	0.525	0.118	0.200	0.155	0.235	0.126	0.264
	2	0.435	0.252	0.532	0.110	0.252	0.173	0.131	0.189	0.633	0.254	0.192	0.218	0.310	0.200	0.206
	3	0.369	0.297	0.303	0.145	0.414	0.180	0.279	0.194	0.542	0.207	0.198	0.200	0.233	0.200	0.198
	4	0.566	0.608	0.365	0.267	0.515	0.151	0.459	0.341	0.621	0.376	0.422	0.525	0.462	0.368	0.284
AP ML DST ST MaxLat	1	0.326	0.259	0.290	0.094	0.360	0.142	0.091	0.147	0.510	0.118	0.200	0.155	0.234	0.123	0.264
	2	0.432	0.252	0.533	0.110	0.252	0.246	0.132	0.189	0.540	0.254	0.194	0.218	0.307	0.200	0.205
	3	0.369	0.295	0.304	0.145	0.414	0.179	0.279	0.195	0.525	0.206	0.230	0.200	0.233	0.200	0.228
	4	0.566	0.606	0.365	0.267	0.544	0.151	0.447	0.341	0.624	0.376	0.422	0.520	0.461	0.368	0.284
AP ML DST CellTrig MaxLat	1	0.326	0.260	0.288	0.091	0.359	0.142	0.091	0.148	0.510	0.118	0.200	0.155	0.236	0.126	0.264
	2	0.448	0.252	0.532	0.110	0.252	0.248	0.132	0.189	0.540	0.254	0.194	0.217	0.308	0.200	0.207
	3	0.367	0.297	0.305	0.144	0.414	0.180	0.291	0.205	0.525	0.207	0.240	0.200	0.233	0.200	0.228
	4	0.564	0.603	0.365	0.267	0.524	0.151	0.472	0.345	0.621	0.383	0.414	0.519	0.462	0.368	0.280
AP ML ST CellTrig MaxLat	1	0.326	0.260	0.289	0.101	0.396	0.142	0.091	0.148	0.510	0.118	0.200	0.155	0.236	0.126	0.279
	2	0.448	0.252	0.532	0.113	0.262	0.248	0.132	0.189	0.540	0.254	0.194	0.218	0.308	0.200	0.216
	3	0.369	0.297	0.305	0.147	0.442	0.180	0.296	0.210	0.525	0.207	0.246	0.200	0.233	0.200	0.228
	4	0.566	0.641	0.365	0.277	0.672	0.151	0.467	0.345	0.677	0.412	0.466	0.556	0.462	0.368	0.284
AP DST ST CellTrig MaxLat	1	0.165	0.140	0.132	0.083	0.258	0.082	0.084	0.106	0.350	0.081	0.087	0.085	0.110	0.089	0.114
	2	0.189	0.128	0.177	0.086	0.218	0.187	0.110	0.085	0.330	0.086	0.090	0.089	0.099	0.085	0.106
	3	0.127	0.147	0.133	0.087	0.289	0.093	0.179	0.088	0.257	0.091	0.129	0.086	0.104	0.085	0.128
	4	0.295	0.269	0.162	0.169	0.303	0.091	0.273	0.175	0.287	0.184	0.176	0.235	0.208	0.166	0.143
ML DST ST CellTrig MaxLat	1	0.186	0.189	0.215	0.094	0.267	0.142	0.091	0.132	0.410	0.118	0.200	0.155	0.196	0.122	0.226
	2	0.256	0.201	0.378	0.110	0.153	0.248	0.110	0.189	0.410	0.252	0.194	0.218	0.288	0.200	0.187
	3	0.306	0.217	0.234	0.145	0.313	0.160	0.163	0.195	0.357	0.204	0.230	0.200	0.208	0.200	0.228
	4	0.450	0.363	0.240	0.169	0.271	0.142	0.244	0.200	0.333	0.228	0.275	0.344	0.262	0.230	0.194
AP ML DST ST	1	0.338	0.259	0.288	0.094	0.360	0.138	0.088	0.146	0.525	0.117	0.200	0.155	0.233	0.123	0.264
	2	0.436	0.252	0.533	0.110	0.242	0.171	0.131	0.189	0.628	0.254	0.192	0.218	0.308	0.200	0.205
	3	0.369	0.295	0.303	0.145	0.414	0.179	0.279	0.194	0.541	0.205	0.198	0.200	0.233	0.200	0.198
	4	0.566	0.606	0.365	0.267	0.544	0.151	0.447	0.341	0.626	0.376	0.422	0.525	0.461	0.368	0.284
AP ML DST CellTrig	1	0.338	0.260	0.287	0.091	0.359	0.138	0.087	0.148	0.525	0.118	0.200	0.155	0.235	0.126	0.264
	2	0.436	0.251	0.532	0.109	0.252	0.173	0.131	0.189	0.633	0.253	0.191	0.217	0.310	0.200	0.207
	3	0.367	0.297	0.303	0.144	0.414	0.180	0.281	0.194	0.542	0.207	0.194	0.200	0.233	0.200	0.198
	4	0.564	0.603	0.365	0.267	0.510	0.151	0.446	0.341	0.621	0.373	0.413	0.524	0.462	0.368	0.280
AP ML DST MaxLat	1	0.338	0.259	0.289	0.089	0.359	0.142	0.090	0.147	0.510	0.117	0.200	0.155	0.234	0.123	0.264
	2	0.432	0.252	0.533	0.110	0.252	0.246	0.132	0.189	0.540	0.254	0.194	0.217	0.307	0.200	0.206
	3	0.367	0.294	0.304	0.144	0.414	0.179	0.281	0.195	0.524	0.206	0.227	0.200	0.233	0.200	0.228
	4	0.564	0.602	0.365	0.267	0.539	0.151	0.445	0.341	0.624	0.372	0.413	0.519	0.461	0.368	0.280

AP ML ST CellTrig	1	0.338	0.260	0.287	0.094	0.396	0.138	0.089	0.148	0.525	0.118	0.200	0.155	0.235	0.126	0.279
	2	0.435	0.252	0.532	0.110	0.252	0.173	0.131	0.189	0.633	0.254	0.192	0.218	0.310	0.200	0.216
	3	0.369	0.297	0.303	0.145	0.414	0.180	0.284	0.206	0.542	0.207	0.199	0.200	0.233	0.200	0.198
	4	0.566	0.641	0.365	0.267	0.533	0.151	0.449	0.341	0.677	0.392	0.462	0.557	0.462	0.368	0.284
AP ML ST MaxLat	1	0.338	0.259	0.290	0.094	0.396	0.142	0.091	0.147	0.510	0.118	0.200	0.155	0.234	0.123	0.279
	2	0.432	0.252	0.533	0.110	0.252	0.246	0.132	0.189	0.540	0.254	0.194	0.218	0.307	0.200	0.214
	3	0.369	0.295	0.304	0.145	0.414	0.179	0.284	0.207	0.525	0.206	0.231	0.200	0.233	0.200	0.228
	4	0.566	0.640	0.365	0.267	0.571	0.151	0.448	0.341	0.680	0.392	0.462	0.556	0.461	0.368	0.284
AP ML CellTrig MaxLat	1	0.343	0.260	0.315	0.111	0.411	0.167	0.091	0.148	0.510	0.118	0.200	0.155	0.241	0.126	0.306
	2	0.531	0.258	0.612	0.130	0.285	0.248	0.132	0.200	0.577	0.322	0.200	0.234	0.349	0.202	0.217
	3	0.474	0.322	0.319	0.210	0.503	0.180	0.387	0.244	0.533	0.213	0.253	0.200	0.233	0.200	0.232
	4	0.651	0.697	0.402	0.351	0.673	0.151	0.589	0.413	0.677	0.429	0.480	0.591	0.512	0.403	0.287
AP DST ST CellTrig	1	0.166	0.140	0.132	0.083	0.245	0.078	0.081	0.106	0.200	0.081	0.087	0.085	0.110	0.088	0.113
	2	0.189	0.128	0.177	0.086	0.218	0.085	0.106	0.082	0.273	0.085	0.089	0.089	0.096	0.085	0.105
	3	0.126	0.147	0.132	0.087	0.280	0.093	0.179	0.083	0.233	0.090	0.088	0.086	0.102	0.085	0.085
	4	0.295	0.269	0.162	0.169	0.300	0.091	0.263	0.174	0.287	0.184	0.176	0.226	0.208	0.165	0.143
AP DST ST MaxLat	1	0.165	0.138	0.129	0.083	0.238	0.081	0.084	0.105	0.350	0.081	0.086	0.082	0.108	0.086	0.113
	2	0.189	0.128	0.177	0.086	0.218	0.183	0.110	0.085	0.330	0.086	0.089	0.088	0.097	0.084	0.103
	3	0.126	0.147	0.131	0.087	0.289	0.089	0.179	0.087	0.256	0.088	0.129	0.082	0.102	0.083	0.128
	4	0.295	0.269	0.160	0.169	0.290	0.089	0.263	0.175	0.290	0.184	0.176	0.222	0.208	0.166	0.143
AP DST CellTrig MaxLat	1	0.166	0.140	0.132	0.078	0.257	0.082	0.082	0.106	0.350	0.075	0.079	0.082	0.110	0.089	0.113
	2	0.189	0.127	0.177	0.083	0.218	0.186	0.110	0.084	0.330	0.084	0.081	0.079	0.098	0.085	0.105
	3	0.123	0.147	0.133	0.080	0.289	0.091	0.179	0.086	0.256	0.090	0.121	0.084	0.104	0.082	0.128
	4	0.304	0.265	0.162	0.168	0.300	0.091	0.283	0.175	0.287	0.180	0.172	0.235	0.208	0.166	0.140
AP ST CellTrig MaxLat	1	0.166	0.140	0.132	0.100	0.329	0.082	0.084	0.106	0.350	0.081	0.087	0.085	0.110	0.089	0.129
	2	0.189	0.128	0.177	0.104	0.384	0.187	0.110	0.085	0.330	0.086	0.101	0.108	0.099	0.085	0.145
	3	0.126	0.147	0.133	0.099	0.405	0.093	0.210	0.120	0.257	0.091	0.147	0.086	0.104	0.085	0.140
	4	0.364	0.385	0.162	0.190	0.648	0.091	0.287	0.175	0.354	0.262	0.256	0.272	0.208	0.166	0.143
ML DST ST CellTrig	1	0.198	0.189	0.214	0.094	0.267	0.138	0.089	0.131	0.330	0.118	0.200	0.155	0.195	0.122	0.226
	2	0.260	0.201	0.378	0.110	0.153	0.173	0.109	0.189	0.360	0.252	0.192	0.218	0.290	0.200	0.187
	3	0.306	0.217	0.233	0.145	0.313	0.160	0.163	0.194	0.346	0.204	0.198	0.200	0.207	0.200	0.198
	4	0.450	0.363	0.240	0.169	0.268	0.142	0.234	0.200	0.333	0.228	0.275	0.337	0.262	0.230	0.194
ML DST ST MaxLat	1	0.198	0.188	0.216	0.094	0.267	0.142	0.091	0.130	0.410	0.117	0.200	0.155	0.194	0.119	0.226
	2	0.256	0.201	0.380	0.110	0.153	0.246	0.110	0.189	0.410	0.252	0.194	0.218	0.286	0.200	0.186
	3	0.306	0.215	0.233	0.145	0.313	0.159	0.163	0.195	0.357	0.203	0.230	0.200	0.208	0.200	0.228
	4	0.450	0.362	0.240	0.169	0.257	0.142	0.233	0.200	0.333	0.228	0.275	0.331	0.261	0.230	0.194
ML DST CellTrig MaxLat	1	0.198	0.189	0.214	0.091	0.267	0.142	0.091	0.132	0.410	0.118	0.200	0.155	0.196	0.122	0.225
	2	0.256	0.201	0.377	0.110	0.149	0.248	0.110	0.189	0.410	0.252	0.194	0.217	0.288	0.200	0.185
	3	0.301	0.216	0.234	0.144	0.312	0.160	0.162	0.195	0.357	0.204	0.227	0.200	0.208	0.200	0.228
	4	0.450	0.361	0.240	0.169	0.269	0.141	0.252	0.200	0.333	0.228	0.268	0.344	0.262	0.230	0.190
ML ST CellTrig MaxLat	1	0.198	0.189	0.215	0.109	0.339	0.142	0.091	0.132	0.410	0.118	0.200	0.155	0.196	0.122	0.246
	2	0.256	0.201	0.378	0.126	0.304	0.248	0.110	0.189	0.410	0.252	0.204	0.237	0.288	0.200	0.234
	3	0.306	0.217	0.234	0.159	0.385	0.160	0.189	0.234	0.357	0.204	0.247	0.200	0.208	0.200	0.248
	4	0.450	0.487	0.240	0.195	0.614	0.142	0.258	0.200	0.400	0.307	0.384	0.390	0.262	0.230	0.194
DST ST CellTrig MaxLat	1	0.084	0.088	0.087	0.100	0.237	0.082	0.084	0.087	0.292	0.080	0.087	0.085	0.086	0.085	0.099
	2	0.084	0.088	0.088	0.104	0.286	0.187	0.088	0.085	0.252	0.083	0.101	0.108	0.088	0.085	0.129
	3	0.084	0.089	0.088	0.099	0.327	0.081	0.119	0.119	0.126	0.088	0.147	0.086	0.085	0.085	0.140
	4	0.152	0.195	0.087	0.106	0.407	0.082	0.137	0.084	0.124	0.149	0.168	0.168	0.087	0.084	0.086
AP ML DST	1	0.212	0.260	0.103	0.085	0.306	0.068	0.082	0.138	0.152	0.116	0.200	0.155	0.130	0.136	0.213
	2	0.452	0.243	0.171	0.110	0.249	0.072	0.108	0.188	0.218	0.076	0.227	0.217	0.192	0.203	0.178
	3	0.361	0.275	0.174	0.135	0.303	0.072	0.284	0.139	0.242	0.115	0.274	0.177	0.123	0.200	0.187
	4	0.595	0.617	0.259	0.298	0.606	0.215	0.453	0.336	0.521	0.256	0.432	0.397	0.457	0.402	0.334
AP ML ST	1	0.230	0.381	0.109	0.083	0.411	0.084	0.082	0.138	0.152	0.122	0.400	0.215	0.132	0.158	0.213
	2	0.484	0.402	0.172	0.148	0.316	0.078	0.109	0.190	0.218	0.084	0.415	0.417	0.192	0.258	0.235
	3	0.403	0.415	0.176	0.207	0.406	0.080	0.385	0.150	0.246	0.132	0.443	0.244	0.133	0.274	0.254
	4	0.675	0.760	0.276	0.350	0.693	0.215	0.448	0.413	0.580	0.330	0.546	0.516	0.545	0.508	0.453
AP ML CellTrig	1	0.213	0.261	0.104	0.079	0.318	0.084	0.082	0.140	0.152	0.120	0.200	0.155	0.133	0.138	0.220
	2	0.484	0.243	0.171	0.129	0.317	0.082	0.108	0.199	0.218	0.087	0.246	0.234	0.192	0.205	0.179
	3	0.403	0.288	0.176	0.193	0.397	0.085	0.383	0.156	0.242	0.120	0.304	0.179	0.123	0.200	0.188
	4	0.665	0.647	0.260	0.328	0.709	0.215	0.549	0.399	0.575	0.276	0.471	0.456	0.511	0.430	0.346

AP ML MaxLat	1	0.214	0.260	0.105	0.078	0.305	0.071	0.086	0.139	0.152	0.105	0.200	0.155	0.130	0.136	0.213
	2	0.484	0.243	0.173	0.109	0.249	0.083	0.110	0.189	0.218	0.080	0.225	0.227	0.192	0.203	0.178
	3	0.394	0.275	0.176	0.133	0.303	0.076	0.284	0.140	0.242	0.117	0.293	0.177	0.124	0.200	0.188
	4	0.624	0.600	0.284	0.278	0.577	0.215	0.409	0.336	0.561	0.265	0.448	0.444	0.506	0.425	0.341
AP DST ST	1	0.151	0.140	0.109	0.085	0.176	0.084	0.080	0.093	0.150	0.080	0.118	0.084	0.097	0.081	0.123
	2	0.339	0.126	0.115	0.129	0.390	0.078	0.107	0.072	0.209	0.083	0.168	0.082	0.096	0.086	0.094
	3	0.265	0.133	0.102	0.244	0.422	0.080	0.507	0.078	0.185	0.081	0.269	0.083	0.086	0.083	0.094
	4	0.282	0.472	0.172	0.371	0.687	0.152	0.498	0.360	0.266	0.190	0.293	0.198	0.209	0.222	0.254
AP DST CellTrig	1	0.151	0.142	0.104	0.085	0.176	0.084	0.078	0.097	0.149	0.085	0.097	0.083	0.096	0.081	0.124
	2	0.333	0.127	0.113	0.130	0.384	0.082	0.104	0.080	0.207	0.087	0.121	0.085	0.092	0.089	0.096
	3	0.285	0.134	0.103	0.243	0.413	0.085	0.498	0.080	0.180	0.085	0.176	0.083	0.081	0.085	0.097
	4	0.283	0.368	0.174	0.359	0.717	0.153	0.594	0.337	0.265	0.181	0.239	0.188	0.210	0.204	0.235
AP DST MaxLat	1	0.150	0.140	0.105	0.085	0.176	0.068	0.084	0.096	0.151	0.080	0.098	0.076	0.094	0.084	0.125
	2	0.330	0.127	0.113	0.104	0.277	0.083	0.108	0.083	0.207	0.077	0.120	0.082	0.095	0.086	0.094
	3	0.268	0.135	0.103	0.156	0.310	0.075	0.333	0.085	0.180	0.075	0.184	0.078	0.082	0.081	0.098
	4	0.282	0.369	0.193	0.315	0.573	0.152	0.485	0.290	0.265	0.189	0.238	0.188	0.209	0.205	0.235
AP ST CellTrig	1	0.287	0.478	0.154	0.347	0.655	0.088	0.310	0.209	0.149	0.228	0.600	0.359	0.142	0.281	0.249
	2	0.463	0.584	0.155	0.590	0.765	0.082	0.407	0.213	0.209	0.088	0.596	0.549	0.163	0.309	0.329
	3	0.377	0.543	0.208	0.600	0.800	0.119	0.738	0.231	0.204	0.180	0.600	0.308	0.218	0.351	0.355
	4	0.645	0.866	0.330	0.567	0.796	0.287	0.618	0.504	0.572	0.526	0.632	0.583	0.485	0.586	0.669
AP ST MaxLat	1	0.270	0.413	0.154	0.268	0.506	0.085	0.303	0.209	0.150	0.199	0.424	0.285	0.141	0.230	0.242
	2	0.453	0.493	0.155	0.492	0.639	0.083	0.386	0.207	0.209	0.083	0.402	0.500	0.165	0.309	0.335
	3	0.354	0.447	0.208	0.500	0.659	0.116	0.647	0.238	0.204	0.167	0.436	0.294	0.215	0.327	0.361
	4	0.592	0.785	0.320	0.483	0.767	0.283	0.498	0.473	0.559	0.526	0.564	0.582	0.515	0.559	0.630
AP CellTrig MaxLat	1	0.270	0.227	0.106	0.229	0.399	0.141	0.200	0.173	0.139	0.190	0.200	0.160	0.108	0.199	0.238
	2	0.491	0.222	0.115	0.362	0.609	0.083	0.268	0.202	0.207	0.105	0.200	0.176	0.095	0.171	0.170
	3	0.386	0.240	0.134	0.411	0.651	0.132	0.607	0.220	0.180	0.119	0.281	0.154	0.095	0.172	0.187
	4	0.492	0.530	0.215	0.418	0.786	0.261	0.659	0.465	0.361	0.369	0.360	0.392	0.349	0.364	0.361
ML DST ST	1	0.137	0.188	0.087	0.085	0.165	0.084	0.083	0.129	0.104	0.110	0.242	0.156	0.118	0.136	0.171
	2	0.368	0.196	0.136	0.159	0.318	0.076	0.086	0.188	0.099	0.084	0.312	0.217	0.172	0.200	0.165
	3	0.276	0.205	0.151	0.287	0.346	0.079	0.469	0.139	0.134	0.119	0.471	0.179	0.126	0.200	0.174
	4	0.350	0.517	0.171	0.333	0.691	0.210	0.451	0.397	0.267	0.153	0.363	0.260	0.257	0.281	0.273
ML DST CellTrig	1	0.137	0.189	0.082	0.085	0.165	0.084	0.083	0.131	0.102	0.114	0.221	0.155	0.117	0.137	0.171
	2	0.368	0.196	0.135	0.159	0.308	0.082	0.085	0.189	0.097	0.087	0.267	0.217	0.172	0.200	0.165
	3	0.296	0.204	0.152	0.287	0.337	0.084	0.460	0.140	0.128	0.120	0.382	0.179	0.123	0.200	0.175
	4	0.351	0.413	0.172	0.320	0.721	0.210	0.547	0.375	0.266	0.146	0.310	0.250	0.260	0.264	0.254
ML DST MaxLat	1	0.137	0.188	0.081	0.085	0.166	0.071	0.086	0.130	0.102	0.099	0.221	0.155	0.114	0.136	0.170
	2	0.368	0.196	0.135	0.134	0.201	0.078	0.088	0.189	0.098	0.079	0.268	0.217	0.172	0.200	0.165
	3	0.276	0.205	0.152	0.203	0.233	0.074	0.295	0.140	0.130	0.116	0.374	0.177	0.124	0.200	0.175
	4	0.350	0.411	0.192	0.274	0.564	0.210	0.428	0.325	0.267	0.153	0.310	0.250	0.257	0.264	0.254
ML ST CellTrig	1	0.260	0.588	0.132	0.349	0.634	0.088	0.327	0.253	0.103	0.264	0.800	0.474	0.180	0.357	0.327
	2	0.474	0.708	0.187	0.627	0.665	0.082	0.381	0.390	0.099	0.088	0.801	0.751	0.274	0.500	0.449
	3	0.388	0.657	0.275	0.671	0.703	0.118	0.705	0.315	0.153	0.234	0.815	0.445	0.282	0.546	0.477
	4	0.632	0.913	0.326	0.566	0.800	0.338	0.559	0.575	0.555	0.498	0.692	0.638	0.526	0.641	0.691
ML ST MaxLat	1	0.242	0.528	0.133	0.269	0.490	0.085	0.311	0.253	0.103	0.218	0.624	0.406	0.179	0.298	0.322
	2	0.465	0.616	0.187	0.531	0.539	0.081	0.352	0.383	0.099	0.084	0.618	0.708	0.274	0.499	0.456
	3	0.363	0.572	0.275	0.571	0.562	0.115	0.605	0.315	0.153	0.221	0.653	0.431	0.271	0.523	0.492
	4	0.587	0.835	0.314	0.474	0.765	0.334	0.432	0.539	0.535	0.499	0.628	0.638	0.556	0.618	0.652
ML CellTrig MaxLat	1	0.236	0.284	0.083	0.229	0.382	0.141	0.200	0.215	0.091	0.201	0.400	0.266	0.138	0.260	0.319
	2	0.502	0.328	0.139	0.404	0.508	0.083	0.231	0.354	0.098	0.105	0.413	0.365	0.172	0.330	0.256
	3	0.387	0.340	0.186	0.486	0.553	0.132	0.563	0.305	0.130	0.162	0.498	0.281	0.132	0.330	0.300
	4	0.527	0.583	0.208	0.410	0.777	0.331	0.594	0.529	0.363	0.344	0.444	0.460	0.407	0.447	0.389
DST ST CellTrig	1	0.196	0.413	0.132	0.360	0.507	0.088	0.311	0.200	0.100	0.222	0.621	0.359	0.130	0.278	0.202
	2	0.343	0.531	0.127	0.611	0.712	0.082	0.367	0.213	0.083	0.088	0.640	0.549	0.143	0.300	0.304
	3	0.272	0.471	0.184	0.682	0.710	0.118	0.762	0.226	0.107	0.180	0.709	0.308	0.218	0.348	0.335
	4	0.386	0.746	0.237	0.561	0.797	0.255	0.604	0.514	0.327	0.410	0.545	0.434	0.288	0.456	0.590
DST ST MaxLat	1	0.178	0.357	0.132	0.276	0.353	0.085	0.303	0.200	0.101	0.195	0.445	0.285	0.130	0.228	0.200
	2	0.334	0.440	0.127	0.515	0.584	0.081	0.346	0.207	0.083	0.083	0.447	0.500	0.145	0.299	0.314
	3	0.252	0.375	0.184	0.582	0.570	0.115	0.662	0.232	0.107	0.167	0.526	0.294	0.207	0.325	0.344
	4	0.327	0.658	0.224	0.482	0.768	0.251	0.482	0.479	0.293	0.410	0.478	0.432	0.319	0.428	0.550

DST CellTrig MaxLat	1	0.175	0.157	0.083	0.237	0.243	0.141	0.200	0.165	0.087	0.185	0.221	0.160	0.096	0.199	0.196
	2	0.380	0.178	0.082	0.377	0.555	0.083	0.229	0.202	0.077	0.105	0.244	0.176	0.083	0.165	0.156
	3	0.284	0.176	0.107	0.504	0.561	0.132	0.619	0.215	0.075	0.119	0.370	0.154	0.095	0.172	0.174
	4	0.249	0.386	0.133	0.420	0.796	0.247	0.639	0.471	0.140	0.256	0.271	0.257	0.184	0.239	0.287
ST CellTrig MaxLat	1	0.310	0.435	0.132	0.503	0.584	0.141	0.464	0.317	0.089	0.364	0.600	0.418	0.150	0.421	0.385
	2	0.470	0.532	0.128	0.721	0.809	0.084	0.511	0.380	0.084	0.106	0.596	0.549	0.145	0.385	0.367
	3	0.365	0.505	0.218	0.779	0.824	0.185	0.819	0.420	0.107	0.218	0.628	0.372	0.218	0.410	0.420
	4	0.499	0.712	0.272	0.582	0.852	0.396	0.650	0.581	0.362	0.538	0.545	0.548	0.402	0.519	0.576
AP ML	1	0.214	0.260	0.103	0.077	0.306	0.068	0.082	0.138	0.152	0.116	0.200	0.155	0.130	0.136	0.213
	2	0.452	0.243	0.171	0.108	0.249	0.072	0.108	0.188	0.218	0.076	0.221	0.217	0.192	0.203	0.178
	3	0.379	0.275	0.174	0.133	0.303	0.072	0.276	0.139	0.242	0.115	0.243	0.177	0.123	0.200	0.187
	4	0.590	0.570	0.259	0.278	0.537	0.215	0.409	0.336	0.521	0.256	0.406	0.396	0.457	0.390	0.394
AP DST	1	0.150	0.140	0.102	0.085	0.176	0.064	0.077	0.093	0.149	0.080	0.097	0.076	0.094	0.079	0.123
	2	0.330	0.126	0.112	0.103	0.277	0.071	0.103	0.072	0.207	0.070	0.119	0.082	0.088	0.085	0.090
	3	0.265	0.133	0.098	0.156	0.310	0.069	0.333	0.078	0.180	0.070	0.154	0.075	0.072	0.081	0.090
	4	0.282	0.368	0.172	0.314	0.545	0.152	0.462	0.290	0.265	0.179	0.238	0.188	0.209	0.204	0.296
AP ST	1	0.271	0.413	0.154	0.268	0.507	0.084	0.247	0.209	0.149	0.212	0.400	0.285	0.141	0.229	0.242
	2	0.431	0.433	0.155	0.396	0.565	0.078	0.319	0.201	0.209	0.083	0.400	0.400	0.163	0.258	0.269
	3	0.351	0.432	0.208	0.400	0.600	0.115	0.550	0.210	0.204	0.166	0.400	0.262	0.206	0.275	0.291
	4	0.553	0.697	0.313	0.454	0.653	0.272	0.477	0.408	0.529	0.433	0.492	0.483	0.465	0.468	0.571
AP CellTrig	1	0.271	0.227	0.104	0.228	0.388	0.141	0.200	0.172	0.138	0.204	0.200	0.160	0.108	0.199	0.238
	2	0.458	0.222	0.115	0.310	0.547	0.082	0.251	0.188	0.207	0.105	0.200	0.176	0.092	0.168	0.170
	3	0.370	0.240	0.133	0.342	0.591	0.132	0.531	0.209	0.180	0.119	0.222	0.153	0.090	0.172	0.187
	4	0.473	0.517	0.210	0.406	0.671	0.261	0.585	0.406	0.361	0.352	0.356	0.355	0.348	0.358	0.416
AP MaxLat	1	0.242	0.140	0.144	0.073	0.182	0.068	0.139	0.204	0.163	0.076	0.093	0.067	0.127	0.084	0.133
	2	0.429	0.168	0.235	0.140	0.258	0.099	0.179	0.197	0.328	0.200	0.079	0.135	0.198	0.155	0.201
	3	0.336	0.171	0.170	0.139	0.259	0.074	0.260	0.196	0.300	0.183	0.139	0.141	0.181	0.141	0.196
	4	0.427	0.418	0.324	0.221	0.428	0.216	0.342	0.320	0.393	0.337	0.301	0.298	0.377	0.319	0.379
ML DST	1	0.137	0.188	0.078	0.085	0.165	0.068	0.082	0.129	0.102	0.110	0.221	0.155	0.113	0.136	0.170
	2	0.368	0.196	0.134	0.134	0.201	0.068	0.085	0.188	0.097	0.075	0.266	0.217	0.172	0.200	0.165
	3	0.276	0.205	0.150	0.203	0.233	0.069	0.295	0.139	0.128	0.115	0.359	0.177	0.123	0.200	0.174
	4	0.350	0.412	0.171	0.274	0.537	0.209	0.405	0.325	0.267	0.145	0.310	0.250	0.257	0.264	0.315
ML ST	1	0.242	0.528	0.132	0.269	0.488	0.084	0.257	0.252	0.103	0.240	0.600	0.406	0.179	0.298	0.322
	2	0.450	0.556	0.187	0.434	0.465	0.076	0.288	0.378	0.099	0.084	0.616	0.617	0.274	0.449	0.391
	3	0.362	0.556	0.275	0.471	0.503	0.114	0.513	0.287	0.153	0.220	0.643	0.399	0.266	0.469	0.417
	4	0.573	0.742	0.308	0.437	0.654	0.326	0.411	0.464	0.520	0.396	0.582	0.551	0.523	0.546	0.598
ML CellTrig	1	0.236	0.284	0.082	0.228	0.375	0.141	0.200	0.214	0.091	0.223	0.400	0.266	0.137	0.260	0.319
	2	0.470	0.328	0.138	0.353	0.445	0.082	0.214	0.343	0.097	0.105	0.412	0.365	0.172	0.327	0.256
	3	0.374	0.341	0.185	0.415	0.494	0.131	0.493	0.288	0.128	0.162	0.466	0.281	0.132	0.330	0.300
	4	0.511	0.564	0.203	0.388	0.664	0.331	0.520	0.459	0.363	0.314	0.443	0.422	0.407	0.441	0.443
ML MaxLat	1	0.213	0.188	0.120	0.078	0.173	0.071	0.141	0.250	0.115	0.099	0.224	0.155	0.155	0.136	0.179
	2	0.447	0.247	0.268	0.174	0.191	0.095	0.156	0.346	0.178	0.200	0.225	0.317	0.305	0.320	0.305
	3	0.335	0.255	0.230	0.189	0.206	0.074	0.250	0.252	0.230	0.229	0.305	0.260	0.246	0.300	0.310
	4	0.472	0.442	0.311	0.191	0.415	0.278	0.285	0.365	0.384	0.304	0.373	0.368	0.433	0.391	0.407
DST ST	1	0.179	0.357	0.132	0.276	0.356	0.084	0.248	0.200	0.100	0.208	0.421	0.285	0.129	0.226	0.200
	2	0.305	0.380	0.127	0.418	0.512	0.076	0.280	0.201	0.083	0.083	0.444	0.400	0.143	0.249	0.250
	3	0.251	0.360	0.184	0.482	0.510	0.114	0.566	0.208	0.107	0.166	0.509	0.262	0.202	0.273	0.273
	4	0.277	0.546	0.218	0.443	0.643	0.242	0.469	0.403	0.261	0.308	0.405	0.334	0.264	0.341	0.491
DST CellTrig	1	0.175	0.157	0.080	0.237	0.231	0.141	0.200	0.164	0.084	0.198	0.221	0.160	0.093	0.199	0.195
	2	0.335	0.178	0.081	0.328	0.494	0.082	0.213	0.188	0.074	0.105	0.244	0.176	0.079	0.162	0.156
	3	0.264	0.176	0.106	0.432	0.502	0.131	0.545	0.206	0.070	0.119	0.332	0.153	0.090	0.172	0.174
	4	0.216	0.366	0.128	0.400	0.673	0.247	0.577	0.401	0.139	0.226	0.267	0.219	0.183	0.233	0.339
DST MaxLat	1	0.161	0.078	0.119	0.085	0.092	0.068	0.140	0.196	0.118	0.072	0.115	0.076	0.107	0.080	0.087
	2	0.309	0.118	0.190	0.160	0.204	0.095	0.156	0.197	0.161	0.200	0.123	0.142	0.186	0.150	0.188
	3	0.263	0.114	0.154	0.216	0.198	0.072	0.270	0.196	0.176	0.183	0.211	0.141	0.181	0.140	0.184
	4	0.171	0.267	0.231	0.208	0.420	0.195	0.342	0.312	0.158	0.216	0.215	0.180	0.187	0.202	0.308
ST CellTrig	1	0.311	0.435	0.132	0.503	0.589	0.141	0.449	0.317	0.088	0.397	0.600	0.418	0.150	0.420	0.384
	2	0.427	0.532	0.128	0.705	0.782	0.082	0.493	0.369	0.083	0.106	0.596	0.549	0.143	0.382	0.364
	3	0.344	0.505	0.218	0.742	0.791	0.184	0.776	0.408	0.107	0.218	0.622	0.372	0.218	0.410	0.419
	4	0.474	0.700	0.268	0.574	0.770	0.396	0.587	0.531	0.362	0.521	0.544	0.518	0.401	0.517	0.637

ST MaxLat	**1**	0.270	0.357	0.183	0.268	0.353	0.085	0.353	0.375	0.113	0.195	0.424	0.285	0.170	0.228	0.207
	2	0.402	0.441	0.247	0.495	0.474	0.097	0.395	0.364	0.165	0.200	0.402	0.500	0.280	0.372	0.427
	3	0.307	0.410	0.278	0.500	0.459	0.115	0.498	0.380	0.196	0.307	0.436	0.362	0.353	0.374	0.431
	4	0.427	0.580	0.391	0.363	0.558	0.321	0.348	0.435	0.389	0.506	0.472	0.462	0.438	0.466	0.592
CellTrig MaxLat	**1**	0.270	0.157	0.122	0.229	0.243	0.141	0.289	0.312	0.099	0.185	0.224	0.160	0.127	0.199	0.203
	2	0.436	0.231	0.192	0.412	0.456	0.100	0.322	0.344	0.164	0.216	0.202	0.257	0.186	0.264	0.285
	3	0.319	0.224	0.177	0.442	0.451	0.132	0.478	0.363	0.176	0.226	0.282	0.246	0.190	0.262	0.315
	4	0.355	0.400	0.265	0.307	0.551	0.325	0.455	0.444	0.237	0.425	0.334	0.341	0.336	0.359	0.437

Appendix C

This appendix shows the tables of stability index values obtained with the median filter (Table C.1), values obtained with the averaging filter (Table C.2), and the difference in the calculated index values (Table C.3). The mean difference between the data sets divided by the mean value of the averaging filter data yields a 3.13% mean difference between the median filter and averaging filter data sets.

Table C.1: Stability index values calculated from raw F-Scan data filtered with a median filter.

	Level	Subjects														
		1	2	3	4	5	6	7	8	9	10	11	12	13	14	15
SIX PARAMS	1	0.372	0.259	0.288	0.090	0.359	0.142	0.089	0.146	0.510	0.117	0.200	0.155	0.233	0.123	0.264
	2	0.437	0.251	0.533	0.109	0.242	0.171	0.132	0.189	0.601	0.254	0.190	0.218	0.308	0.200	0.206
	3	0.368	0.294	0.301	0.144	0.414	0.179	0.281	0.194	0.540	0.204	0.194	0.200	0.233	0.200	0.198
	4	0.568	0.606	0.365	0.267	0.540	0.151	0.444	0.341	0.629	0.373	0.420	0.518	0.460	0.368	0.281
AP ML DST ST CellTrig	1	0.326	0.260	0.287	0.094	0.360	0.138	0.089	0.148	0.525	0.118	0.200	0.155	0.235	0.126	0.264
	2	0.435	0.252	0.532	0.110	0.252	0.173	0.131	0.189	0.633	0.254	0.192	0.218	0.310	0.200	0.206
	3	0.369	0.297	0.303	0.145	0.414	0.180	0.279	0.194	0.542	0.207	0.198	0.200	0.233	0.200	0.198
	4	0.566	0.608	0.365	0.267	0.515	0.151	0.459	0.341	0.621	0.376	0.422	0.525	0.462	0.368	0.284
AP ML DST ST MaxLat	1	0.326	0.259	0.290	0.094	0.360	0.142	0.091	0.147	0.510	0.118	0.200	0.155	0.234	0.123	0.264
	2	0.432	0.252	0.533	0.110	0.252	0.246	0.132	0.189	0.540	0.254	0.194	0.218	0.307	0.200	0.205
	3	0.369	0.295	0.304	0.145	0.414	0.179	0.279	0.195	0.525	0.206	0.230	0.200	0.233	0.200	0.228
	4	0.566	0.606	0.365	0.267	0.544	0.151	0.447	0.341	0.624	0.376	0.422	0.520	0.461	0.368	0.284
AP ML DST CellTrig MaxLat	1	0.326	0.260	0.288	0.091	0.359	0.142	0.091	0.148	0.510	0.118	0.200	0.155	0.236	0.126	0.264
	2	0.448	0.252	0.532	0.110	0.252	0.248	0.132	0.189	0.540	0.254	0.194	0.217	0.308	0.200	0.207
	3	0.367	0.297	0.305	0.144	0.414	0.180	0.291	0.205	0.525	0.207	0.240	0.200	0.233	0.200	0.228
	4	0.564	0.603	0.365	0.267	0.524	0.151	0.472	0.345	0.621	0.383	0.414	0.519	0.462	0.368	0.280
AP ML ST CellTrig MaxLat	1	0.326	0.260	0.289	0.101	0.396	0.142	0.091	0.148	0.510	0.118	0.200	0.155	0.236	0.126	0.279
	2	0.448	0.252	0.532	0.113	0.262	0.248	0.132	0.189	0.540	0.254	0.194	0.218	0.308	0.200	0.216
	3	0.369	0.297	0.305	0.147	0.442	0.180	0.296	0.210	0.525	0.207	0.246	0.200	0.233	0.200	0.228
	4	0.566	0.641	0.365	0.277	0.672	0.151	0.467	0.345	0.677	0.412	0.466	0.556	0.462	0.368	0.284
AP DST ST CellTrig MaxLat	1	0.165	0.140	0.132	0.083	0.258	0.082	0.084	0.106	0.350	0.081	0.087	0.085	0.110	0.089	0.114
	2	0.189	0.128	0.177	0.086	0.218	0.187	0.110	0.085	0.330	0.086	0.090	0.089	0.099	0.085	0.106
	3	0.127	0.147	0.133	0.087	0.289	0.093	0.179	0.088	0.257	0.091	0.129	0.086	0.104	0.085	0.128
	4	0.295	0.269	0.162	0.169	0.303	0.091	0.273	0.175	0.287	0.184	0.176	0.235	0.208	0.166	0.143
ML DST ST CellTrig MaxLat	1	0.186	0.189	0.215	0.094	0.267	0.142	0.091	0.132	0.410	0.118	0.200	0.155	0.196	0.122	0.226
	2	0.256	0.201	0.378	0.110	0.153	0.248	0.110	0.189	0.410	0.252	0.194	0.218	0.288	0.200	0.187
	3	0.306	0.217	0.234	0.145	0.313	0.160	0.163	0.195	0.357	0.204	0.230	0.200	0.208	0.200	0.228
	4	0.450	0.363	0.240	0.169	0.271	0.142	0.244	0.200	0.333	0.228	0.275	0.344	0.262	0.230	0.194
AP ML DST ST	1	0.338	0.259	0.288	0.094	0.360	0.138	0.088	0.146	0.525	0.117	0.200	0.155	0.233	0.123	0.264
	2	0.436	0.252	0.533	0.110	0.242	0.171	0.131	0.189	0.628	0.254	0.192	0.218	0.308	0.200	0.205
	3	0.369	0.295	0.303	0.145	0.414	0.179	0.279	0.194	0.541	0.205	0.198	0.200	0.233	0.200	0.198
	4	0.566	0.606	0.365	0.267	0.544	0.151	0.447	0.341	0.626	0.376	0.422	0.525	0.461	0.368	0.284
AP ML DST CellTrig	1	0.338	0.260	0.287	0.091	0.359	0.138	0.087	0.148	0.525	0.118	0.200	0.155	0.235	0.126	0.264
	2	0.436	0.251	0.532	0.109	0.252	0.173	0.131	0.189	0.633	0.253	0.191	0.217	0.310	0.200	0.207
	3	0.367	0.297	0.303	0.144	0.414	0.180	0.281	0.194	0.542	0.207	0.194	0.200	0.233	0.200	0.198
	4	0.564	0.603	0.365	0.267	0.510	0.151	0.446	0.341	0.621	0.373	0.413	0.524	0.462	0.368	0.280
AP ML DST MaxLat	1	0.338	0.259	0.289	0.089	0.359	0.142	0.090	0.147	0.510	0.117	0.200	0.155	0.234	0.123	0.264
	2	0.432	0.252	0.533	0.110	0.252	0.246	0.132	0.189	0.540	0.254	0.194	0.217	0.307	0.200	0.206
	3	0.367	0.294	0.304	0.144	0.414	0.179	0.281	0.195	0.524	0.206	0.227	0.200	0.233	0.200	0.228
	4	0.564	0.602	0.365	0.267	0.539	0.151	0.445	0.341	0.624	0.372	0.413	0.519	0.461	0.368	0.280
AP ML ST CellTrig	1	0.338	0.260	0.287	0.094	0.396	0.138	0.089	0.148	0.525	0.118	0.200	0.155	0.235	0.126	0.279
	2	0.435	0.252	0.532	0.110	0.252	0.173	0.131	0.189	0.633	0.254	0.192	0.218	0.310	0.200	0.216
	3	0.369	0.297	0.303	0.145	0.414	0.180	0.284	0.206	0.542	0.207	0.199	0.200	0.233	0.200	0.198
	4	0.566	0.641	0.365	0.267	0.533	0.151	0.449	0.341	0.677	0.392	0.462	0.557	0.462	0.368	0.284

AP ML ST MaxLat	1	0.338	0.259	0.290	0.094	0.396	0.142	0.091	0.147	0.510	0.118	0.200	0.155	0.234	0.123	0.279
	2	0.432	0.252	0.533	0.110	0.252	0.246	0.132	0.189	0.540	0.254	0.194	0.218	0.307	0.200	0.214
	3	0.369	0.295	0.304	0.145	0.414	0.179	0.284	0.207	0.525	0.206	0.231	0.200	0.233	0.200	0.228
	4	0.566	0.640	0.365	0.267	0.571	0.151	0.448	0.341	0.680	0.392	0.462	0.556	0.461	0.368	0.284
AP ML CellTrig MaxLat	1	0.343	0.260	0.315	0.111	0.411	0.167	0.091	0.148	0.510	0.118	0.200	0.155	0.241	0.126	0.306
	2	0.531	0.258	0.612	0.130	0.285	0.248	0.132	0.200	0.577	0.322	0.200	0.234	0.349	0.202	0.217
	3	0.474	0.322	0.319	0.210	0.503	0.180	0.387	0.244	0.533	0.213	0.253	0.200	0.233	0.200	0.232
	4	0.651	0.697	0.402	0.351	0.673	0.151	0.589	0.413	0.677	0.429	0.480	0.591	0.512	0.403	0.287
AP DST ST CellTrig	1	0.166	0.140	0.132	0.083	0.245	0.078	0.081	0.106	0.200	0.081	0.087	0.085	0.110	0.088	0.113
	2	0.189	0.128	0.177	0.086	0.218	0.085	0.106	0.082	0.273	0.085	0.089	0.089	0.096	0.085	0.105
	3	0.126	0.147	0.132	0.087	0.280	0.093	0.179	0.083	0.233	0.090	0.088	0.086	0.102	0.085	0.085
	4	0.295	0.269	0.162	0.169	0.300	0.091	0.263	0.174	0.287	0.184	0.176	0.226	0.208	0.165	0.143
AP DST ST MaxLat	1	0.165	0.138	0.129	0.083	0.238	0.081	0.084	0.105	0.350	0.081	0.086	0.082	0.108	0.086	0.113
	2	0.189	0.128	0.177	0.086	0.218	0.183	0.110	0.085	0.330	0.086	0.089	0.088	0.097	0.084	0.103
	3	0.126	0.147	0.131	0.087	0.289	0.089	0.179	0.087	0.256	0.088	0.129	0.082	0.102	0.083	0.128
	4	0.295	0.269	0.160	0.169	0.290	0.089	0.263	0.175	0.290	0.184	0.176	0.222	0.208	0.166	0.143
AP DST CellTrig MaxLat	1	0.166	0.140	0.132	0.078	0.257	0.082	0.082	0.106	0.350	0.075	0.079	0.082	0.110	0.089	0.113
	2	0.189	0.127	0.177	0.083	0.218	0.186	0.110	0.084	0.330	0.084	0.081	0.079	0.098	0.085	0.105
	3	0.123	0.147	0.133	0.080	0.289	0.091	0.179	0.086	0.256	0.090	0.121	0.084	0.104	0.082	0.128
	4	0.304	0.265	0.162	0.168	0.300	0.091	0.283	0.175	0.287	0.180	0.172	0.235	0.208	0.166	0.140
AP ST CellTrig MaxLat	1	0.166	0.140	0.132	0.100	0.329	0.082	0.084	0.106	0.350	0.081	0.087	0.085	0.110	0.089	0.129
	2	0.189	0.128	0.177	0.104	0.384	0.187	0.110	0.085	0.330	0.086	0.101	0.108	0.099	0.085	0.145
	3	0.126	0.147	0.133	0.099	0.405	0.093	0.210	0.120	0.257	0.091	0.147	0.086	0.104	0.085	0.140
	4	0.364	0.385	0.162	0.190	0.648	0.091	0.287	0.175	0.354	0.262	0.256	0.272	0.208	0.166	0.143
ML DST ST CellTrig	1	0.198	0.189	0.214	0.094	0.267	0.138	0.089	0.131	0.330	0.118	0.200	0.155	0.195	0.122	0.226
	2	0.260	0.201	0.378	0.110	0.153	0.173	0.109	0.189	0.360	0.252	0.192	0.218	0.290	0.200	0.187
	3	0.306	0.217	0.233	0.145	0.313	0.160	0.163	0.194	0.346	0.204	0.198	0.200	0.207	0.200	0.198
	4	0.450	0.363	0.240	0.169	0.268	0.142	0.234	0.200	0.333	0.228	0.275	0.337	0.262	0.230	0.194
ML DST ST MaxLat	1	0.198	0.188	0.216	0.094	0.267	0.142	0.091	0.130	0.410	0.117	0.200	0.155	0.194	0.119	0.226
	2	0.256	0.201	0.380	0.110	0.153	0.246	0.110	0.189	0.410	0.252	0.194	0.218	0.286	0.200	0.186
	3	0.306	0.215	0.233	0.145	0.313	0.159	0.163	0.195	0.357	0.203	0.230	0.200	0.208	0.200	0.228
	4	0.450	0.362	0.240	0.169	0.257	0.142	0.233	0.200	0.333	0.228	0.275	0.331	0.261	0.230	0.194
ML DST CellTrig MaxLat	1	0.198	0.189	0.214	0.091	0.267	0.142	0.091	0.132	0.410	0.118	0.200	0.155	0.196	0.122	0.225
	2	0.256	0.201	0.377	0.110	0.149	0.248	0.110	0.189	0.410	0.252	0.194	0.217	0.288	0.200	0.185
	3	0.301	0.216	0.234	0.144	0.312	0.160	0.162	0.195	0.357	0.204	0.227	0.200	0.208	0.200	0.228
	4	0.450	0.361	0.240	0.169	0.269	0.141	0.252	0.200	0.333	0.228	0.268	0.344	0.262	0.230	0.190
ML ST CellTrig MaxLat	1	0.198	0.189	0.215	0.109	0.339	0.142	0.091	0.132	0.410	0.118	0.200	0.155	0.196	0.122	0.246
	2	0.256	0.201	0.378	0.126	0.304	0.248	0.110	0.189	0.410	0.252	0.204	0.237	0.288	0.200	0.234
	3	0.306	0.217	0.234	0.159	0.385	0.160	0.189	0.234	0.357	0.204	0.247	0.200	0.208	0.200	0.248
	4	0.450	0.487	0.240	0.195	0.614	0.142	0.258	0.200	0.400	0.307	0.384	0.390	0.262	0.230	0.194
DST ST CellTrig MaxLat	1	0.084	0.088	0.087	0.100	0.237	0.082	0.084	0.087	0.292	0.080	0.087	0.085	0.086	0.085	0.099
	2	0.084	0.088	0.088	0.104	0.286	0.187	0.088	0.085	0.252	0.083	0.101	0.108	0.088	0.085	0.129
	3	0.084	0.089	0.088	0.099	0.327	0.081	0.119	0.119	0.126	0.088	0.147	0.086	0.085	0.085	0.140
	4	0.152	0.195	0.087	0.106	0.407	0.082	0.137	0.084	0.124	0.149	0.168	0.168	0.087	0.084	0.086

Table C.2: Stability index values calculated from raw F-Scan data filtered with an averaging filter.

	Level		Subjects													
		1	2	3	4	5	6	7	8	9	10	11	12	13	14	15
SIX PARAMS	1	0.381	0.260	0.336	0.078	0.429	0.109	0.084	0.144	0.505	0.113	0.200	0.155	0.213	0.136	0.295
	2	0.535	0.249	0.442	0.108	0.361	0.200	0.109	0.188	0.558	0.247	0.221	0.218	0.310	0.207	0.187
	3	0.415	0.282	0.308	0.133	0.435	0.178	0.277	0.202	0.564	0.201	0.245	0.200	0.233	0.200	0.188
	4	0.573	0.634	0.378	0.280	0.543	0.203	0.424	0.362	0.442	0.342	0.453	0.516	0.481	0.385	0.439
AP ML DST ST CellTrig	1	0.332	0.261	0.336	0.082	0.438	0.106	0.084	0.147	0.503	0.114	0.200	0.156	0.215	0.138	0.295
	2	0.535	0.251	0.441	0.110	0.369	0.200	0.108	0.189	0.581	0.247	0.223	0.218	0.311	0.208	0.187
	3	0.419	0.283	0.307	0.134	0.430	0.179	0.278	0.202	0.570	0.204	0.255	0.200	0.233	0.200	0.188
	4	0.573	0.632	0.382	0.280	0.514	0.203	0.439	0.374	0.551	0.347	0.451	0.503	0.484	0.385	0.365
AP ML DST ST MaxLat	1	0.333	0.260	0.336	0.082	0.438	0.111	0.086	0.146	0.505	0.113	0.200	0.155	0.214	0.136	0.295
	2	0.535	0.251	0.441	0.110	0.363	0.275	0.110	0.189	0.548	0.248	0.223	0.218	0.310	0.208	0.187
	3	0.416	0.282	0.307	0.134	0.427	0.178	0.278	0.202	0.516	0.203	0.288	0.200	0.233	0.200	0.188
	4	0.573	0.632	0.378	0.280	0.548	0.203	0.429	0.346	0.513	0.347	0.451	0.502	0.482	0.385	0.365
AP ML DST CellTrig MaxLat	1	0.333	0.261	0.336	0.079	0.438	0.111	0.086	0.147	0.505	0.113	0.200	0.155	0.216	0.138	0.295
	2	0.558	0.250	0.439	0.109	0.369	0.275	0.110	0.189	0.548	0.248	0.223	0.217	0.311	0.207	0.187
	3	0.429	0.282	0.307	0.133	0.454	0.179	0.284	0.215	0.516	0.204	0.291	0.200	0.233	0.200	0.188
	4	0.588	0.629	0.382	0.280	0.528	0.203	0.445	0.346	0.513	0.341	0.451	0.502	0.484	0.385	0.362
AP ML ST CellTrig MaxLat	1	0.333	0.261	0.336	0.082	0.458	0.111	0.086	0.147	0.505	0.114	0.200	0.156	0.216	0.138	0.295
	2	0.558	0.251	0.439	0.112	0.428	0.275	0.110	0.189	0.548	0.248	0.223	0.218	0.311	0.217	0.187
	3	0.432	0.282	0.307	0.136	0.499	0.179	0.295	0.217	0.516	0.204	0.304	0.200	0.233	0.200	0.188
	4	0.588	0.673	0.382	0.290	0.671	0.203	0.444	0.346	0.538	0.364	0.490	0.544	0.484	0.385	0.365
AP DST ST CellTrig MaxLat	1	0.165	0.142	0.131	0.082	0.431	0.083	0.085	0.105	0.350	0.081	0.087	0.085	0.110	0.086	0.130
	2	0.259	0.128	0.166	0.086	0.268	0.185	0.109	0.085	0.331	0.089	0.089	0.089	0.098	0.086	0.097
	3	0.163	0.140	0.138	0.087	0.283	0.094	0.178	0.129	0.285	0.087	0.130	0.085	0.103	0.085	0.099
	4	0.335	0.278	0.177	0.183	0.300	0.112	0.272	0.204	0.338	0.219	0.188	0.198	0.210	0.177	0.223
ML DST ST CellTrig MaxLat	1	0.193	0.189	0.256	0.082	0.390	0.111	0.086	0.132	0.405	0.114	0.200	0.156	0.185	0.137	0.259
	2	0.367	0.203	0.305	0.110	0.278	0.275	0.088	0.189	0.417	0.244	0.223	0.218	0.291	0.208	0.174
	3	0.310	0.204	0.221	0.134	0.318	0.159	0.163	0.203	0.412	0.204	0.288	0.200	0.208	0.200	0.175
	4	0.463	0.369	0.226	0.170	0.267	0.163	0.228	0.230	0.374	0.218	0.289	0.318	0.282	0.230	0.306
AP ML DST ST	1	0.344	0.260	0.336	0.082	0.438	0.106	0.083	0.144	0.503	0.113	0.200	0.155	0.213	0.136	0.295
	2	0.535	0.251	0.442	0.110	0.379	0.200	0.108	0.188	0.582	0.247	0.223	0.218	0.310	0.208	0.187
	3	0.416	0.283	0.307	0.134	0.427	0.178	0.278	0.201	0.569	0.202	0.255	0.200	0.233	0.200	0.188
	4	0.573	0.632	0.378	0.280	0.544	0.203	0.429	0.374	0.551	0.347	0.451	0.502	0.482	0.385	0.365
AP ML DST CellTrig	1	0.344	0.261	0.336	0.079	0.438	0.106	0.082	0.147	0.503	0.113	0.200	0.155	0.215	0.138	0.295
	2	0.535	0.249	0.440	0.109	0.369	0.200	0.108	0.189	0.581	0.247	0.222	0.217	0.311	0.207	0.187
	3	0.417	0.282	0.307	0.133	0.427	0.179	0.276	0.202	0.570	0.204	0.243	0.200	0.233	0.200	0.188
	4	0.573	0.629	0.382	0.280	0.513	0.203	0.425	0.374	0.550	0.341	0.447	0.502	0.484	0.385	0.362
AP ML DST MaxLat	1	0.345	0.260	0.336	0.077	0.438	0.111	0.086	0.146	0.505	0.113	0.200	0.155	0.214	0.136	0.295
	2	0.535	0.250	0.441	0.109	0.359	0.275	0.110	0.189	0.548	0.248	0.223	0.217	0.310	0.207	0.187
	3	0.413	0.282	0.307	0.133	0.427	0.178	0.276	0.202	0.515	0.203	0.279	0.200	0.233	0.200	0.188
	4	0.573	0.629	0.378	0.280	0.547	0.203	0.425	0.346	0.513	0.341	0.448	0.501	0.482	0.385	0.362
AP ML ST CellTrig	1	0.344	0.261	0.336	0.082	0.458	0.106	0.084	0.147	0.503	0.114	0.200	0.156	0.215	0.138	0.295
	2	0.535	0.251	0.441	0.110	0.379	0.200	0.108	0.189	0.581	0.247	0.223	0.218	0.311	0.217	0.187
	3	0.419	0.283	0.307	0.134	0.465	0.179	0.283	0.216	0.570	0.204	0.256	0.200	0.233	0.200	0.188
	4	0.573	0.673	0.382	0.280	0.525	0.203	0.429	0.376	0.605	0.347	0.490	0.544	0.484	0.385	0.365
AP ML ST MaxLat	1	0.345	0.260	0.336	0.082	0.458	0.111	0.086	0.146	0.505	0.113	0.200	0.155	0.214	0.136	0.295
	2	0.535	0.251	0.441	0.110	0.373	0.275	0.110	0.189	0.548	0.248	0.223	0.218	0.310	0.217	0.187
	3	0.416	0.282	0.307	0.134	0.465	0.178	0.283	0.217	0.516	0.203	0.289	0.200	0.233	0.200	0.188
	4	0.573	0.674	0.378	0.280	0.569	0.203	0.429	0.346	0.538	0.347	0.490	0.543	0.482	0.385	0.365
AP ML CellTrig MaxLat	1	0.364	0.261	0.400	0.079	0.465	0.111	0.086	0.147	0.505	0.113	0.200	0.155	0.221	0.138	0.307
	2	0.635	0.258	0.484	0.129	0.469	0.275	0.110	0.200	0.586	0.308	0.248	0.234	0.352	0.218	0.187
	3	0.520	0.295	0.321	0.193	0.515	0.179	0.383	0.233	0.518	0.210	0.344	0.200	0.233	0.200	0.188
	4	0.629	0.740	0.402	0.364	0.674	0.203	0.562	0.411	0.563	0.361	0.530	0.612	0.554	0.420	0.370
AP DST ST CellTrig	1	0.165	0.142	0.131	0.082	0.354	0.078	0.081	0.105	0.188	0.081	0.087	0.085	0.109	0.085	0.130
	2	0.259	0.128	0.166	0.086	0.268	0.082	0.106	0.082	0.234	0.087	0.089	0.089	0.097	0.086	0.096
	3	0.163	0.140	0.138	0.087	0.260	0.094	0.178	0.124	0.243	0.086	0.089	0.085	0.102	0.085	0.096
	4	0.298	0.278	0.177	0.183	0.296	0.111	0.262	0.192	0.264	0.205	0.187	0.197	0.210	0.177	0.183
AP DST ST MaxLat	1	0.165	0.140	0.131	0.082	0.348	0.081	0.085	0.104	0.350	0.080	0.087	0.082	0.107	0.084	0.130
	2	0.234	0.128	0.166	0.086	0.262	0.184	0.109	0.085	0.331	0.089	0.089	0.088	0.096	0.084	0.095
	3	0.162	0.140	0.138	0.087	0.280	0.089	0.178	0.105	0.284	0.085	0.130	0.081	0.102	0.083	0.098
	4	0.335	0.278	0.176	0.183	0.289	0.109	0.262	0.204	0.338	0.205	0.188	0.198	0.209	0.177	0.183
AP DST CellTrig MaxLat	1	0.166	0.142	0.131	0.078	0.430	0.083	0.083	0.105	0.350	0.075	0.079	0.082	0.110	0.086	0.130
	2	0.259	0.127	0.165	0.083	0.267	0.183	0.108	0.084	0.331	0.087	0.081	0.079	0.098	0.086	0.097
	3	0.160	0.140	0.138	0.081	0.287	0.090	0.177	0.128	0.285	0.086	0.119	0.083	0.103	0.082	0.099
	4	0.336	0.272	0.177	0.181	0.299	0.111	0.282	0.204	0.338	0.212	0.184	0.198	0.210	0.177	0.222
AP ST CellTrig MaxLat	1	0.166	0.142	0.131	0.082	0.471	0.083	0.085	0.105	0.350	0.081	0.087	0.085	0.110	0.086	0.204
	2	0.259	0.128	0.166	0.104	0.414	0.185	0.109	0.085	0.331	0.089	0.100	0.108	0.098	0.097	0.097
	3	0.163	0.140	0.138	0.099	0.384	0.094	0.209	0.153	0.285	0.087	0.147	0.085	0.103	0.085	0.099
	4	0.407	0.394	0.177	0.204	0.654	0.112	0.286	0.204	0.363	0.259	0.277	0.250	0.210	0.177	0.223

ML DST ST CellTrig	**1**	0.204	0.189	0.256	0.082	0.387	0.106	0.084	0.131	0.323	0.114	0.200	0.156	0.183	0.137	0.259
	2	0.367	0.203	0.305	0.110	0.278	0.200	0.085	0.189	0.347	0.244	0.223	0.218	0.291	0.208	0.174
	3	0.310	0.204	0.221	0.134	0.315	0.159	0.162	0.202	0.357	0.204	0.255	0.200	0.207	0.200	0.175
	4	0.463	0.369	0.226	0.170	0.267	0.163	0.217	0.238	0.349	0.218	0.289	0.318	0.282	0.230	0.266
ML DST ST MaxLat	**1**	0.205	0.188	0.256	0.082	0.387	0.111	0.086	0.131	0.405	0.113	0.200	0.155	0.183	0.136	0.259
	2	0.367	0.203	0.306	0.110	0.272	0.275	0.088	0.189	0.417	0.244	0.223	0.218	0.289	0.208	0.174
	3	0.307	0.204	0.222	0.134	0.315	0.158	0.163	0.202	0.412	0.203	0.288	0.200	0.208	0.200	0.175
	4	0.463	0.369	0.222	0.170	0.257	0.163	0.218	0.230	0.374	0.218	0.289	0.317	0.281	0.230	0.266
ML DST CellTrig MaxLat	**1**	0.205	0.189	0.256	0.079	0.389	0.111	0.086	0.132	0.405	0.113	0.200	0.155	0.185	0.137	0.259
	2	0.367	0.203	0.304	0.109	0.277	0.275	0.088	0.189	0.417	0.244	0.223	0.217	0.291	0.206	0.174
	3	0.306	0.204	0.221	0.133	0.320	0.159	0.158	0.204	0.412	0.204	0.279	0.200	0.208	0.200	0.175
	4	0.463	0.369	0.226	0.169	0.266	0.163	0.234	0.230	0.374	0.217	0.284	0.317	0.282	0.230	0.303
ML ST CellTrig MaxLat	**1**	0.205	0.189	0.256	0.082	0.430	0.111	0.086	0.132	0.405	0.114	0.200	0.156	0.185	0.137	0.259
	2	0.367	0.203	0.305	0.125	0.429	0.275	0.088	0.189	0.417	0.244	0.233	0.238	0.291	0.224	0.174
	3	0.310	0.204	0.221	0.148	0.425	0.159	0.190	0.235	0.412	0.204	0.302	0.200	0.208	0.200	0.175
	4	0.463	0.495	0.226	0.196	0.622	0.163	0.242	0.230	0.399	0.258	0.399	0.383	0.282	0.230	0.306
DST ST CellTrig MaxLat	**1**	0.085	0.089	0.086	0.082	0.398	0.083	0.085	0.087	0.292	0.080	0.087	0.085	0.086	0.085	0.138
	2	0.124	0.088	0.087	0.104	0.354	0.185	0.087	0.085	0.252	0.083	0.100	0.108	0.086	0.096	0.086
	3	0.086	0.089	0.086	0.099	0.295	0.082	0.119	0.152	0.210	0.087	0.147	0.085	0.085	0.085	0.087
	4	0.197	0.197	0.086	0.105	0.408	0.081	0.138	0.125	0.256	0.167	0.169	0.135	0.085	0.085	0.189

Table C.3: Difference in stability index value between the averaging filter values (Table C.2) and the median filter values (Table C.1). The difference between the two data sets has an average of 3.13%.

	Subjects														
	1	2	3	4	5	6	7	8	9	10	11	12	13	14	15
SIX PARAMS	0.009	0.001	0.048	-0.012	0.070	-0.033	-0.006	-0.001	-0.005	-0.005	0.000	0.000	-0.021	0.013	0.031
	0.099	-0.002	-0.091	-0.001	0.119	0.029	-0.023	-0.001	-0.042	-0.007	0.031	0.000	0.001	0.007	-0.019
	0.047	-0.011	0.007	-0.011	0.022	-0.001	-0.004	0.008	0.023	-0.003	0.051	0.000	0.000	0.000	-0.010
	0.005	0.027	0.013	0.013	0.002	0.052	-0.020	0.021	-0.187	-0.030	0.034	-0.001	0.021	0.016	0.158
AP ML DST ST CellTrig	0.006	0.001	0.048	-0.012	0.079	-0.032	-0.005	-0.001	-0.022	-0.005	0.000	0.000	-0.021	0.012	0.031
	0.100	-0.001	-0.091	0.000	0.117	0.027	-0.023	0.000	-0.052	-0.006	0.030	0.000	0.002	0.008	-0.019
	0.050	-0.014	0.003	-0.011	0.016	-0.001	-0.001	0.008	0.028	-0.003	0.056	0.000	0.000	0.000	-0.011
	0.007	0.024	0.017	0.013	-0.001	0.052	-0.020	0.033	-0.070	-0.030	0.029	-0.022	0.022	0.016	0.081
AP ML DST ST MaxLat	0.007	0.001	0.046	-0.012	0.079	-0.032	-0.005	-0.001	-0.005	-0.005	0.000	0.000	-0.021	0.013	0.031
	0.104	-0.001	-0.093	0.000	0.112	0.029	-0.023	0.000	0.008	-0.006	0.029	0.000	0.003	0.008	-0.018
	0.047	-0.013	0.003	-0.011	0.013	-0.001	-0.001	0.008	-0.009	-0.003	0.058	0.000	0.000	0.000	-0.040
	0.007	0.026	0.013	0.013	0.004	0.052	-0.019	0.005	-0.111	-0.030	0.029	-0.018	0.021	0.016	0.081
AP ML DST CellTrig MaxLat	0.007	0.001	0.048	-0.012	0.079	-0.032	-0.005	-0.001	-0.005	-0.005	0.000	0.000	-0.021	0.012	0.031
	0.110	-0.002	-0.093	-0.001	0.117	0.027	-0.023	0.000	0.008	-0.006	0.029	0.000	0.003	0.007	-0.020
	0.062	-0.015	0.002	-0.011	0.041	-0.001	-0.006	0.010	-0.009	-0.003	0.051	0.000	0.000	0.000	-0.040
	0.024	0.025	0.017	0.013	0.004	0.052	-0.027	0.001	-0.108	-0.041	0.038	-0.017	0.022	0.016	0.082
AP ML ST CellTrig MaxLat	0.007	0.001	0.047	-0.019	0.062	-0.032	-0.005	-0.001	-0.005	-0.005	0.000	0.000	-0.021	0.012	0.016
	0.110	-0.001	-0.093	0.000	0.166	0.027	-0.023	0.000	0.008	-0.006	0.029	0.000	0.003	0.017	-0.029
	0.063	-0.015	0.002	-0.011	0.057	-0.001	-0.001	0.007	-0.009	-0.003	0.057	0.000	0.000	0.000	-0.040
	0.022	0.033	0.017	0.013	-0.001	0.052	-0.024	0.001	-0.139	-0.048	0.025	-0.012	0.022	0.016	0.081
AP DST ST CellTrig MaxLat	0.000	0.003	-0.001	-0.001	0.173	0.001	0.001	-0.001	0.000	-0.001	0.001	0.000	-0.001	-0.003	0.017
	0.070	0.000	-0.012	0.000	0.050	-0.003	-0.001	0.000	0.001	0.003	0.000	0.000	-0.001	0.000	-0.008
	0.036	-0.007	0.006	0.000	-0.006	0.001	-0.001	0.041	0.028	-0.004	0.001	-0.001	0.000	0.000	-0.030
	0.040	0.009	0.016	0.013	-0.004	0.020	-0.001	0.029	0.050	0.035	0.011	-0.037	0.001	0.011	0.081
ML DST ST CellTrig MaxLat	0.007	0.000	0.041	-0.012	0.122	-0.032	-0.005	0.000	-0.005	-0.004	0.000	0.000	-0.011	0.016	0.033
	0.110	0.002	-0.073	0.000	0.125	0.027	-0.022	0.000	0.007	-0.008	0.029	0.000	0.003	0.008	-0.014
	0.004	-0.013	-0.013	-0.011	0.005	-0.001	0.000	0.008	0.055	0.000	0.058	0.000	0.000	0.000	-0.053
	0.013	0.006	-0.014	0.000	-0.004	0.022	-0.016	0.030	0.040	-0.010	0.014	-0.027	0.020	0.000	0.113
AP ML DST ST	0.006	0.001	0.048	-0.012	0.079	-0.032	-0.005	-0.001	-0.022	-0.005	0.000	0.000	-0.021	0.013	0.031
	0.099	-0.001	-0.091	0.000	0.137	0.029	-0.023	-0.001	-0.046	-0.006	0.030	0.000	0.002	0.008	-0.018
	0.047	-0.012	0.005	-0.011	0.013	0.000	-0.001	0.008	0.028	-0.003	0.056	0.000	0.000	0.000	-0.010
	0.007	0.026	0.013	0.013	0.000	0.052	-0.019	0.033	-0.075	-0.030	0.029	-0.023	0.021	0.016	0.081
AP ML DST CellTrig	0.006	0.001	0.049	-0.012	0.079	-0.032	-0.005	-0.001	-0.022	-0.005	0.000	0.000	-0.021	0.012	0.031
	0.100	-0.002	-0.092	-0.001	0.117	0.027	-0.023	0.000	-0.052	-0.007	0.031	0.000	0.002	0.007	-0.020
	0.050	-0.014	0.003	-0.011	0.013	-0.001	-0.004	0.008	0.028	-0.003	0.050	0.000	0.000	0.000	-0.011
	0.009	0.025	0.017	0.013	0.002	0.052	-0.021	0.033	-0.070	-0.031	0.034	-0.022	0.022	0.016	0.082
AP ML DST MaxLat	0.007	0.001	0.047	-0.012	0.079	-0.032	-0.005	-0.001	-0.005	-0.005	0.000	0.000	-0.021	0.013	0.031
	0.104	-0.002	-0.093	-0.001	0.107	0.029	-0.023	0.000	0.008	-0.006	0.029	0.000	0.003	0.007	-0.019
	0.047	-0.012	0.003	-0.011	0.013	-0.001	-0.004	0.008	-0.009	-0.003	0.052	0.000	0.000	0.000	-0.040
	0.009	0.027	0.013	0.013	0.007	0.052	-0.020	0.005	-0.111	-0.030	0.034	-0.019	0.021	0.016	0.082
AP ML ST CellTrig	0.006	0.001	0.048	-0.012	0.062	-0.032	-0.005	-0.001	-0.022	-0.005	0.000	0.000	-0.021	0.012	0.016
	0.100	-0.001	-0.091	0.000	0.127	0.027	-0.023	0.000	-0.052	-0.006	0.030	0.000	0.002	0.017	-0.029
	0.050	-0.014	0.003	-0.011	0.051	-0.001	-0.001	0.010	0.028	-0.003	0.056	0.000	0.000	0.000	-0.011
	0.007	0.033	0.017	0.013	-0.008	0.052	-0.020	0.035	-0.071	-0.046	0.028	-0.013	0.022	0.016	0.081
AP ML ST MaxLat	0.007	0.001	0.046	-0.012	0.062	-0.032	-0.005	-0.001	-0.005	-0.005	0.000	0.000	-0.021	0.013	0.016
	0.104	-0.001	-0.093	0.000	0.122	0.029	-0.023	0.000	0.008	-0.006	0.029	0.000	0.003	0.017	-0.027
	0.047	-0.013	0.003	-0.011	0.051	-0.001	-0.001	0.010	-0.009	-0.003	0.058	0.000	0.000	0.000	-0.040
	0.007	0.034	0.013	0.013	-0.002	0.052	-0.019	0.005	-0.143	-0.046	0.028	-0.013	0.021	0.016	0.081
AP ML CellTrig MaxLat	0.021	0.001	0.085	-0.032	0.054	-0.057	-0.005	-0.001	-0.005	-0.005	0.000	0.000	-0.021	0.012	0.000
	0.105	0.000	-0.128	-0.001	0.184	0.027	-0.023	0.000	0.009	-0.014	0.048	0.000	0.003	0.015	-0.030
	0.046	-0.027	0.002	-0.017	0.011	-0.001	-0.004	-0.011	-0.015	-0.003	0.091	0.000	0.000	0.000	-0.044
	-0.022	0.043	0.000	0.014	0.001	0.052	-0.027	-0.002	-0.115	-0.068	0.050	0.021	0.042	0.016	0.083
AP DST ST CellTrig	0.000	0.003	-0.001	-0.001	0.110	0.000	0.000	-0.001	-0.011	-0.001	0.000	0.000	-0.001	-0.003	0.017
	0.070	0.000	-0.012	0.000	0.050	-0.003	0.000	0.000	-0.039	0.002	0.000	0.000	0.001	0.000	-0.009
	0.037	-0.007	0.006	0.000	-0.020	0.001	-0.001	0.041	0.010	-0.004	0.001	-0.001	0.000	0.000	0.012
	0.003	0.009	0.016	0.013	-0.005	0.021	-0.001	0.018	-0.023	0.021	0.011	-0.029	0.001	0.011	0.041
AP DST ST MaxLat	0.000	0.002	0.002	-0.001	0.111	0.001	0.001	-0.001	0.000	-0.001	0.001	0.000	-0.001	-0.002	0.017
	0.046	0.000	-0.011	0.000	0.044	0.001	-0.001	0.000	0.001	0.002	0.000	0.000	-0.001	0.000	-0.008
	0.036	-0.007	0.007	0.000	-0.009	0.001	-0.001	0.017	0.028	-0.003	0.001	-0.001	0.000	0.000	-0.030
	0.040	0.009	0.016	0.013	-0.001	0.020	-0.001	0.029	0.047	0.022	0.011	-0.024	0.000	0.011	0.041
AP DST CellTrig MaxLat	0.000	0.003	-0.001	0.000	0.173	0.001	0.001	-0.001	0.000	-0.001	0.001	0.000	-0.001	-0.003	0.017
	0.070	0.000	-0.012	0.000	0.049	-0.003	-0.002	0.000	0.001	0.003	0.000	0.000	-0.001	0.000	-0.008
	0.037	-0.007	0.005	0.000	-0.002	0.000	-0.002	0.042	0.028	-0.004	-0.002	-0.001	0.000	0.001	-0.029
	0.032	0.007	0.016	0.013	-0.001	0.020	-0.001	0.029	0.050	0.032	0.012	-0.037	0.001	0.011	0.082
AP ST CellTrig MaxLat	0.000	0.003	-0.001	-0.018	0.142	0.001	0.001	-0.001	0.000	-0.001	0.001	0.000	-0.001	-0.003	0.075
	0.070	0.000	-0.012	-0.001	0.031	-0.003	-0.001	0.000	0.001	0.003	0.000	0.000	-0.001	0.011	-0.048
	0.037	-0.007	0.006	0.000	-0.021	0.001	-0.001	0.033	0.028	-0.004	0.000	-0.001	0.000	0.000	-0.041
	0.042	0.010	0.016	0.013	0.006	0.020	0.000	0.029	0.009	-0.003	0.020	-0.022	0.001	0.011	0.081

ML DST ST CellTrig	0.006	0.000	0.042	-0.012	0.120	-0.032	-0.005	0.000	-0.007	-0.004	0.000	0.000	-0.011	0.016	0.033
	0.106	0.002	-0.073	0.000	0.125	0.027	-0.023	0.000	-0.013	-0.008	0.030	0.000	0.001	0.008	-0.014
	0.004	-0.013	-0.012	-0.011	0.002	-0.001	0.000	0.008	0.011	0.000	0.056	0.000	0.000	0.000	-0.023
	0.013	0.006	-0.014	0.000	0.000	0.022	-0.017	0.038	0.015	-0.010	0.014	-0.019	0.020	0.000	0.073
ML DST ST MaxLat	0.007	0.000	0.040	-0.012	0.120	-0.032	-0.005	0.000	-0.005	-0.004	0.000	0.000	-0.011	0.016	0.033
	0.110	0.002	-0.074	0.000	0.120	0.029	-0.022	0.000	0.007	-0.008	0.029	0.000	0.003	0.008	-0.012
	0.001	-0.011	-0.011	-0.011	0.002	-0.001	0.000	0.008	0.055	0.000	0.058	0.000	0.000	0.000	-0.053
	0.013	0.007	-0.018	0.000	0.000	0.022	-0.015	0.030	0.040	-0.010	0.014	-0.014	0.020	0.000	0.073
ML DST CellTrig MaxLat	0.007	0.000	0.042	-0.012	0.122	-0.032	-0.005	0.000	-0.005	-0.004	0.000	0.000	-0.011	0.016	0.035
	0.110	0.002	-0.073	-0.001	0.128	0.027	-0.022	0.000	0.007	-0.008	0.029	0.000	0.003	0.006	-0.011
	0.005	-0.012	-0.013	-0.011	0.008	-0.001	-0.004	0.008	0.055	0.000	0.052	0.000	0.000	0.000	-0.053
	0.013	0.008	-0.014	0.000	-0.003	0.022	-0.017	0.030	0.040	-0.010	0.016	-0.027	0.020	0.000	0.113
ML ST CellTrig MaxLat	0.007	0.000	0.041	-0.027	0.091	-0.032	-0.005	0.000	-0.005	-0.004	0.000	0.000	-0.011	0.016	0.014
	0.110	0.002	-0.073	-0.001	0.125	0.027	-0.022	0.000	0.007	-0.008	0.028	0.000	0.003	0.024	-0.061
	0.004	-0.013	-0.013	-0.011	0.040	-0.001	0.001	0.002	0.055	0.000	0.055	0.000	0.000	0.000	-0.073
	0.013	0.007	-0.014	0.000	0.007	0.022	-0.016	0.030	-0.001	-0.049	0.015	-0.008	0.020	0.000	0.113
DST ST CellTrig MaxLat	0.000	0.000	-0.002	-0.018	0.161	0.001	0.001	0.000	0.001	0.000	0.001	0.000	0.000	0.000	0.039
	0.040	0.000	-0.001	-0.001	0.068	-0.003	0.000	0.000	0.000	0.000	0.000	0.000	-0.002	0.011	-0.043
	0.001	0.000	-0.002	0.000	-0.032	0.001	0.001	0.033	0.084	0.000	0.000	-0.001	0.000	0.000	-0.053
	0.045	0.003	-0.001	0.000	0.000	-0.001	0.001	0.041	0.132	0.018	0.001	-0.032	-0.002	0.000	0.103

Appendix D

This appendix shows the mean stability index values for each subject, across all trials, for each stability level, from the best 11 parameter combinations (Section 5.2.4).

Table D.1: Stability index values for each subject across all trials for each stability level. The standard deviations of each value are in parentheses.

	Stability Level	Subjects														
		1	2	3	4	5	6	7	8	9	10	11	12	13	14	15
SIX PARAMS	1	0.38 (0.09)	0.26 (0.06)	0.34 (0.07)	0.08 (0.03)	0.43 (0.17)	0.11 (0.00)	0.08 (0.01)	0.14 (0.05)	0.51 (0.05)	0.11 (0.03)	0.20 (0.00)	0.16 (0.03)	0.21 (0.04)	0.14 (0.03)	0.30 (0.07)
	2	0.54 (0.09)	0.25 (0.07)	0.44 (0.07)	0.11 (0.03)	0.36 (0.10)	0.20 (0.04)	0.11 (0.05)	0.19 (0.02)	0.56 (0.09)	0.25 (0.05)	0.22 (0.03)	0.22 (0.02)	0.31 (0.09)	0.21 (0.00)	0.19 (0.05)
	3	0.41 (0.11)	0.28 (0.08)	0.31 (0.11)	0.13 (0.03)	0.44 (0.04)	0.18 (0.08)	0.28 (0.08)	0.20 (0.07)	0.56 (0.02)	0.20 (0.01)	0.25 (0.03)	0.20 (0.00)	0.23 (0.06)	0.20 (0.00)	0.19 (0.00)
	4	0.57 (0.15)	0.63 (0.12)	0.38 (0.15)	0.28 (0.09)	0.54 (0.12)	0.20 (0.02)	0.42 (0.08)	0.36 (0.11)	0.44 (0.16)	0.34 (0.11)	0.45 (0.13)	0.52 (0.10)	0.48 (0.14)	0.38 (0.11)	0.44 (0.12)
AP ML DST ST CellTrig	1	0.33 (0.11)	0.26 (0.06)	0.34 (0.06)	0.08 (0.03)	0.44 (0.17)	0.11 (0.00)	0.08 (0.01)	0.15 (0.06)	0.50 (0.08)	0.11 (0.03)	0.20 (0.00)	0.16 (0.03)	0.21 (0.04)	0.14 (0.03)	0.29 (0.07)
	2	0.54 (0.09)	0.25 (0.07)	0.44 (0.07)	0.11 (0.03)	0.37 (0.12)	0.20 (0.04)	0.11 (0.05)	0.19 (0.02)	0.58 (0.08)	0.25 (0.05)	0.22 (0.03)	0.22 (0.03)	0.31 (0.08)	0.21 (0.00)	0.19 (0.04)
	3	0.42 (0.11)	0.28 (0.08)	0.31 (0.11)	0.13 (0.03)	0.43 (0.04)	0.18 (0.08)	0.28 (0.08)	0.20 (0.07)	0.57 (0.02)	0.20 (0.01)	0.25 (0.04)	0.20 (0.00)	0.23 (0.06)	0.20 (0.00)	0.19 (0.00)
	4	0.57 (0.15)	0.63 (0.12)	0.38 (0.15)	0.28 (0.09)	0.51 (0.10)	0.20 (0.02)	0.44 (0.10)	0.37 (0.11)	0.55 (0.15)	0.35 (0.11)	0.45 (0.14)	0.50 (0.13)	0.48 (0.13)	0.38 (0.11)	0.37 (0.12)
AP ML DST ST MaxLat	1	0.33 (0.11)	0.26 (0.06)	0.34 (0.07)	0.08 (0.03)	0.44 (0.17)	0.11 (0.00)	0.09 (0.01)	0.15 (0.05)	0.51 (0.05)	0.11 (0.03)	0.20 (0.00)	0.16 (0.03)	0.21 (0.04)	0.14 (0.03)	0.30 (0.07)
	2	0.54 (0.09)	0.25 (0.07)	0.44 (0.07)	0.11 (0.03)	0.36 (0.12)	0.27 (0.07)	0.11 (0.05)	0.19 (0.02)	0.55 (0.02)	0.25 (0.05)	0.22 (0.03)	0.22 (0.03)	0.31 (0.08)	0.21 (0.00)	0.19 (0.04)
	3	0.42 (0.11)	0.28 (0.08)	0.31 (0.11)	0.13 (0.03)	0.43 (0.04)	0.18 (0.08)	0.28 (0.08)	0.20 (0.07)	0.52 (0.04)	0.20 (0.01)	0.29 (0.08)	0.20 (0.00)	0.23 (0.06)	0.20 (0.00)	0.19 (0.07)
	4	0.57 (0.15)	0.63 (0.12)	0.38 (0.15)	0.28 (0.09)	0.55 (0.12)	0.20 (0.02)	0.43 (0.08)	0.35 (0.11)	0.51 (0.15)	0.35 (0.11)	0.45 (0.14)	0.50 (0.12)	0.48 (0.14)	0.38 (0.11)	0.37 (0.12)
AP ML DST CellTrig MaxLat	1	0.33 (0.11)	0.26 (0.06)	0.34 (0.07)	0.08 (0.03)	0.44 (0.17)	0.11 (0.00)	0.09 (0.01)	0.15 (0.05)	0.51 (0.05)	0.11 (0.03)	0.20 (0.00)	0.16 (0.03)	0.22 (0.04)	0.14 (0.03)	0.29 (0.07)
	2	0.56 (0.10)	0.25 (0.07)	0.44 (0.07)	0.11 (0.03)	0.37 (0.12)	0.27 (0.07)	0.11 (0.05)	0.19 (0.02)	0.55 (0.02)	0.25 (0.05)	0.22 (0.03)	0.22 (0.02)	0.31 (0.08)	0.21 (0.00)	0.19 (0.05)
	3	0.43 (0.11)	0.28 (0.08)	0.31 (0.11)	0.13 (0.03)	0.45 (0.04)	0.18 (0.08)	0.28 (0.08)	0.22 (0.07)	0.52 (0.05)	0.20 (0.01)	0.29 (0.08)	0.20 (0.00)	0.23 (0.06)	0.20 (0.00)	0.19 (0.07)
	4	0.59 (0.15)	0.63 (0.12)	0.38 (0.15)	0.28 (0.09)	0.53 (0.10)	0.20 (0.02)	0.45 (0.12)	0.35 (0.11)	0.51 (0.15)	0.34 (0.14)	0.45 (0.13)	0.50 (0.12)	0.48 (0.13)	0.38 (0.11)	0.36 (0.12)
AP ML ST CellTrig MaxLat	1	0.33 (0.11)	0.26 (0.06)	0.34 (0.07)	0.08 (0.04)	0.46 (0.21)	0.11 (0.00)	0.09 (0.01)	0.15 (0.05)	0.51 (0.05)	0.11 (0.03)	0.20 (0.00)	0.16 (0.03)	0.22 (0.04)	0.14 (0.03)	0.29 (0.09)
	2	0.56 (0.10)	0.25 (0.07)	0.44 (0.07)	0.11 (0.03)	0.43 (0.13)	0.27 (0.07)	0.11 (0.05)	0.19 (0.02)	0.55 (0.02)	0.25 (0.05)	0.22 (0.03)	0.22 (0.03)	0.31 (0.08)	0.22 (0.00)	0.19 (0.05)
	3	0.43 (0.11)	0.28 (0.08)	0.31 (0.11)	0.14 (0.03)	0.50 (0.04)	0.18 (0.08)	0.29 (0.08)	0.22 (0.08)	0.52 (0.05)	0.20 (0.01)	0.30 (0.08)	0.20 (0.00)	0.23 (0.06)	0.20 (0.00)	0.19 (0.07)
	4	0.59 (0.15)	0.67 (0.15)	0.38 (0.11)	0.29 (0.10)	0.67 (0.08)	0.20 (0.02)	0.44 (0.11)	0.35 (0.11)	0.54 (0.19)	0.36 (0.19)	0.49 (0.15)	0.54 (0.15)	0.48 (0.13)	0.38 (0.11)	0.37 (0.12)
AP ML DST ST	1	0.34 (0.11)	0.26 (0.06)	0.34 (0.07)	0.08 (0.03)	0.44 (0.17)	0.11 (0.00)	0.08 (0.01)	0.14 (0.05)	0.50 (0.05)	0.11 (0.03)	0.20 (0.00)	0.16 (0.03)	0.21 (0.04)	0.14 (0.03)	0.30 (0.07)
	2	0.54 (0.10)	0.25 (0.07)	0.44 (0.07)	0.11 (0.03)	0.38 (0.12)	0.20 (0.07)	0.11 (0.05)	0.19 (0.02)	0.58 (0.02)	0.25 (0.05)	0.22 (0.03)	0.22 (0.02)	0.31 (0.08)	0.21 (0.00)	0.19 (0.05)
	3	0.42 (0.11)	0.28 (0.08)	0.31 (0.11)	0.13 (0.03)	0.43 (0.04)	0.18 (0.08)	0.28 (0.08)	0.20 (0.07)	0.57 (0.05)	0.20 (0.01)	0.25 (0.08)	0.20 (0.00)	0.23 (0.06)	0.20 (0.00)	0.19 (0.07)
	4	0.57 (0.15)	0.63 (0.12)	0.38 (0.15)	0.28 (0.09)	0.54 (0.10)	0.20 (0.02)	0.43 (0.12)	0.37 (0.11)	0.55 (0.15)	0.35 (0.14)	0.45 (0.13)	0.50 (0.12)	0.48 (0.13)	0.38 (0.11)	0.37 (0.12)
AP ML DST CellTrig	1	0.34 (0.10)	0.26 (0.06)	0.34 (0.05)	0.08 (0.00)	0.44 (0.15)	0.11 (0.03)	0.08 (0.00)	0.15 (0.05)	0.50 (0.09)	0.11 (0.03)	0.20 (0.00)	0.16 (0.03)	0.21 (0.03)	0.14 (0.01)	0.29 (0.07)
	2	0.54 (0.03)	0.25 (0.06)	0.44 (0.09)	0.11 (0.03)	0.37 (0.08)	0.20 (0.00)	0.11 (0.05)	0.19 (0.03)	0.58 (0.06)	0.25 (0.06)	0.22 (0.04)	0.22 (0.02)	0.31 (0.09)	0.21 (0.02)	0.19 (0.05)
	3	0.42 (0.19)	0.28 (0.07)	0.31 (0.10)	0.13 (0.04)	0.43 (0.06)	0.18 (0.08)	0.28 (0.09)	0.20 (0.10)	0.57 (0.03)	0.20 (0.01)	0.24 (0.05)	0.20 (0.00)	0.23 (0.06)	0.20 (0.00)	0.19 (0.03)
	4	0.57 (0.06)	0.63 (0.13)	0.38 (0.09)	0.28 (0.07)	0.51 (0.08)	0.20 (0.08)	0.43 (0.09)	0.37 (0.19)	0.55 (0.11)	0.34 (0.09)	0.45 (0.15)	0.50 (0.03)	0.48 (0.13)	0.38 (0.07)	0.36 (0.16)
AP ML DST MaxLat	1	0.34 (0.10)	0.26 (0.06)	0.34 (0.05)	0.08 (0.00)	0.44 (0.15)	0.11 (0.04)	0.09 (0.00)	0.15 (0.05)	0.51 (0.05)	0.11 (0.03)	0.20 (0.00)	0.16 (0.03)	0.21 (0.02)	0.14 (0.00)	0.30 (0.07)
	2	0.54 (0.03)	0.25 (0.06)	0.44 (0.09)	0.11 (0.03)	0.36 (0.09)	0.27 (0.11)	0.11 (0.05)	0.19 (0.02)	0.55 (0.03)	0.25 (0.06)	0.22 (0.04)	0.22 (0.02)	0.31 (0.09)	0.21 (0.02)	0.19 (0.05)
	3	0.41 (0.19)	0.28 (0.07)	0.31 (0.10)	0.13 (0.04)	0.43 (0.06)	0.18 (0.08)	0.28 (0.09)	0.20 (0.10)	0.51 (0.07)	0.20 (0.01)	0.28 (0.08)	0.20 (0.00)	0.23 (0.06)	0.20 (0.00)	0.19 (0.03)
	4	0.57 (0.06)	0.63 (0.13)	0.38 (0.09)	0.28 (0.07)	0.55 (0.11)	0.20 (0.08)	0.43 (0.09)	0.35 (0.13)	0.51 (0.11)	0.34 (0.09)	0.45 (0.15)	0.50 (0.04)	0.48 (0.13)	0.38 (0.07)	0.36 (0.16)
AP ML ST CellTrig	1	0.34 (0.10)	0.26 (0.06)	0.34 (0.05)	0.08 (0.00)	0.46 (0.18)	0.11 (0.03)	0.08 (0.00)	0.15 (0.05)	0.50 (0.09)	0.11 (0.03)	0.20 (0.00)	0.16 (0.03)	0.21 (0.03)	0.14 (0.01)	0.29 (0.07)
	2	0.54 (0.03)	0.25 (0.06)	0.44 (0.09)	0.11 (0.03)	0.38 (0.08)	0.20 (0.00)	0.11 (0.05)	0.19 (0.03)	0.58 (0.06)	0.25 (0.06)	0.22 (0.04)	0.22 (0.03)	0.31 (0.09)	0.22 (0.04)	0.19 (0.05)
	3	0.42 (0.19)	0.28 (0.07)	0.31 (0.10)	0.13 (0.04)	0.47 (0.10)	0.18 (0.08)	0.28 (0.08)	0.22 (0.10)	0.57 (0.03)	0.20 (0.01)	0.26 (0.06)	0.20 (0.00)	0.23 (0.06)	0.20 (0.00)	0.19 (0.03)
	4	0.57 (0.06)	0.67 (0.14)	0.38 (0.09)	0.28 (0.07)	0.53 (0.09)	0.20 (0.08)	0.43 (0.10)	0.38 (0.19)	0.61 (0.14)	0.35 (0.09)	0.49 (0.17)	0.54 (0.04)	0.48 (0.13)	0.38 (0.07)	0.37 (0.16)
AP ML ST MaxLat	1	0.34 (0.10)	0.26 (0.06)	0.34 (0.05)	0.08 (0.00)	0.46 (0.18)	0.11 (0.04)	0.09 (0.00)	0.15 (0.05)	0.51 (0.05)	0.11 (0.03)	0.20 (0.00)	0.16 (0.03)	0.21 (0.02)	0.14 (0.00)	0.30 (0.07)
	2	0.54 (0.03)	0.25 (0.06)	0.44 (0.09)	0.11 (0.03)	0.37 (0.09)	0.27 (0.11)	0.11 (0.05)	0.19 (0.02)	0.55 (0.03)	0.25 (0.06)	0.22 (0.04)	0.22 (0.03)	0.31 (0.09)	0.22 (0.04)	0.19 (0.05)
	3	0.42 (0.19)	0.28 (0.07)	0.31 (0.10)	0.13 (0.04)	0.47 (0.10)	0.18 (0.08)	0.28 (0.08)	0.22 (0.10)	0.52 (0.07)	0.20 (0.01)	0.29 (0.08)	0.20 (0.00)	0.23 (0.06)	0.20 (0.00)	0.19 (0.03)
	4	0.57 (0.06)	0.67 (0.14)	0.38 (0.09)	0.28 (0.07)	0.57 (0.14)	0.20 (0.08)	0.43 (0.10)	0.35 (0.13)	0.54 (0.13)	0.35 (0.09)	0.49 (0.17)	0.54 (0.04)	0.48 (0.13)	0.38 (0.07)	0.37 (0.16)
AP ML CellTrig MaxLat	1	0.36 (0.11)	0.26 (0.06)	0.40 (0.07)	0.08 (0.00)	0.47 (0.17)	0.11 (0.04)	0.09 (0.00)	0.15 (0.05)	0.51 (0.05)	0.11 (0.03)	0.20 (0.00)	0.16 (0.03)	0.22 (0.04)	0.14 (0.01)	0.31 (0.09)
	2	0.64 (0.03)	0.26 (0.06)	0.48 (0.18)	0.13 (0.07)	0.47 (0.11)	0.27 (0.11)	0.11 (0.05)	0.20 (0.03)	0.59 (0.06)	0.31 (0.11)	0.25 (0.09)	0.23 (0.05)	0.35 (0.11)	0.22 (0.03)	0.19 (0.05)
	3	0.52 (0.19)	0.29 (0.10)	0.32 (0.09)	0.19 (0.08)	0.51 (0.16)	0.18 (0.08)	0.38 (0.19)	0.23 (0.07)	0.52 (0.07)	0.21 (0.10)	0.34 (0.17)	0.20 (0.04)	0.23 (0.06)	0.20 (0.00)	0.19 (0.03)
	4	0.63 (0.09)	0.74 (0.20)	0.40 (0.14)	0.36 (0.12)	0.67 (0.06)	0.20 (0.08)	0.56 (0.15)	0.41 (0.12)	0.56 (0.15)	0.36 (0.13)	0.53 (0.21)	0.61 (0.04)	0.55 (0.13)	0.42 (0.12)	0.37 (0.16)